

This study of airborne observations of halogenated VOCs (HVOCs) represents a valuable addition to the knowledge of these compounds over the Southern Ocean, where few data exist. The study confirms the current view that the main sources of  $\text{CHBr}_3$  and  $\text{CH}_2\text{Br}_2$  are biological, and that  $\text{CH}_3\text{I}$  has both biological and non-biological sources. The authors have put forward a novel concept of using enrichment ratios of HVOCs to  $\text{O}_2$  to infer the contribution or otherwise of ocean biological sources, and propose a new function to estimate non-biological emission fluxes of  $\text{CH}_3\text{I}$ . The dataset has been used to evaluate the CAM-Chem HVOC emission scheme at high latitudes in the Southern Hemisphere. The take home message/s from this evaluation are rather opaque – they could do with being put in context. E.g., do they infer that fluxes from these regions are poorly known, or problems with the models mixing /convection schemes special to these latitudes, or issues with photo-oxidation rates?. In terms of presentation, the paper has a number of typographical and other errors, listed below, and needs a thorough reading (I doubt I captured all of them). However overall, I think this manuscript presents sufficiently novel results to be suitable for publication, once these matters have been attended to.

We appreciate the reviewer's time and comments. We have done our best to clarify the goals and findings of this study. We argue that emissions of HVOCs over the Southern Ocean are poorly known using mixing ratio comparisons with a global climate model and state of the art biogenic flux parameterizations based on chl *a* that show persistent model biases. Thereafter, we seek to address this problem by proposing new approaches to estimate regional HVOC fluxes using airborne observations. We demonstrate two additional approaches for deriving HVOC flux estimates using airborne observations, and model output. We hope that the reviewer finds our article suitable for publication following these revisions.

L34-38 The regional enrichment ratios should be put in context here - there is no explanation as their relevance.

We no longer report enrichment ratios in the abstract. We do however, attempt to explain the role of  $\text{O}_2$ -HVOC enrichment ratios in inferring a biological flux of HVOCs. This passage now reads, "The first approach takes advantage of the robust relationships that were found between airborne observations of  $\text{O}_2$  and  $\text{CHBr}_3$ ,  $\text{CH}_2\text{Br}_2$ , and  $\text{CHClBr}_2$ ; we use these linear regressions with  $\text{O}_2$  and modeled  $\text{O}_2$  distributions to infer a biological flux of HVOCs." L30-33.

L51- 52 "Indeed, HVOCs may be among the most important sources of inorganic bromine to the whole atmosphere ..... (Murphy et al., in review)." This is not conventional wisdom and thus quite a bold statement. Are the authors confident that the Murphy et al paper will be published soon?

Murphy et al. (2019) has now been published and the citation has been revised. We have also moderated the language to reflect that this statement challenges conventional wisdom. This passage L50-54 now reads, "In the marine boundary layer and lower troposphere, sea salt is the main source of reactive bromine (Finlayson-Pitts 1982, Simpson et al. 2019). Yet HVOCs may also be a more important source of inorganic bromine to the whole atmosphere than previously thought, according to a recent study, which indicates that sea salt is scarce and insufficient to control the bromine budget in the middle and upper troposphere (Murphy et al., 2019)."

L61-64 The anthropogenic sources of CH<sub>3</sub>Br have changed over time and now are dominated by quarantine and pre-shipment (QPS) applications (not controlled by the Montreal Protocol). Please stick to the most recent information from WMO 2018 (and update the reference).

Both the information and citation on anthropogenic sources of CH<sub>3</sub>Br have been revised in L65-68: “CH<sub>3</sub>I is also formed through non-biological reactions in surface seawater, and CH<sub>3</sub>Br is emitted as a result of quarantine and pre-shipment activities, which are not regulated by the Montreal Protocol (e.g., Moore and Zafiriou; 1994, WMO 2018).

L119- 130 The last paragraph of the introduction would benefit from an introduction to the concept of enrichment ratios of HVOCs to O<sub>2</sub>, which feature prominently in the abstract.

We have revised this passage in L122-139 to read, “In Section 3.1 and 3.2, we report new airborne observations of CHBr<sub>3</sub>, CH<sub>2</sub>Br<sub>2</sub>, CH<sub>3</sub>I, CHClBr<sub>2</sub>, CHBrCl<sub>2</sub>, and CH<sub>3</sub>Br from high latitudes in the Southern Hemisphere, where data are scarce, and large-scale regional mixing ratio comparisons for HVOCs with the community earth system model (CESM) atmospheric component with chemistry (CAM-Chem). In section 3.4, we present two novel approaches to estimate regional fluxes of HVOCs for comparison with global climate models’ parameterizations or climatologies. One approach uses correlations of HVOCs to marine, oxygen (O<sub>2</sub>) of marine origin, as measured by deviations in the ratio of O<sub>2</sub> to nitrogen (N<sub>2</sub>) ( $\delta(O_2/N_2)$  see Sect. 2.1.2 and 3.1.2) to determine the importance of regional biological HVOC sources. The robust correlations of CHBr<sub>3</sub> and CH<sub>2</sub>Br<sub>2</sub> with  $\delta(O_2/N_2)$  are indicative of a strong biological source. Our first approach exploits the ratio of HVOCs to oxygen (O<sub>2</sub>) determined from linear regressions (i.e. the enrichment ratio), and the ocean flux of O<sub>2</sub> from CESM’s ocean component, to estimate the marine biogenic flux of several HVOCs. The second approach relies on observed HVOC mixing ratios, the Stochastic Time-Inverted Lagrangian Transport (STILT) particle dispersion model and geophysical datasets (see Sect. 2.3 and 3.3). We assess contributions from previously hypothesized regional sources for the Southern Ocean, and estimate HVOC fluxes based on regressions between upstream influences and observed mixing ratios and distributions of remotely sensed data.”

L235-245 The fact that the polyhalogenated bromocarbons are likely co-emitted is not new – there are numerous papers that show this, and the discussion could elaborate on those a bit more. What is also missing from this paragraph is a discussion of macroalgal sources of these compounds, although this is presumably not relevant for the Antarctic.

We have expanded the discussion of previous findings of co-emitted polyhalogenated bromocarbons and cited several additional studies. This passage L390 - 401 now reads, “Previous studies have documented co-located source regions of CHBr<sub>3</sub> and CH<sub>2</sub>Br<sub>2</sub> in the Southern Ocean (e.g. Hughes et al., 2009; Carpenter et al., 2000; Nightingale et al. 1995; Laturmus et al. 1996), and laboratory studies have demonstrated that phytoplankton and their associated bacteria cultures, including a cold water diatom isolated from coastal waters along the Antarctic Peninsula and common to the Southern Ocean, produce both CHBr<sub>3</sub> and CH<sub>2</sub>Br<sub>2</sub> (Hughes et al., 2013; Tokarczyk and Moore 1994, Sturges et al., 1993). The non-linearity observed in ratios of these two gases at low CHBr<sub>3</sub> may reflect the different rates of their production or loss in seawater, or possibly, the influence of air masses from distant, more productive low-latitude source regions. Several studies have documented bacterially mediated loss of CH<sub>2</sub>Br<sub>2</sub>, but not

CHBr<sub>3</sub>, and report distinct ratios of CH<sub>2</sub>Br<sub>2</sub> to CHBr<sub>3</sub> in seawater during the growth and senescent phases of a phytoplankton bloom (e.g. Carpenter et al. 2009, Hughes et al 2013). ”

L244-245 “For instance, Huges et al. (2013) also report distinct seawater slopes between CH<sub>2</sub>Br<sub>2</sub> to CHBr<sub>3</sub> , when chl a was increasing.” It is not clear what is meant by this. Please rephrase

This statement has been rephrased on L398, “Several studies have documented bacterially mediated loss of CH<sub>2</sub>Br<sub>2</sub>, but not CHBr<sub>3</sub>, and report distinct ratios of CH<sub>2</sub>Br<sub>2</sub> to CHBr<sub>3</sub> in seawater during the growth and senescent phases of a phytoplankton bloom (e.g. Carpenter et al. 2009, Hughes et al 2013).”

L361- 366 “In both regions, the model under predicts CH<sub>3</sub>I above the MBL, which may indicate slower observed photochemical loss than the model predicts.” Has this been found in other CAM-Chem studies – e.g. is it a general result? If not, could a different source emission distribution (i.e. more homogeneous source) explain these results?

We have revised the text to reflect that indeed this result has been found in other CAM-Chem studies, and that the observed difference at high latitudes in the SH at ~10 km altitude may be due to the zonal transport of air masses from lower latitudes, where differences in CH<sub>3</sub>I in the UTLS have also been observed. For instance, in Ordonez et al. (2012), Fig. 10 illustrates the consistent under prediction of the observed CH<sub>3</sub>I mixing ratios, and these authors attribute this discrepancy to the strength of convective cells rapidly transporting air masses to the UTLS. This section L494-499 now reads as follows: “In both regions, the model under predicts CH<sub>3</sub>I in the upper troposphere and lower stratosphere (UTLS), likely stemming from the poleward transport of lower latitude air masses, where CAM-Chem also exhibits a negative bias. Mixing ratio comparisons with CAM-Chem over the tropics (see Ordonez et al. Figure 10) depict similar or larger discrepancies, and have been attributed to stronger than anticipated convective cells in the tropics.”

L555-L560 onwards. There is no mention in Moore and Zarifou 1994 nor Richter and Wallace 2004 as far as I can see on the influence of iron availability – do the authors mean iodide availability?!

We have both fixed a typo and clarified the discussion on proposed non-biological chemical mechanisms for CH<sub>3</sub>I production in the ocean, which include the radical recombination reaction proposed by Moore and Zarifou (1994), and the substitution reaction, requiring an oxidant such as iron III, proposed by Williams et al. (2007). This passage L563-569 now reads, “This non-biological source, though not fully understood, requires light, a humic like substance at the surface ocean supplying a carbon source and methyl group, and reactive iodine (Moore and Zarifou 1994; Richter and Wallace 2004). Thus far, two chemical mechanisms have been proposed for the non-biological production of methyl iodide, one – a radical recombination of a methyl group and iodine involving UV photolysis (e.g. Moore and Zarifou 1994), and the second, a substitution reaction involving the reduction of an oxidant, such as iron III (e.g. Williams et al. 2007).”

L1036 – Note that units should be pmol m<sup>-2</sup> hr<sup>-1</sup> (not m<sup>2</sup>). Please state whether the values given for the observations are means or medians. It would be also be good to include their ranges.

We have corrected this typo on L1068. The units on Table 1 now read “ $\text{pmol m}^{-2} \text{hr}^{-1}$ .”

Ln 82. atmopsheric Ln 213. “oppose” should be “opposed” Ln 213. “Huges” should be “Hughes” Ln 242 : “HOVCs” Ln 469. “Zafarou” should be “Zafariou” Ln 980. “includind” LN 1015. “fluxed”

L81, L253, L391, L518, L1171- Typos have been corrected to read, “Atmospheric,” “opposed,” “HVOCs,” “Zafariou,” and “fluxes.” Other typos previously listed have been deleted from the text.

## Response to Reviewer #2

The paper presented by Asher et al., provides a valuable contribution to the understanding of the distribution and sources of halogenated organic substances from the Southern Ocean. The work publishes airborne observations of VHOC in an understudied region and applies new concepts for source determinations related to measurements of O<sub>2</sub> and CO<sub>2</sub> and geophysical datasets. It underlines current knowledge of the biological sources of CHBr<sub>3</sub> and CH<sub>2</sub>Br<sub>2</sub> by applying their ratio to oceanic oxygen emissions. CH<sub>3</sub>I appears to have a dominant biological source in the area of the Patagonian shelf, while closer to Antarctica a photochemical source appears to be dominant. The paper also compares the derived emissions of the novel concepts to the output of a global climate model. I agree that the presentation of data from several compounds and several campaigns is a difficult task. Also the loaded content of the paper: evaluation of model predictions, calculation of biogenic enrichment ratios, identification of regional sources, and novel means of parameterizing ocean fluxes, which was only summarized clearly in the conclusion section of the paper, makes the task of writing not easier. While the authors present their results and outcomes, which are not totally exciting and sometimes are also not very convincing due to poor correlations, their novel approaches and novel concepts are more exciting, but are poorly presented. They could do a much better job in explaining and presenting their concepts and the overall goal of the paper, which for me remains more a concept than a result paper. The results underline the novel approaches, as they do not contradict earlier studies and the novel approaches can be more useful and should be tested for and in future studies. The authors should think about a different setup of their paper, putting their concepts more into the focus, but clearly their approaches need to be described more clearly and in more detail throughout the text. Also they authors should think about the title. Also technically the paper needs improvement, as abbreviations are sometimes not introduced, sometimes edits are not clearly overworked, which led to typos and grammar mistakes and also I wonder if it would be possible to make some sentences less bulky and loaded. Some figures are too small, some legends appear odd and there appear to be misunderstandings with some references. Overall I think the work behind the paper is very valuable and should be published in ACP, but the presentation of the work needs prior strong improvement.

We appreciate the reviewer's constructive criticism. We have refocused our paper on the approaches and concepts outlined here, rather than our results. We also argue that emissions of HVOCs over the Southern ocean are poorly known and seek to address this problem by proposing new approaches to estimate regional HVOC fluxes using airborne observations. We have sought to better outline the two novel approaches to estimate HVOC fluxes and explain why these approaches represent an important step forward in the field. We have also done our best to improve the presentation by reorganizing the structure of the paper, simplified the language and corrected typos and grammar errors. We hope that the reviewer finds our article suitable for publication following these revisions.

L22- 25 We also use CH<sub>3</sub>Br from the University of Miami Advanced Whole Air Sampler(AWAS) on ORCAS and from the UC Irvine Whole Air Sampler (WAS) on ATom-2. In connection with the first and the third sentence, this is a strange sentence. I think there is too much detail in the first two sentences about the instrumentation, which could be abandoned for the abstract and only explained later in the text.

We agree with the reviewer and have revised the text to include less detail on instrumentation. This section on L22-25 now reads: "We present observations of CHBr<sub>3</sub>, CH<sub>2</sub>Br<sub>2</sub>, CH<sub>3</sub>I, CHClBr<sub>2</sub>, CHBrCl<sub>2</sub>,

and CH<sub>3</sub>Br during the O<sub>2</sub>/N<sub>2</sub> Ratio and CO<sub>2</sub> Airborne Southern Ocean (ORCAS) study and the 2<sup>nd</sup> Atmospheric Tomography mission (ATom-2), in January and February of 2016 and 2017.”

L32-38 Based on these relationships What does this refer to?... it is unclear

We have done our best to clarify how the regressions of HVOC mixing ratios with upwind influences and O<sub>2</sub> are used to estimate basin-wide fluxes on L30-33: “... we demonstrate two novel approaches to estimate HVOC fluxes; the first approach takes advantage of the robust relationships that were found between airborne observations of O<sub>2</sub> and CHBr<sub>3</sub>, CH<sub>2</sub>Br<sub>2</sub>, and CHClBr<sub>2</sub>; we use these linear regressions with O<sub>2</sub> and modeled O<sub>2</sub> distributions to infer a biological flux of HVOCs.”

L49-53 Indeed, HVOCs may be among the most important sources of inorganic bromine to the whole atmosphere, since recent evidence indicates that sea salt is scarce.. This is not true, as there is enough literature out to show how sea salt aerosol dominates the bromine in the lower troposphere. If the authors want to keep this sentence they have to provide more evidence, than just an upcoming paper. I suggest rewriting and specifying the statement to the known literature.

We have added a sentence to reflect that sea salt aerosol is critical to the bromine budget in the lower troposphere, and have moderated the language of the sentence regarding the contribution of bromocarbons to the middle and upper troposphere to reflect that this statement challenges conventional wisdom. This passage L50-54 now reads, “In the marine boundary layer and lower troposphere, sea salt is the main source of reactive bromine (Finlayson-Pitts 1982, Simpson et al. 2019). Yet HVOCs may also be a more important source of inorganic bromine to the whole atmosphere than previously thought, according to a recent study, which indicates that sea salt is scarce and insufficient to control the bromine budget in the middle and upper troposphere (Murphy et al., 2019).”

L75-80 There is an important observational paper missing which the authors need to relate to in the discussion of their results later on in the paper. It is: Regional sinks of bromoform in the Southern Ocean from 2013 from Mattsson et al. in GRL, where he shows the heterogeneity of the sources, which make the ocean a sink at times. Therefore also the next sentence needs to be revised: These studies indicate moderate ocean sources of CHBr<sub>3</sub> and CH<sub>2</sub>Br<sub>2</sub> at high latitudes in the Southern Hemisphere, and refer to Mattsson., possibly in line 79.

This passage has been revised on L79-84: “Mattsson et al. (2013) noted that the ocean also acts as a sink for HVOCs, when HVOC undersaturated surface waters equilibrate with air masses transported from source regions. The spatially heterogeneous ocean sources of CHBr<sub>3</sub> and CH<sub>2</sub>Br<sub>2</sub> at high latitudes in the Southern Hemisphere are often underestimated in global atmospheric models (Hossaini et al., 2013; Ordoñez et al., 2012; Ziska et al., 2013).”

L94-103 Here you need to relate to Salawitch (2011?).. –most trace gases in tropospheric air enter the stratosphere in the tropics, move poleward and descend to the troposphere at middle and high latitudes. Salawitch claims, that the polar bromine can be influenced by large scale subsidence from the lower latitudes. . .

This passage has been rewritten to reflect this on L99-103, “As a result of limited vertical transport in these regions, however, air-sea fluxes lead to strong vertical gradients. Zonal transport from lower latitudes has a large impact on the vertical gradients of trace gas mixing ratios over polar regions (Salawitch 2010). Given their extended photochemical lifetimes at high latitudes (see Sect. 2.3 for a brief discussion), many HVOC distributions are particularly sensitive to zonal transport at altitude.”

L105-106 Few constraints on HVOC mixing ratios or emissions based on airborne data exist at high latitudes in the Southern Hemisphere. What does this mean?

This sentence has been rewritten (L108-109) and is hopefully more clear: “Few airborne observations of HVOCs exist at high latitudes in the Southern Hemisphere.”

L117 This is pmol. . . not nmol mol<sup>-1</sup>

The correction has been made on 119, “ACE-1 measurements of CH<sub>3</sub>I in the MBL indicate a strong ocean source between 40° S and 50° S in austral summer, with mixing ratios above 1.2 pmol below ~1 km (Blake et al., 1999).”

L131 – 136 Here you could (you need to do it somewhere) elaborate on the O<sub>2</sub>/N<sub>2</sub> concept and why you chose to relate the HVOHCs to those.

We now discuss the concept and purpose of relating HVOCs to O<sub>2</sub>/N<sub>2</sub> in L126-L134: “In section 3.4, we present two novel approaches to estimate regional fluxes of HVOCs for comparison with global climate models’ parameterizations or climatologies. One approach uses correlations of HVOCs to marine, oxygen (O<sub>2</sub>) of marine origin, as measured by deviations in the ratio of O<sub>2</sub> to nitrogen (N<sub>2</sub>) ( $\delta(O_2/N_2)$ ) see Sect. 2.1.2 and 3.1.2) to determine the importance of regional biological HVOC sources. The robust correlations of CHBr<sub>3</sub> and CH<sub>2</sub>Br<sub>2</sub> with  $\delta(O_2/N_2)$  are indicative of a strong biological source. Our first approach exploits the ratio of HVOCs to oxygen (O<sub>2</sub>) determined from linear regressions (i.e. the enrichment ratio), and the ocean flux of O<sub>2</sub> from CESM’s ocean component, to estimate the marine biogenic flux of several HVOCs.”

L141-144 Please include the regions into Figure 1.

We now include the regions in Fig. 1.

L144-152 If you only refer to two flights from ATom-2, the sentence could be easier to read.

This sentence has been revised to read, “On Feb. 10 and 13, 2017 the sixth and seventh ATom-2 research flights passed over the eastern Pacific sector poleward of 60° S (defined here as Region 1) and over the Patagonian Shelf between 40° S and 55° S and between 70° W and 55° W (defined here as Region 2), respectively.”

L204 [Model is missing](#)

Although this passage has been revised, “Model” has been added when CESM is first introduced in the introduction on L126: “In Section 3.1 and 3.2, we report new airborne observations of  $\text{CHBr}_3$ ,  $\text{CH}_2\text{Br}_2$ ,  $\text{CH}_3\text{I}$ ,  $\text{CHClBr}_2$ ,  $\text{CHBrCl}_2$ , and  $\text{CH}_3\text{Br}$  from high latitudes in the Southern Hemisphere, where data are scarce, and large-scale regional mixing ratio comparisons for HVOCs with the community earth system model (CESM) atmospheric component with chemistry (CAM-Chem).”

L207 [You did not introduce CAM.](#)

CAM is now referred to here as “CESM’s atmosphere component. Please see above comment.

L1215 [What is a broadening effect?](#)

L217 We have specified “pressure broadening effect” on the  $\text{CO}_2$  and  $\text{CH}_4$  spectrum in cavity ring down instruments, which has been observed in several studies due to the influence of water vapor (e.g. Chen et al. 2013). This sentence now reads, “Dry-air mole fractions were calculated using empirical corrections to account for dilution and pressure broadening effects as determined in the laboratory before and after the campaign deployments, and in-flight calibrations were used to determine an offset correction for each flight.”

L243-L252 [We note that the non-linearity observed in ratios of these two gases at low  \$\text{CHBr}\_3\$  levels likely reflects the differences in emissions during strong phytoplankton blooms, as oppose to other periods. The ratio may simply \(and more likely\) reflect other air masses from more distant source regions, which is reflected in a ratio which favors the longer lived compound \( \$\text{CH}\_2\text{Br}\_2\$ \) over the shorter-lived compound \( \$\text{CHBr}\_3\$ \) which is emitted in larger quantities in a biological source region \(refer to Yokouchi, 20xx\) but more rapidly degraded during transport.](#)

Our analysis focuses on the bottom 2 km of the atmosphere, and as such largely reflects recent enhancements in HVOCs. Nevertheless, we have clarified this passage to reflect that contributions from zonal transport from low latitude regions cannot fully be ruled out, and have further expanded on the differences in  $\text{CH}_2\text{Br}_2$  and  $\text{CHBr}_3$  production and loss rates in surface waters. This passage L395-405 now reads, “The non-linearity observed in ratios of these two gases at low  $\text{CHBr}_3$  may reflect the different rates of their production or loss in seawater, or possibly, the influence of air masses from distant, more productive low-latitude source regions. Several studies have documented bacterially mediated loss of  $\text{CH}_2\text{Br}_2$ , but not  $\text{CHBr}_3$ , and report distinct ratios of  $\text{CH}_2\text{Br}_2$  to  $\text{CHBr}_3$  in seawater during the growth and senescent phases of a phytoplankton bloom (e.g. Carpenter et al. 2009, Hughes et al 2013). Although this analysis is restricted to the bottom 2 km of the atmosphere, zonal transport of air masses with lower ratios of  $\text{CH}_2\text{Br}_2$  to  $\text{CHBr}_3$  ratios, as have been observed in the MBL over productive, low-latitude regions, may also have influenced our observations (Yokouchi et al. 2005).”

L246-248 [For instance, Huges et al. \(2013\) also report distinct seawater slopes between  \$\text{CH}\_2\text{Br}\_2\$  to  \$\text{CHBr}\_3\$ , when chl a was increasing. This is a weak sentence; can you give it more meaning?](#)



This sentence has been rewritten on L398, “Several studies have documented bacterially mediated loss of  $\text{CH}_2\text{Br}_2$ , but not  $\text{CHBr}_3$ , and report distinct ratios of  $\text{CH}_2\text{Br}_2$  to  $\text{CHBr}_3$  in seawater during the growth and senescent phases of a phytoplankton bloom (e.g. Carpenter et al. 2009, Hughes et al 2013).”

L257-258 please explain the concept: What do you expect from the ratio of the HVOHCs and the marine oxygen.

L415-418 We have revised this passage, “We sought to test if the biologically mediated production of bromocarbons and oxygen result in similar atmospheric distributions. Conversely, we expected HVOHC atmospheric distributions and  $\text{CO}_2$  distributions to anticorrelate because  $\text{CO}_2$  fixation in surface waters is proportional to the production of oxygen.”

L288 238/241-242: Where did you get this equilibration times? Support them by reference or evidence. And also the air-sea fluxes of  $\text{O}_2$  and  $\text{CHBr}_3$  are not very similar. Revise. L444 This sentence now reads, “The bulk air-sea equilibration time for an excess of  $\text{CHBr}_3$  and other HVOHCs is less than two weeks, although the photochemical loss of HVOHCs will alter their ratio over time (see Supplement for details on calculations of bulk sea air equilibration times).” The section in the supplement (L1177-1185) reads as follows: “To support the interpretation of our results, we calculate nominal equilibration times. For estimates of bulk sea air equilibration times for HVOHCs,  $\text{O}_2$ , and  $\text{CO}_2$ , we assume a mixed layer depth of 30 m, a temperature of  $0^\circ\text{C}$ , a salinity of 35 PSU, and carbonate buffering according to eq. 8.3.10 in Sarmiento and Gruber (2006), and transfer velocities according to Nightingale et al., (2000). The Schmidt number (i.e. the ratio of the kinematic viscosity of a gas, divided by the molecular diffusivity) for  $\text{O}_2$ ,  $\text{CO}_2$  and  $\text{CH}_3\text{Br}$  were calculated according to Wanninkhof (2014), and the Schmidt numbers for  $\text{CHBr}_3$  and  $\text{CH}_3\text{I}$  were calculated according to Quack and Wallace (2003) and Moore and Groszko (1999), respectively. The results are provided in Sect. 3.1.2.”

L291-300 This paragraph is a little back and forth between compounds and regions; it can be sorted for easier reading.

We have done our best to clarify this paragraph in L455-465: “Our observations suggest a biological source for  $\text{CHBr}_3$  and  $\text{CH}_2\text{Br}_2$  in both Region 1 and Region 2 (Fig. 4). Interestingly, the slope of the regression between  $\text{CHBr}_3$  and  $\text{O}_2$  appears distinct in Region 1 and Region 2, but between  $\text{CH}_2\text{Br}_2$  is the same. Molar enrichment ratios are  $0.20 \pm 0.01$ , and  $0.07 \pm 0.004$  pmol : mol for  $\text{CHBr}_3$  and  $\text{CH}_2\text{Br}_2$  to  $\text{O}_2$  in Region 1, and  $0.32 \pm 0.02$ , and  $0.07 \pm 0.004$  pmol : mol in Region 2. We observe a weaker relationship between  $\text{CH}_3\text{I}$  and  $\text{CHClBr}_2$  and  $\text{O}_2$  in Region 1 (Fig. 4c, d), consistent with the existence of other, non-biological sources of  $\text{CH}_3\text{I}$  in this region. Figure 4f illustrates a strong relationship between  $\text{CH}_3\text{I}$  and  $\text{O}_2$ , as well as  $\text{CHClBr}_2$  and  $\text{O}_2$ , in Region 2, however, which implies that the dominant sources of  $\text{CH}_3\text{I}$  and  $\text{CHClBr}_2$  emissions over the Patagonian Shelf are biological. The corresponding molar enrichment ratios of  $\text{CH}_3\text{I}$  to  $\text{O}_2$  and  $\text{CHClBr}_2$  to  $\text{O}_2$  in Region 2 are  $0.38 \pm 0.03$  pmol : mol and  $0.19 \pm 0.04$  pmol : mol, respectively.”

263. This should have come earlier, when you start with the equilibria (238, 241). And do you also reference the atmospheric lifetimes?

L44 We now refer the reader to the supplement here for further reading on the calculation of equilibration times. Please see two responses up for details.

L336 – 337 [FINN and MEGAN 2.1 products. I guess the abbreviations need to be explained a bit as well as the products](#)

L247 “The model uses chemistry described by Tilmes et al. (2016), biomass burning and biogenic emissions from the Fire INventory of NCAR (FINN; Wiedinmyer et al. 2011) and MEGAN (Model of Emissions of Gasses and Aerosols from Nature) 2.1 products (Guenther et al., 2012) with additional tropospheric halogen chemistry described in Fernandez et al. (2014) and Saiz-Lopez et al. (2014), including ocean emissions of  $\text{CHBr}_3$ ,  $\text{CH}_2\text{Br}_2$ ,  $\text{CHBr}_2\text{Cl}$ , and  $\text{CHBrCl}_2$ , with parameterized emissions based on chlorophyll *a* (*chl a*) concentrations and scaled by a factor of 2.5 over coastal regions, as opposed to open ocean regions (Ordoñez et al. 2012).”

L341 [from this sentence it is not clear where the oceanic emissions are derived from. I guess its Ordonez, 2012?](#) Done. Ordonez et al. (2012) has been cited. Please see above.

L343 [Ordonez, 2012 does not include  \$\text{CH}\_3\text{Br}\$ . Revise](#)

We respectfully disagree with the reviewer. Indeed, Ordonez does prescribe a lower boundary condition for  $\text{CH}_3\text{Br}$  and show mixing ratio comparisons for this compound. There is not a biogenic flux prescribed for  $\text{CH}_3\text{Br}$ .

L393 [GDAS has to be introduced.](#)

L271 “STILT was run using 0.5° Global Data Assimilation System (GDAS) reanalysis winds to investigate the transport history of air sampled along the flight track (Stephens et al., 2018).”

416-418 [We consider the wind direction error to evaluate the possible size of spatial errors in footprint location. There appears to be something wrong with the grammar? The sentence is not understandable. Given median wind speeds in this domain, this corresponds to a possible error of 260 km/day possible error. Here is also something wrong.](#)

L287 We have revised this passage to read, “For wind speed, a small bias may be present, where we find a median difference between observations and reanalysis of 0.68 m/s, a 5% relative bias. The 1-sigma of the wind speed difference is 2.3 m/s, corresponding to a 19% 1-sigma uncertainty in wind speed. In its simplest approximation, the surface influence strength error is perfectly correlated with the wind speed error, and thus we take 19% as an approximation of the surface influence strength uncertainty. The uncertainty in surface influence location depends on the error in the wind direction. We find a 1-sigma error of 14 degrees in wind speed, which corresponds to a possible error of 260 km/day.”

L448- 449 OCI and GIOP have to be introduced. What does . . .and its uncertainty . . .mean? how do you obtain a  $0.25^\circ \times 0.25^\circ$  gridded uncertainty in the detrital material absorption? It is also not clear from section 5.2.

OCI and GIOP are introduced, and we have done our best to clarify the meaning of GIOP absorption uncertainty in L350-362: “Due to persistent cloud cover over the Southern Ocean, which often precludes the retrieval of remotely sensed ocean color data, we used 8-day mean composite Aqua MODIS L3 distributions of chl *a* from the Ocean Color Index (OCI) algorithm and absorption due to gelbstoff and detrital material at 443 nm from the Generalized Inherent Optical Properties (GIOP) model (NASA Goddard Space Flight Center, 2014). Absorption due to gelbstoff and detrital material at 443 nm is used as a proxy for colored dissolved organic matter (CDOM; <https://oceancolor.gsfc.nasa.gov/atbd/giop/>). CDOM is hypothesized to be an important source of carbon for the photochemical production of  $\text{CH}_3\text{I}$  (Moore et al., 1994). The GIOP model also publishes an uncertainty in the absorption due to gelbstoff and detrital material at 443 nm. Raw 4 km x 4 km data were geometrically averaged, based on lognormal probability density functions, to a spatial resolution of  $0.25^\circ \times 0.25^\circ$  for use with gridded surface influences. We used the ratio of the  $0.25^\circ \times 0.25^\circ$  gridded uncertainty in the detrital material absorption to the absorption as the relative uncertainty for flux calculations (see Sect. 3.4.2).”

L477 and elsewhere – Is the new terminology geophysical influence function something different than the surface influence function? Or why do you change the wording? Its unclear.

We do not mean to confuse the reader with superfluous terminology: “geophysical influence function” has been replaced everywhere with “surface influence function.”

403 to 404. Can you give an example for *H* and *s*. What is the potential geophysical source distribution *s*?

*H* is the surface influence based on a sample’s back trajectories in the boundary layer ( $\text{ppt m}^2 \text{ s pmol}^{-1}$ ). An example of *s* would be the distribution of chl. *a* at the ocean surface ( $\mu\text{g m}^{-3}$ ) or the distribution of fractional sea ice at the ocean surface, which is unitless.

412: here the potential source distributions is *Hs1*, *Hs2*. . .? And not *s*? Is *HS1* the same as *Hs1*? 415-416: We used the standard deviation of the regression coefficients and the relative uncertainty in the source fields, added in quadrature, to estimate the uncertainty in these fluxes (see Fig. 7 and Sect. 5.2 for fractional uncertainties). 418: How did you calculate and do you report the relative uncertainty of the regression coefficients? There is no standard deviation of the regression coefficients in Fig 7 and sect 5.2 does not explain fractional uncertainties and no explanation is found about relative uncertainties in source fields. Or are you relating to surface influence strength uncertainty here. There needs to be more explanation about this added here.

L316-L333 Yes *Hs1* is the same as *HS2*. This passage has been revised and two capitalization typos have been corrected to clarify the role of upstream influence functions and geophysical source distributions in these regressions with surface influence functions. Also an example of a geophysical source distribution *s*, was given, Chl. *a*, now L304. The relative uncertainty of regression coefficients for Figure 9 is reported, and used to calculate the flux shown in Figure 11 as described in Sect. 3.4.2. To clarify, in

those regressions where a flux was not calculated based on the relationship (e.g. Fig 7-8), the uncertainty in the regression coefficients is not reported.

L501 why did you include. . . such as CH<sub>3</sub>I in Region 1? The second half sentence does not add information?

The phrase “such as CH<sub>3</sub>I in Region 1” has been deleted.

L500-501 Note, sea ice did not include land ice; however, we also found a negative correlation between upstream land ice influence and mixing ratios of HVOCs. Why do you add the sentence starting with however? How did you get the correlations when it is not included and does it help the interpretation of the results? It appears misleading and redundant.

This statement on L521 has been revised to read, “We found no positive relationships between upstream sea-ice influence and any measured HVOC Region 1 (Fig. 7).”

L506 We note that over-turned first year sea-ice, which can expose under-ice algae colonies to the air, likely still present a local source of CHBr<sub>3</sub>, CH<sub>2</sub>Br<sub>2</sub>, or other VOHCs to the MBL. How does this speculation relate to your study and how does it help your interpretations? It stands a bit loose currently.

The statements regarding land ice and overturned first-year ice have been deleted.

Sect. 4.2 What was the temporal resolution of the input data shortwave and detrital material- add in section 4.2.

The temporal resolution of the input shortwave radiation data is every six hours and detrital data is every eight days, as specified elsewhere on L351 (a) and L365 (b).

a) “Due to persistent cloud cover over the Southern Ocean, which often precludes the retrieval of remotely sensed ocean color data, we used 8-day mean composite Aqua MODIS L3 distributions of chl *a* from the Ocean Color Index (OCI) algorithm and absorption due to gelbstoff and detrital material at 443 nm from the Generalized Inherent Optical Properties (GIOP) model (NASA Goddard Space Flight Center, 2014).”

b) “The National Center for Environmental Prediction (NCEP) provides Final Global Data Assimilation System (GDAS/FNL) global data of downward shortwave radiation at the surface at 0.25 degree and 6-hour resolution (NCEP, 2015).”

L557-562 This section is wrong. There is no study (at least not the referenced ones) which proves a relationship between iron availability and methyl iodide. The authors have misinterpreted the cited studies. Please check and revise.

L565-569 A typo has been corrected and this passage has been revised and clarified. The role of iron is briefly explicitly discussed as a possible oxidant for one of two proposed abiotic CH<sub>3</sub>I reactions: “This

non-biological source, though not fully understood, requires light, a humic like substance at the surface ocean supplying a carbon source and methyl group, and reactive iodine (Moore and Zarifou 1994; Richter and Wallace 2004). Thus far, two chemical mechanisms have been proposed for the non-biological production of methyl iodide, one – a radical recombination of a methyl group and iodine involving UV photolysis (e.g. Moore and Zarifou 1994), and the second, a substitution reaction involving the reduction of an oxidant, such as iron III (e.g. Williams et al. 2007).”

L564-565 citing the link between temperature and PAR to the solar radiation..this wording is strange..also add which temperature is needed. . .water . may be its easier to just write revealing the link to solar radiation ..or similar

L570 Done, this statement has been revised, “Several previous studies have correlated mixing ratios of CH<sub>3</sub>I to satellite retrievals of PAR and surface ocean temperature, revealing a link to solar radiation (e.g. Happell et al., 1996; Yokouchi et al., 2001).”

L424 please introduce TUV. This section appears to be in the wrong place. I would expect this earlier in the description of the model, e.g. in 4.1., where you also talk about uncertainties due to meteorology.

TUV is now introduced. Note, this section L419-429 has been moved up as suggested to the end of Sect. 2.3 L295-306: “Finally, we note that photochemical loss during transport is not accounted for in this analysis. Low OH mixing ratios, cold temperatures, and lower photolysis rates due to angled sunlight at high latitudes lead to longer than average HVOC lifetimes. For instance, assuming an average diurnal OH concentration of 0.03 pptv, and average photochemical loss according to the Tropospheric Ultraviolet and Visible (TUV) radiation model and the Mainz Spectral data site ([http://satellite.mpic.de/spectral\\_atlas](http://satellite.mpic.de/spectral_atlas)) for Jan. 29 under clear sky conditions at 60° S, CHBr<sub>3</sub> has a lifetime of 30 days, CH<sub>2</sub>Br<sub>2</sub> has a lifetime of 270 days, CH<sub>3</sub>I has a lifetime of 7 days, and CHClBr<sub>2</sub> has a lifetime of 63 days. As such, the photochemical lifetimes of these gases are greater than or equal to the time of our back-trajectory analysis. Moreover, OH concentrations in this region have large uncertainties, the inclusion of which would lead to more, not less, uncertainty in surface influence based regression coefficients and estimated fluxes.”

L571-576.

as explained earlier the concept needs to be introduced more clearly earlier..e.g. why do you not take the VOHC directly but apply their relationship to oxygen?

Our goal was not to suggest the “correct” regional flux of HVOCs based on data from two austral summers (and relatively few measurements from the Atom-2 campaign in 2017), but to demonstrate that airborne data can be used to develop other empirically based parameterizations, which could work better. We argue that despite the its inherent uncertainties in the parameterization of biogenic HVOC fluxes based on O<sub>2</sub>, the current CAM-Chem scheme based on chl. *a* leads to biases that exceed 50-100% for these compounds. Moreover, the uncertainties in remotely sensed chl. *a* are rarely considered in such parameterizations.

How can a model and an observation based flux-estimate be wrong by around 50%? And why do you think that a simple down scaling of the calculated oxygen fluxes leads to a robust flux estimate for VOHC, respectively why is this better, than taking just the VOHC fluxes? Can you explain this concept in the text please? Also it is unclear why you calculate all your influence functions to the VOHC mixing ratios directly, and not to their relation to oxygen and why for the flux calculation this now appears better?

O<sub>2</sub> and CO<sub>2</sub> fluxes are not well constrained at high latitudes in the southern hemispheres. In fact, the ORCAS campaign sought primarily to address this problem. Please see Stephens et al. (2018) for details. Although we agree with the reviewer that the simple downscaling is crude, this large discrepancy between observations and model or climatological mean values is due to inter-annual variability. The uncertainty discussed in L546-548 is meant to account for errors in the spatial variability in the fluxes, and does not include the mean absolute difference that is adjusted for in downscaling.

L632-634 I strongly believe that the calculation of the regression surface influence functions need to be shown in the text not in the legend of figure 9. Regression coefficients from the MLR with surface influence functions are now shown in here on L641-644 not in the legend of Fig. 9, “We used a multiple linear regression ( $\pm$  1 standard deviations; Equation 2), where Hs1 and Hs2 are the surface influence functions of downward shortwave radiation and detrital absorption, respectively, with an intercept  $b = 0.19 \pm 0.01$ , and influence coefficients  $a_1 = 3.7E-5 \pm 1.3E-5$ ,  $a_2 = 3.5 \pm 0.74$ , and an interaction term with the coefficient  $-5.2E-4 \pm 1.5E-4$  (c).”

Table 1. You need to indicate in table1 ,which method you used in “This study” to derive the reported flux, as there are several methods here.

The approaches (O<sub>2</sub> vs. MLR using surface influence functions) has been clarified here.

L678-680 this also appears true for CHBr<sub>3</sub>, CHClBr<sub>2</sub> in region 1 ..and for the entire troposphere for CHBrCl<sub>2</sub>

We have rewritten this passage. L692-704: “Our flux estimates based on the relationship of HVOC mixing ratios to other airborne observations and remotely sensed parameters compared relatively well with those derived from global models and ship-based studies (Table 1). Our emission estimates of CHBr<sub>3</sub>, CH<sub>2</sub>Br<sub>2</sub>, and CHClBr<sub>2</sub> are significantly higher than CAM-Chem’s globally prescribed emissions in Region 1, where HVOC mixing ratios are under predicted (Table 1; Fig. 5). Similarly, our estimate of CHClBr<sub>2</sub> emissions is also significantly higher than CAM-Chem’s in Region 2, where CHClBr<sub>2</sub> mixing ratios remained under predicted. Nevertheless, our emission estimates of CHBr<sub>3</sub>, CH<sub>2</sub>Br<sub>2</sub>, CH<sub>3</sub>I, are lower than most prior estimates based on either other models or localized studies using seawater-side measurements from the Antarctic polar region in summer. In the case of CH<sub>3</sub>I, our estimated emissions suggest that the prescribed emissions in CAM-Chem may be too high in Region 1 and Region 2. Our parameterizations of the CH<sub>3</sub>I flux could be used to explore inter-annual variability in emissions, which is not captured by the Bell et al. (2002) CH<sub>3</sub>I climatology currently employed in CAM-Chem.”

L660-664 although they were significantly higher than CAM-Chem's prescribed emissions in Region 1, where VOHC mixing ratios are under predicted (Table 1; Fig. 5). Can you please add the comparison to CAM-Chem at the beginning. It would be better structured if you don't jump between comparisons.

We have clarified these two passages. Please see above.

L675 – 684 parameterizations..these are different ..and you need to add which compounds you are referring to in this sentence. Here it would be good to extend on the methods and why they appear so useful and how you would extend them to other species.

L705-711 We have done our best to clarify this passage: "To extend these relationships to year-round and global parameterizations for use in global climate models, they must be studied using airborne observations in other seasons and regions. These approaches may help parameterize emissions of new species that can be correlated with surface influence functions or the biological production of oxygen or may improve existing emissions, where persistent biases exist. Finally, future airborne observations of HVOCs have the potential to further improve our understanding of air-sea flux rates and their drivers for these chemically and climatically important gases over the Southern Ocean."

Figure 2. Are the data of the campaigns merged? Detection limits need to be added. The label of CH3I is odd.

Yes, the data are merged. Detection limits have been added to the legend.

Figure 3. Please specify one name for the campaigns and keep it. Here in one figure the authors switch between Atom-2, Atom and Atom. Line 937 to 939 in the legend : This sentence does not make sense.

All mentions of ATom are now listed as ATom-2.

Figure 4. There appears to be an old legend as d, g and h are missing as well as CHClBr2. The applied regressions appear to be the same, thus it would be good to elaborate in the text about the method to reduce the legend, e.g. what means. using variables scaled to their range? In the legend? Also here only regressions above 0.2 are shown.

The legend has been revised, and a statement has been added to say that only regressions with  $r^2 > 0.2$  are shown.

Figure 5,6. Switching between CESM in the figure and CAM-Chem1.2 does not help clarity. . . . multiplied by the percentage of data below detection.. . . was it used for calculating the mean? ..rephrase for clarity.

CESM in all the figure axes has been relabeled CAM-Chem. The sentence regarding data below the DL has been revised to read, "Again, the binned mean includes measurements below the detection limit (DL), which for this calculation are assigned a value equal to the DL multiplied by the percentage of data below detection."

Figure 7,8. Talking of statistical significance with  $r^2 \ll 0.2$  and looking at the plots with scattered values and no surface influence, is a bold exaggeration. And the p-values can be abandoned from the figure and just the threshold mentioned, as they do not help the statistics.

P-values listed on the plots have been replaced with p-value thresholds (e.g.  $p < 0.001$ ).

Figure 9. The labeling of the figures is too small, the p- value redundant and the legend for figure c.) too intricate. I strongly believe that the calculation of the regression surface influence functions need to be shown in the text not in the legend of figure 9.

The size of figure labels is larger. The calculation is now shown in the text as discussed above.

Figure 10. The figures and labeling of a to c are too small. ( I suggest single plots, resolution as Figure 1?. It must be  $\text{pmol m}^{-2} \text{ hr}^{-1}$  also in the legend. Also clarify that these are model results. How do the mentioned CESM (CAM- Chem 1.2)  $\text{O}_2$  fluxes relate to the figure? And is this also 2016?

The labeling is now larger, and as now stated in the figure legend, represents the year 2016. CESM ocean component  $\text{O}_2$  fluxes (not shown here) were multiplied by the regression coefficients shown in Fig. 4 to infer a biological flux of HVOCs, as explained in Sect. 5.1.

Figure 11. fluxes not fluxed

Done, and now reads, “fluxes.”



### Response to Reviewer #3

Anonymous Referee #3 The manuscript of Asher et al. describes airborne observations of halogenated volatile organic compounds over the Southern Ocean and improved emission flux estimates, based on modeling studies and correlative O<sub>2</sub> observations. This is an important and interesting study that should be published in Atmos. Chem. Phys. after consideration of the following points. The authors should consider improving the presentation by first presenting their data and methods and then discussing the results. This study contains important new methods and approaches compared to previous studies but the presentation is not always clear. As an example, a key result is the presentation of “regional enrichment ratios” for HVOCs, but it did not become sufficiently clear to me, how they are defined and how they were calculated.

We appreciate the reviewer’s comments and suggestions. We have done our best to reorganize the paper accordingly, by first discussing our methods and data sources and discussing our results second. We have paid particular attention to clarifying the discussion of regional enrichment ratios for HVOCs in the abstract as well as in sections 3.12 and 3.31.

#### Specific Comments:

Specific comments: L32-34: in the same sentence “halogenated hydrocarbon” and “halogenated volatile organic compounds (HVOCs)” are used. If the two mean the same, use only one name. If there is a distinction, please define.

Indeed- these are the same. The wording has been revised. Only the term “halogenated volatile organic compounds (HVOCs)” is now used.

L47-49: Is there a particular logic for the order of the citations given? They are neither sorted according to year, nor alphabetically.

This has been corrected and special attention has been paid to the order of citations throughout the paper.

L50: “recent evidence indicates that sea salt is scarce and insufficient”: this is a strong statement that should be backed up with more than a manuscript in review.

We appreciate the reviewer’s comment. Although this study is now published, this statement has been amended to better reflect current understanding on L50 – 54: “In the marine boundary layer and lower troposphere, sea salt is the main source of reactive bromine. Yet HVOCs may also be a more important source of inorganic bromine to the whole atmosphere than previously thought, according to a recent study, which indicates that sea salt is scarce and insufficient to control the bromine budget in the middle and upper troposphere (Murphy et al., 2019).”

L66: You may cite Abrahamsson et al. (2018) already at this stage.

Done. L670: “Over the Southern Ocean specifically, hypothesized sources of HVOCs include: coastal macroalgae, phytoplankton, sea ice algae, and photochemical or dust stimulated non-biological production at the sea surface (e.g., Abrahamsson et al. 2018, Manley and Dastoor 1998; Moore and Zafiriou 1994; Moore et al., 1996; Richter and Wallace 2004; Williams et al., 2007; Tokarczyk and Moore 1994; Sturges et al., 1992).”

L96: The point “support quantitative air-sea flux estimates” is less obvious than the other points so a reference may be helpful here.

Thank you, we have revised this sentence on L106 to read, “Aircraft observations can rapidly map basin-wide vertical distributions, support quantitative flux estimates, and provide spatial constraints to atmospheric models (e.g. Xiang et al. 2010x; Stephens et al 2018; Wofsy et al. 2011).”

L211: “We note that the non-linearity observed in ratios of these two gases at low  $\text{CHBr}_3$  levels likely reflects the differences in emissions during strong phytoplankton blooms, as oppose to other periods.” Could not the different lifetimes also effect this?

L395-409 Thank you, this passage has been amended to reflect this possibility, and we have done our best to clarify the wording: “The non-linearity observed in ratios of these two gases at low  $\text{CHBr}_3$  may reflect the different rates of their production or loss in seawater, or possibly, the influence of air masses from distant, more productive low-latitude source regions. Several studies have documented bacterially mediated loss of  $\text{CH}_2\text{Br}_2$ , but not  $\text{CHBr}_3$ , and report distinct ratios of  $\text{CH}_2\text{Br}_2$  to  $\text{CHBr}_3$  in seawater during the growth and senescent phases of a phytoplankton bloom (e.g. Carpenter et al. 2009, Hughes et al 2013). Although this analysis is restricted to the bottom 2 km of the atmosphere, zonal transport of air masses with lower ratios of  $\text{CH}_2\text{Br}_2$  to  $\text{CHBr}_3$  ratios, as have been observed in the MBL over productive, low-latitude regions, may also have influenced our observations (Yokouchi et al. 2005).”

Fig. 3. Units missing for the axes

This has been corrected- thank you for brining it to our attention.

Fig. 4. Why are some units given as nmol/mol and others as ppt ?

This too has now been corrected, the axes all read ppt. Again, thank you for brining this to our attention.

L222: Sorry, but I don't know what a type II major axis regression is. A few more words may help.

L426-L431 We have added a short passage to clarify the meaning and utility of the type II major axis regression in this analysis: “We used a type II major axis regression model (bivariate) to balance the influences of uncorrelated processes and measurement uncertainty in HVOCs (on the y-axis) and uncorrelated processes and measurement uncertainty in  $\text{O}_2$  and  $\text{CO}_2$  (on the x-axis) on the regression slope (Ayers et al. 2001; Glover et al., 2011). As noted by previous studies, simple least squares linear regressions fail to account for uncertainties in predictor variables (e.g. Cantrell et al. 2008).”

L250: Please explain how the molar enrichment ratios are defined and/or calculated. This seems to be critical, but not well explained. Is this just the slope of the regression between CHBr<sub>3</sub> (or CH<sub>2</sub>Br<sub>2</sub>) and O<sub>2</sub>?

Yes, the molar enrichment ratios are equivalent to the slope of the regression, although the units of O<sub>2</sub> must be converted from O<sub>2</sub>/N<sub>2</sub> (per meg) to equivalent ppm (multiplying O<sub>2</sub>/N<sub>2</sub> by the X<sub>O<sub>2</sub></sub>, in dry air = 0.2093).

L351: “In its simplest approximation, the wind speed error will correlate with surface influence error” I understand that this is in general may be a reasonable assumption, but it is not obvious to me why the error in the influence function (in ppt m<sup>2</sup> s pmol<sup>-1</sup>) should be proportional to the error in wind speed. More justification of this argument would be needed here.

As explained in Xiang et al. 2010, now cited here, the STILT model error (E) represents a combination of source and model transport error. Although model transport error is difficult to quantify precisely, it is influenced first and foremost by differences in simulated and actual wind speed, wind direction, and boundary layer height. This passage L280-294 now reads, “Uncertainty in the surface influence value is strongly influenced by the accuracy of the underlying meteorological transport, as discussed in Xiang et al. (2010). We evaluated the GDAS reanalysis winds by comparing model winds interpolated in space and averaged between corresponding time points and pressure levels to match aircraft observations. By evaluating observed winds compared with modeled winds along the flight tracks we can estimate uncertainty in the surface influence values. We consider the observation-model differences in both wind speed and direction to approximate errors in surface influence strength and location. For wind speed, a small bias may be present, where we find a median difference between observations and reanalysis of 0.68 m/s, a 5% relative bias. The 1-sigma of the wind speed difference is 2.3 m/s, corresponding to a 19% 1-sigma uncertainty in wind speed. In its simplest approximation, the surface influence strength error is perfectly correlated with the wind speed error, and thus we take 19% as an approximation of the surface influence strength uncertainty. The uncertainty in surface influence location depends on the error in the wind direction. We find a 1-sigma error of 14 degrees in wind speed, which corresponds to a possible error of 260 km/day.”

L389: PAR: please spell out (as far as I can see first defined in L476)

L369 Thank you. This is now done.

L431: “We note that over-turned first year sea-ice, which can expose under-ice algae colonies to the air, likely still present a local source of CHBr<sub>3</sub>, CH<sub>2</sub>Br<sub>2</sub>, or other HVOCs to the MBL.” What is this statement based on?

As it is irrelevant to the main objective of the paper, this statement has been removed.

L499: Reference to Fig.9 in L499 was not clear to me. Was really Fig.9 meant here?

594 Fig. 10 is now referenced here, “For  $\text{CHBr}_3$ ,  $\text{CH}_2\text{Br}_2$ , and  $\text{CHClBr}_2$  we construct ocean emission inventories for January and February using a scaled version of gridded modeled air-sea  $\text{O}_2$  fluxes and the slopes (i.e. molar ratios) of linear correlations between  $\delta(\text{O}_2/\text{N}_2)$  and HVOC mixing ratios (Fig. 10).”

Fig. 9c: Caption not very clear, would be helpful if the description in the caption can be improved.

The wording of this caption has been rewritten. As now discussed elsewhere in the text (Sect. 2.3.1) the surface influence function (e.g.  $\text{HS}_1$ ) is the product of the surface influence and a relevant surface source field.

5.2 Why are STILT based emission estimates presented only for  $\text{CH}_3\text{I}$ ? Why is it not possible to perform this for other HVOCs as well?

Indeed, it is possible to estimate STILT emissions for other gases such as  $\text{CHBr}_3$  and  $\text{CH}_2\text{Br}_2$ . At present, we have not done this, as the correlations with STILT surface influence functions were less strong than those with  $\text{O}_2/\text{N}_2$ , as now stated in the text L653-656.

Figure S4: “Consecutive samples in and out of dips into the MBL”: Sorry, I don’t really understand what is meant here, please re-word.

This has been reworded as requested to read, “Consecutive TOGA VOC sample locations, their back-trajectories and surface influences in the lower troposphere on two different flights (a-c; Jan. 21, 2016, and d-f; Jan. 30, 2016).”

Technical corrections: L134: “low attitude” -> “low altitude”

Done.

L183: citation should be part of the sentence

Done.

1 **Novel approaches to improve estimates of short-lived halocarbon emissions during summer**  
2 **from the Southern Ocean using airborne observations**  
3 Elizabeth Asher<sup>1</sup>, Rebecca S. Hornbrook<sup>1</sup>, Britton B. Stephens<sup>1</sup>, Doug Kinnison<sup>1</sup>, Eric J. Morgan<sup>5</sup>, Ralph F.  
4 Keeling<sup>5</sup>, Elliot L. Atlas<sup>6</sup>, Sue M. Schauffler<sup>1</sup>, Simone Tilmes<sup>1</sup>, Eric A. Kort<sup>2</sup>, Martin S. Hoecker-Martínez<sup>3</sup>,  
5 Matt C. Long<sup>1</sup>, Jean-François Lamarque<sup>1</sup>, Alfonso Saiz-Lopez<sup>4,1</sup>, Kathryn McKain<sup>7,8</sup>, Colm Sweeney<sup>8</sup>, Alan J.  
6 Hills<sup>1</sup>, and Eric C. Apel<sup>1</sup>

7 <sup>1</sup> National Center for Atmospheric Research, Boulder, Colorado, USA

8 <sup>2</sup> University of Michigan, Climate and Space Sciences and Engineering, Ann Arbor, Michigan, USA

9 <sup>3</sup> University of Redlands, Physics Department, Redlands, California, USA

10 <sup>4</sup> Department of Atmospheric Chemistry and Climate, Institute of Physical Chemistry Rocasolano, CSIC,  
11 Madrid, Spain

12 <sup>5</sup> Scripps Institution of Oceanography, University of California, San Diego, California, USA

13 <sup>6</sup> University of Miami, Department of Atmospheric Sciences, Miami, Florida, USA

14 <sup>7</sup> Cooperative Institute for Research in Environmental Sciences, University of Colorado, Boulder,  
15 Colorado, USA

16 <sup>8</sup> National Oceanic and Atmospheric Administration, Boulder, Colorado, USA  
17  
18

## 19 Abstract.

20 Fluxes of halogenated volatile organic compounds (HVOCs) over the Southern Ocean remain  
21 poorly understood, and few atmospheric measurements exist to constrain modeled emissions of  
22 these compounds. We present observations of  $\text{CHBr}_3$ ,  $\text{CH}_2\text{Br}_2$ ,  $\text{CH}_3\text{I}$ ,  $\text{CHClBr}_2$ ,  $\text{CHBrCl}_2$ , and  
23  $\text{CH}_3\text{Br}$  during the  $\text{O}_2/\text{N}_2$  Ratio and  $\text{CO}_2$  Airborne Southern Ocean (ORCAS) study and the 2<sup>nd</sup>  
24 Atmospheric Tomography mission (ATom-2), in January and February of 2016 and 2017. Good  
25 model-measurement correlations were obtained between these observations and simulations from  
26 the Community Earth System Model (CESM) atmospheric component with chemistry (CAM-  
27 Chem) for  $\text{CHBr}_3$ ,  $\text{CH}_2\text{Br}_2$ ,  $\text{CH}_3\text{I}$ , and  $\text{CHClBr}_2$  but all showed significant differences in  
28 model:measurement ratios. The model:measurement comparison for  $\text{CH}_3\text{Br}$  was satisfactory and  
29 for  $\text{CHBrCl}_2$  the low levels present precluded us from making a complete assessment.  
30 Thereafter, we demonstrate two novel approaches to estimate HVOC fluxes; the first approach  
31 takes advantage of the robust relationships that were found between airborne observations of  $\text{O}_2$   
32 and  $\text{CHBr}_3$ ,  $\text{CH}_2\text{Br}_2$ , and  $\text{CHClBr}_2$ ; we use these linear regressions with  $\text{O}_2$  and modeled  $\text{O}_2$   
33 distributions to infer a biological flux of HVOCs. The second approach uses the Stochastic  
34 Time-Inverted Lagrangian Transport (STILT) particle dispersion model to explore the  
35 relationships between observed mixing ratios and the product of the upstream surface influence  
36 and sea ice, chl *a*, absorption due to detritus, and downward shortwave radiation at the surface,  
37 which in turn relate to various regional hypothesized sources of HVOCs such as marine  
38 phytoplankton, phytoplankton in sea ice brines, and decomposing organic matter in surface  
39 seawater. These relationships can help evaluate the likelihood of particular HVOC sources, and  
40 in the case of statistically significant correlations, such as was found for  $\text{CH}_3\text{I}$ , may be used to  
41 derive an estimated flux field. Our results are consistent with a biogenic regional source of  
42  $\text{CHBr}_3$ , and both non-biological and biological sources of  $\text{CH}_3\text{I}$  over these regions.

43

## 44 1 Introduction

45 Emissions of halogenated volatile organic compounds (HVOCs) influence regional atmospheric  
46 chemistry and global climate. Through the production of reactive halogen radicals at high  
47 latitudes, HVOCs contribute to tropospheric and stratospheric ozone destruction, and alter the  
48 sulfur, mercury, nitrogen oxide and hydrogen oxide cycles (e.g. Schroeder et al., 1998; Boucher  
49 et al., 2003; Bloss et al., 2005; von Glasow and Crutzen; 2007; Saiz-Lopez et al., 2007; Obrist et  
50 al., 2011; WMO, 2018). In the marine boundary layer and lower troposphere, sea salt is the main  
51 source of reactive bromine (Finlayson-Pitts 1982, Simpson et al., 2015). Yet HVOCs may also  
52 be a more important source of inorganic bromine to the whole atmosphere than previously  
53 thought, according to a recent study, which indicates that sea salt is scarce and insufficient to  
54 control the bromine budget in the middle and upper troposphere (Murphy et al., 2019).

55 Phytoplankton and macroalgae in the ocean are the main sources to the atmosphere of several  
56 very short-lived bromocarbons, including bromoform ( $\text{CHBr}_3$ ), dibromomethane ( $\text{CH}_2\text{Br}_2$ ),  
57 dibromochloromethane ( $\text{CHClBr}_2$ ), and bromodichloromethane ( $\text{CHBrCl}_2$ ) (Moore et al., 1996;  
58 Carpenter et al. 2003; Butler et al., 2007; Raimund et al., 2011). Other HVOCs, such as methyl

Elizabeth Asher 7/5/2019 2:01 PM

Deleted: -side

Elizabeth Asher 7/5/2019 2:05 PM

Deleted: We show mixing ratio comparisons

Elizabeth Asher 7/6/2019 2:51 PM

Deleted: Thereafter, we

63 iodide (CH<sub>3</sub>I), and methyl bromide (CH<sub>3</sub>Br) have many natural sources, such as coastal  
64 macroalgae, phytoplankton, temperate forest soil and litter, and biomass burning (e.g., Bell et al.,  
65 2002; Sive et al., 2007; Colomb et al. 2008; Drewer et al., 2008). CH<sub>3</sub>I is also formed through  
66 non-biological reactions in surface seawater, and CH<sub>3</sub>Br is emitted as a result of quarantine and  
67 pre-shipment activities, which are not regulated by the Montreal Protocol (e.g., Moore and  
68 Zafiriou; 1994, WMO 2018). Over the Southern Ocean specifically, hypothesized sources of  
69 HVOCs include: coastal macroalgae, phytoplankton, sea ice algae, and photochemical or dust  
70 stimulated non-biological production at the sea surface (e.g., Abrahamsson et al. 2018, Manley  
71 and Dastoor 1998; Moore and Zafiriou 1994; Moore et al., 1996; Richter and Wallace 2004;  
72 Williams et al., 2007; Tokarczyk and Moore 1994; Sturges et al., 1992).

73 We largely owe our current understanding of marine HVOC emissions over the Southern Ocean  
74 to ship-based field campaigns and laboratory process studies (e.g., Abrahamsson et al. 2004a,b;  
75 Atkinson et al., 2012; Carpenter et al., 2007; Moore et al., 1996; Chuck et al., 2005; Butler et al.,  
76 2007; Raimund et al., 2011; Hughes et al., 2009; Mattsson et al. 2013; Hughes et al., 2013).  
77 These studies have reported surface water and sea-ice HVOC supersaturation and corresponding  
78 elevated levels of HVOCs in the marine boundary layer (MBL) in summer, and have identified  
79 numerous biological and non-biological ocean sources for these compounds. Mattsson et al.  
80 (2013) noted that the ocean also acts as a sink for HVOCs, when HVOC undersaturated surface  
81 waters equilibrate with air masses transported from source regions. The spatially heterogeneous  
82 ocean sources of CHBr<sub>3</sub> and CH<sub>2</sub>Br<sub>2</sub> at high latitudes in the Southern Hemisphere, are often  
83 underestimated in global atmospheric models (Hossaini et al., 2013; Ordoñez et al., 2012; Ziska  
84 et al., 2013). Ship-based and Lagrangian float observations provide invaluable information on  
85 the sources and temporal variability of compounds in the surface ocean. These methods offer the  
86 advantage of simultaneous measurements of both air and seawater to evaluate the gases'  
87 saturation state in the surface ocean and calculate fluxes. Yet ship-based measurements onboard  
88 these slow moving platforms also have drawbacks: they under sample the spatial variability of  
89 HVOCs (e.g., Butler et al., 2007) and require assumptions about gas-exchange rates to estimate  
90 fluxes.

91 To disentangle the roles of atmospheric transport and spatial variability of emissions on HVOC  
92 distributions requires large-scale atmospheric observations. At low latitudes, large-scale  
93 convection at the intertropical convergence zone carries bromocarbons and other HVOCs into  
94 the free troposphere and lower stratosphere (e.g., Liang et al., 2014; Navarro et al., 2015). Polar  
95 regions are characterized by stable boundary layers in summer. Wind shear, frontal systems, and  
96 internal gravity waves create turbulence and control vertical mixing within and across a stable  
97 polar boundary layer (e.g. Anderson et al., 2008), and small, convective plumes may form over  
98 the marginal sea ice zone, related to sea ice leads as well as winds from ice-covered to open-  
99 ocean waters (e.g. Schnell et al., 1989). As a result of limited vertical transport in these regions,  
100 however, air-sea fluxes lead to strong vertical gradients. Zonal transport from lower latitudes has  
101 a large impact on the vertical gradients of trace gas mixing ratios over polar regions (Salawitch  
102 2010). Given their extended photochemical lifetimes at high latitudes (see Sect. 2.3 for a brief  
103 discussion), many HVOC distributions are particularly sensitive to zonal transport at altitude.

Elizabeth Asher 7/7/2019 9:48 AM

Deleted: the

Elizabeth Asher 7/7/2019 9:49 AM

Deleted: ,

106 Aircraft observations can rapidly map basin-wide vertical distributions, support quantitative flux  
107 estimates, and provide spatial constraints to atmospheric models (e.g. Xiang et al., 2010;  
108 Stephens et al., 2018; Wofsy et al., 2011). Few airborne observations of HVOCs exist at high  
109 latitudes in the Southern Hemisphere. Two earlier aircraft campaigns that have measured  
110 summertime HVOCs in this region are the first Aerosol Characterization Experiment (ACE-1;  
111 Bates et al., 1999) and the first High-performance Instrumented Airborne Platform for  
112 Environmental Research (HIAPER) Pole-to-Pole Observations (HIPPO; Wofsy, 2011)  
113 campaign. For these two aircraft campaigns, whole air samples were collected onboard the  
114 NSF/NCAR C-130 and the NSF/NCAR Gulfstream V (GV) during latitudinal transects over the  
115 Pacific Ocean as far south as 60° S and 67° S, respectively. However, the ACE-1 and HIPPO  
116 campaigns obtained relatively few whole air samples in this region, with ≤100 samples poleward  
117 of 60° S combined (e.g., Blake et al., 1999; Hossaini et al., 2013). ACE-1 measurements of CH<sub>3</sub>I  
118 in the MBL indicate a strong ocean source between 40° S and 50° S in austral summer, with  
119 mixing ratios above 1.2 pmol below ~1 km (Blake et al., 1999).

Elizabeth Asher 6/16/2019 4:20 PM

Deleted: air-sea

120 HVOC emissions are frequently incorporated into earth system models, using either  
121 climatologies or parameterizations based on satellite observations of chlorophyll and  
122 geographical region and evaluated using mixing ratio comparisons with airborne observations. In  
123 Section 3.1 and 3.2, we report new airborne observations of CHBr<sub>3</sub>, CH<sub>2</sub>Br<sub>2</sub>, CH<sub>3</sub>I, CHClBr<sub>2</sub>,  
124 CHBrCl<sub>2</sub>, and CH<sub>3</sub>Br from high latitudes in the Southern Hemisphere, where data are scarce, and  
125 large-scale regional mixing ratio comparisons for HVOCs with the community earth system  
126 model (CESM) atmospheric component with chemistry (CAM-Chem). In section 3.4, we  
127 present two novel approaches to estimate regional fluxes of HVOCs for comparison with global  
128 climate models' parameterizations or climatologies. One approach uses correlations of HVOCs  
129 to marine, oxygen (O<sub>2</sub>) of marine origin, as measured by deviations in the ratio of O<sub>2</sub> to nitrogen  
130 (N<sub>2</sub>) (δ(O<sub>2</sub>/N<sub>2</sub>) see Sect. 2.1.2 and 3.1.2). We exploit robust ratios of HVOCs to oxygen (O<sub>2</sub>)  
131 determined from linear regressions (i.e. the enrichment ratio), and the ocean flux of O<sub>2</sub> from  
132 CESM's ocean component, to estimate the marine biogenic flux of several HVOCs. The second  
133 approach relies on observed HVOC mixing ratios, the Stochastic Time-Inverted Lagrangian  
134 Transport (STILT) particle dispersion model and geophysical datasets (see Sect. 2.3 and 3.3).  
135 We assess contributions from previously hypothesized regional sources for the Southern Ocean,  
136 and estimate HVOC fluxes based on regressions between upstream influences and observed  
137 mixing ratios and distributions of remotely sensed data.

Elizabeth Asher 7/7/2019 10:08 AM

Deleted: climate

## 139 2 Methods

### 140 2.1 Measurements

141 Atmospheric measurements for this study were collected at high latitudes in the Southern  
142 Hemisphere as part of the O<sub>2</sub>/N<sub>2</sub> Ratio and CO<sub>2</sub> Airborne Southern Ocean (ORCAS) study  
143 (Stephens et al., 2018), and the second NASA Atmospheric Tomography Mission (ATom-2),  
144 near Punta Arenas, Chile (Fig. 1). The ORCAS field campaign took place from Jan. 15 – Feb.  
145 29, 2016 onboard the NSF/NCAR GV. On Feb. 10 and 13, 2017 the sixth and seventh ATom-2  
146 research flights passed over the eastern Pacific sector poleward of 60° S (defined here as Region

Elizabeth Asher 7/5/2019 2:13 PM

Deleted: Observations

Elizabeth Asher 7/5/2019 2:13 PM

Deleted: Overview



151 | 1) and over the Patagonian Shelf between 40° S and 55° S and between 70° W and 50° W  
152 | (defined here as Region 2), respectively. The two regions for this study are defined based  
153 | loosely on dynamic biogeochemical provinces identified using bathymetry, algal biomass, sea  
154 | surface temperature and salinity (Reygondeau et al., 2013).

155 | Both projects featured en route vertical profiling from near the ocean surface (~ 150 m) to the  
156 | upper-troposphere, with 74 ORCAS and seven ATom-2 (during the sixth and seventh flights)  
157 | low-altitude level legs in the MBL. These campaigns shared a number of instruments, including  
158 | the NCAR Trace Gas Organic Analyzer (TOGA), the NCAR Atmospheric Oxygen (AO2)  
159 | instrument, a Picarro cavity ringdown spectrometer operated by NOAA, discussed below. More  
160 | information about individual instruments may be found in Stephens et al., 2018 and at  
161 | [https://www.eol.ucar.edu/field\\_projects/orcas](https://www.eol.ucar.edu/field_projects/orcas) and <https://espo.nasa.gov/atom/content/ATom>.

162

### 163 | 2.1.1 Halogenated VOCs

164 | During ORCAS and ATom-2 TOGA provided mixing ratios of over 60 organic compounds,  
165 | including HVOCs. The instrument, described in Apel et al. (2015), continuously collects and  
166 | analyzes samples for  $\text{CHBr}_3$ ,  $\text{CH}_2\text{Br}_2$ ,  $\text{CHClBr}_2$ ,  $\text{CHBrCl}_2$ , and  $\text{CH}_3\text{I}$  among other compounds,  
167 | with a 35-second sampling period and repeats the cycle every two-minutes using online fast gas  
168 | chromatography and mass spectrometry. This study also leverages measurements of  $\text{CH}_3\text{Br}$  from  
169 | whole air samples from the U. Miami / NCAR Advanced Whole Air Sampler (AWAS;  
170 | Schauffler et al., 1999) onboard the GV during the ORCAS campaign and the UC Irvine Whole  
171 | Air Sampler (WAS; Blake et al., 2001) onboard the DC-8 during the ATom-2 campaign.  
172 | HVOCs reported here have an overall  $\pm 15\%$  accuracy and  $\pm 3\%$  relative precision, and detection  
173 | limits of 0.03 ppt for  $\text{CH}_3\text{I}$ , 0.2 ppt for  $\text{CHBr}_3$ , 0.03 ppt for  $\text{CH}_2\text{Br}_2$ , 0.03 ppt for  $\text{CHClBr}_2$ , 0.05  
174 | ppt for  $\text{CHBrCl}_2$ , and 0.2 ppt for  $\text{CH}_3\text{Br} - 0.2$  ppt. In addition, comparisons between onboard  
175 | collected whole air samples and in-flight TOGA measurements, when sharing over half of their  
176 | sampling period with TOGA measurements, showed good correlations for  $\text{CHBr}_3$ ,  $\text{CH}_2\text{Br}_2$ ,  $\text{CH}_3\text{I}$ ,  
177 | and  $\text{CHClBr}_2$ , although there were some calibration differences (Fig. S1 and Fig. S2). In  
178 | addition to the comparison between co-located atmospheric measurements, we also conducted a  
179 | lab inter-comparison following the campaign between NOAA's programmable flask package  
180 | (PFP) and TOGA (Table S1; see supplement for details).

181

### 182 | 2.1.2 $\delta(\text{O}_2/\text{N}_2)$ and $\text{CO}_2$

183 | The AO2 instrument measures variations in atmospheric  $\text{O}_2$ , which are reported as relative  
184 | deviations in the oxygen to nitrogen ratio ( $\delta(\text{O}_2/\text{N}_2)$ ), following a dilution correction for  $\text{CO}_2$   
185 | (Keeling et al., 1998; Stephens et al., 2018). The instrument's precision is  $\pm 2$  per meg units (one  
186 | in one million relative) for a 5 second measurement (Stephens et al., 2003; Stephens et al.,  
187 | manuscript in preparation, 2019). Anthropogenic, biogenic, and oceanic processes introduce  $\text{O}_2$   
188 | perturbations that are superimposed on the background concentrations of  $\text{O}_2$  in air ( $X\text{O}_2$ , in dry  
189 | air = 0.2095). Air-sea  $\text{O}_2$  fluxes are driven by both biological production and consumption of  $\text{O}_2$

Elizabeth Asher 6/16/2019 1:28 PM

Deleted: t

Elizabeth Asher 7/7/2019 10:48 AM

Deleted: 2

Elizabeth Asher 7/5/2019 2:14 PM

Deleted: , at background levels

Elizabeth Asher 7/8/2019 5:29 PM

Deleted: The instrument, described in  
Apel et al. (2015), continuously collects and  
analyzes samples

Elizabeth Asher 7/8/2019 5:29 PM

Deleted:

Elizabeth Asher 7/7/2019 11:02 AM

Formatted: Font:Italic

Elizabeth Asher 8/4/2019 2:03 PM

Deleted: 3

Elizabeth Asher 7/7/2019 11:03 AM

Formatted: Subscript

and by heating and cooling of surface waters. O<sub>2</sub> is consumed when fossil fuels are burned and produced and consumed during terrestrial photosynthesis and respiration. Seasonal changes in the ocean heat content lead to small changes in atmospheric N<sub>2</sub>. As others have done, we isolated the air-sea O<sub>2</sub> signal by subtracting model estimates of the terrestrial O<sub>2</sub>, fossil-fuel O<sub>2</sub>, and air-sea N<sub>2</sub> flux influences from the δ(O<sub>2</sub>/N<sub>2</sub>) measurements (Equation 1; Keeling et al., 1998; Garcia and Keeling, 2001; Stephens et al., 2018). The difference of the δ(O<sub>2</sub>/N<sub>2</sub>) measurement and these modeled components is multiplied by XO<sub>2</sub> to convert to ppm equivalents as needed (ppm eq; Keeling et al., 1998; Equation 1).

$$O_{2\text{-ppm-equiv}} = [\delta(O_2/N_2) - \delta(O_2/N_2)_{\text{Land}} - \delta(O_2/N_2)_{\text{Fossil Fuel}} - \delta(O_2/N_2)_{N_2}] \times XO_2 \quad (1)$$

We obtained the modeled δ(O<sub>2</sub>/N<sub>2</sub>) signal terrestrial influences from the land model component of the CESM, the fossil fuel combustion influences from the Carbon Dioxide Information Analysis Center (CDIAC; Boden et al. 2017), and the air-sea N<sub>2</sub> influences from the oceanic component of CESM. These fluxes were all advected through the specified dynamics version of CESM's atmosphere component, as described below in Sect. 2.2 and in Stephens et al. (2018).

CO<sub>2</sub> measurements were provided by NOAA's Picarro G2401-m cavity ring down spectrometer modified to have a ~1.2 sec measurement interval and a lower cell pressure of 80 Torr, which enabled the instrument to function at the full range of GV altitudes. (McKain et al. manuscript in preparation, 2019). Dry-air mole fractions were calculated using empirical corrections to account for dilution and pressure broadening effects as determined in the laboratory before and after the campaign deployments, and in-flight calibrations were used to determine an offset correction for each flight. Corrected CO<sub>2</sub> data have a total average uncertainty of 0.07 ppm (McKain et al. manuscript in preparation, 2019). To merge them with the TOGA data, these faster O<sub>2</sub> and CO<sub>2</sub> measurements were arithmetically averaged over TOGA's 35-s sampling periods (Stephens et al., 2017 and <https://espo.nasa.gov/atom/content/ATom>).

## 2.2 CAM-Chem model configuration

The CESM version 1, atmospheric component with chemistry (CAM-Chem) is a global three-dimensional chemistry climate model that extends from the Earth's surface to the stratopause. CAM-Chem version 1.2 includes all the physical parameterizations of Neale et al. (2013) and a finite volume dynamical core (Lin, 2004) for tracer advection. The model has a horizontal resolution of 0.9° latitude × 1.25° longitude, with 56 vertical hybrid levels and a time-step of 30 minutes. Meteorology is specified using the NASA Global Modeling and Assimilation Office (GMAO) Goddard Earth Observing System Model, version 5 (GEOS-5; Rienecker et al., 2008) (GEOS-5), following the specified dynamic procedure described by Lamarque et al. (2012). Winds, temperatures, surface pressure, surface stress, and latent and sensible heat fluxes are nudged using a 5-hour relaxation timescale to GEOS-5 1° × 1° meteorology. The sea surface temperature boundary condition is derived from the Merged Hadley-NOAA Optimal Interpolation Sea Surface Temperature and Sea-Ice Concentration product (Hurrell et al., 2008). The model uses chemistry described by Tilmes et al. (2016), biomass burning and biogenic

Elizabeth Asher 6/16/2019 1:28 PM

Deleted: (Keeling et al., 1998; Garcia and Keeling, 2001; Stephens et al., 2018)

Elizabeth Asher 7/7/2019 11:04 AM

Deleted: photosynthesis

Elizabeth Asher 7/7/2019 11:04 AM

Deleted: combustion

Elizabeth Asher 7/7/2019 11:04 AM

Formatted: Subscript

Elizabeth Asher 7/7/2019 11:04 AM

Formatted: Subscript

Elizabeth Asher 7/7/2019 11:05 AM

Deleted: values

Elizabeth Asher 7/8/2019 5:30 PM

Deleted: .

Elizabeth Asher 7/7/2019 11:05 AM

Deleted: land

Elizabeth Asher 7/7/2019 11:09 AM

Deleted: Community Earth System (

Elizabeth Asher 7/7/2019 11:09 AM

Deleted: )

Elizabeth Asher 7/7/2019 11:11 AM

Deleted: 3.1

Elizabeth Asher 8/4/2019 2:04 PM

Deleted: The XO<sub>2</sub> in 2016 is the Tohjima et al. (2005) value from the year 2000 adjusted for the 4 ppm yr<sup>-1</sup> or ~20 per meg yr<sup>-1</sup> decrease in O<sub>2</sub> between 2000 and 2016.

Elizabeth Asher 7/7/2019 11:11 AM

Deleted: ., in prep., 2019

Elizabeth Asher 7/8/2019 5:30 PM

Deleted: in prep.

emissions from the Fire INventory of NCAR (FINN; Wiedinmyer et al., 2011) and MEGAN (Model of Emissions of Gasses and Aerosols from Nature) 2.1 products (Guenther et al., 2012) and additional tropospheric halogen chemistry described in Fernandez et al. (2014) and Saiz-Lopez et al. (2014). These include ocean emissions of  $\text{CHBr}_3$ ,  $\text{CH}_2\text{Br}_2$ ,  $\text{CHBr}_2\text{Cl}$ , and  $\text{CHBrCl}_2$ , with parameterized emissions based on chlorophyll *a* (*chl a*) concentrations and scaled by a factor of 2.5 over coastal regions, as opposed to open ocean regions (Ordoñez et al., 2012). The model used an existing  $\text{CH}_3\text{I}$  flux climatology (Bell et al., 2002), and  $\text{CH}_3\text{Br}$  was constrained to a surface lower boundary condition, also described by Ordoñez et al. (2012). This version of the model was run for the period of the ORCAS field campaign (January and February 2016), following a 24-month spin-up. To facilitate comparisons to ORCAS observations, output included vertical profiles of modeled constituents from the two nearest latitude and two nearest longitude model grid-points (four profiles in total) to the airborne observations at every 30-min model time-step. Following the run, simulated constituent distributions were linearly interpolated to the altitude, latitude and longitude along the flight track, yielding co-located modeled constituents and airborne observations. This version of the model has not yet been run for the ATom-2 period.

### 2.3 STILT model configuration

The Stochastic Time-Inverted Lagrangian Transport (STILT; Lin et al., 2003) particle dispersion model uses a receptor oriented framework to infer surface sources or sinks of trace gases from atmospheric observations collected downstream, thus simulating the upstream influences that are ultimately measured at the receptor site. The model tracks ensembles of particle trajectories backward in time and the resulting distributions of these particles can be used to define surface influence maps for each observation. STILT was run using 0.5° Global Data Assimilation System (GDAS) reanalysis winds to investigate the transport history of air sampled along the flight track (Stephens et al., 2018). For each TOGA observation, an ensemble of 4,096 particles was released from the sampling location and followed over a backwards simulation period of seven days. Particles in the lower half of the simulated MBL are assigned a surface influence value, which quantitatively links observed mixing ratios to surface sources (Lin et al., 2003). The average surface influence of all 4,096 particles per sampling location yields an hourly and spatially gridded surface influence value ( $\text{ppt m}^2 \text{ s pmol}^{-1}$ ) at a spatial resolution of  $0.25^\circ \times 0.25^\circ$  for each sample point.

Uncertainty in the surface influence value is strongly influenced by the accuracy of the underlying meteorological transport, as discussed in Xiang et al. (2010). We evaluated the GDAS reanalysis winds by comparing model winds interpolated in space and averaged between corresponding time points and pressure levels to match aircraft observations. By evaluating observed winds compared with modeled winds along the flight tracks we can estimate uncertainty in the surface influence values. We consider the observation-model differences in both wind speed and direction to approximate errors in surface influence strength and location. For wind speed, a small bias may be present, where we find a median difference between observations and reanalysis of 0.68 m/s, a 5% relative bias. The 1-sigma of the wind speed

difference is 2.3 m/s, corresponding to a 19% 1-sigma uncertainty in wind speed. In its simplest approximation, the surface influence strength error is perfectly correlated with the wind speed error, and thus we take 19% as an approximation of the surface influence strength uncertainty. The uncertainty in surface influence location depends on the error in the wind direction. We find a 1-sigma error of 14 degrees in wind speed, which corresponds to a possible error of 260 km/day.

Finally, we note that photochemical loss during transport is not accounted for in this analysis. Low OH mixing ratios, cold temperatures, and lower photolysis rates due to angled sunlight at high latitudes lead to longer than average HVOC lifetimes. For instance, assuming an average diurnal OH concentration of 0.03 ppt, and average photochemical loss according to the Tropospheric Ultraviolet and Visible (TUV) radiation model and the Mainz Spectral data site ([http://satellite.mpic.de/spectral\\_atlas](http://satellite.mpic.de/spectral_atlas)) for Jan. 29 under clear sky conditions at 60° S,  $\text{CHBr}_3$  has a lifetime of 30 days,  $\text{CH}_2\text{Br}_2$  has a lifetime of 270 days,  $\text{CH}_3\text{I}$  has a lifetime of 7 days, and  $\text{CHClBr}_2$  has a lifetime of 63 days. As such, the photochemical lifetimes of these gases are greater than or equal to the time of our back-trajectory analysis. Moreover, OH concentrations in this region have large uncertainties, the inclusion of which would lead to more, not less, uncertainty in surface influence based regression coefficients and estimated fluxes (see Sect. 2.3 and 3.3 for details).

### 2.3.1 STILT surface influence functions

For this study, we used STILT surface influence distributions with remotely sensed ocean surface and reanalysis data (i.e. surface source fields) in linear and multi-linear regressions to generate empirical STILT influence functions. Surface influence functions can help explain observed mixing ratios of  $\text{CHBr}_3$ ,  $\text{CH}_2\text{Br}_2$ ,  $\text{CH}_3\text{Br}$  and  $\text{CH}_3\text{I}$ , evaluate the likelihood of particular HVOC sources, and in the case of statistically significant correlations, may be used to derive an estimated flux field (See Sect. 3.3 and 3.4.2 for details).

We tested whether observed mixing ratios ( $Z$ ) could be explained by a linear relationship in which the predictor variable is a surface influence function, equal to the product of the surface influence ( $H$ ) and a potential geophysical surface source field(s), such as chl  $a$ , as well as an intercept ( $b$ ), a slope ( $a$ ), and error term  $\xi$  (Equation 2; Fig. S5). This relationship can be generalized as a multiple linear regression with multiple surface influence functions ( $H_{s_1}, H_{s_2}, \dots$ ) and slope coefficients ( $a_1, a_2$ ; Equation 3), when multiple sources contribute to observed HVOC mixing ratios. The multiple linear regression may also include an interaction term ( $H_{s_1 s_2}$ ) between predictor variables (e.g.  $H_{s_1}$  and  $H_{s_2}$ ) with a slope coefficient ( $a_3$ ) to improve the fit. Statistical correlations between mixing ratios and surface influence functions may be used to support or reject hypothesized sources. A flux ( $\mu\text{mol m}^{-2} \text{s}^{-1}$ ) may then be estimated for each grid cell based on the product of the slopes ( $a_1, a_2, \dots$ ) and the potential source fields ( $s_1, s_2, \dots$ ). Grid cell fluxes are averaged over a geographical region to yield the average regional flux. We used the standard deviation of the regression coefficients and the relative uncertainty in the surface source, added in quadrature, to estimate the uncertainty in the flux (see Sect. 3.4.2 for fractional uncertainties).

336 We note that the uncertainty in STILT transport (see Sect. 2.3 for details) is inherently reflected  
337 in the relative uncertainty of the regression coefficients ( $a_1, a_2, \dots$ ).

338 
$$Z = aHs + b + \xi \text{ _____} \quad (2)$$

339 
$$Z = a_1Hs_1 + a_2Hs_2 + (a_3Hs_1Hs_2) \dots + b + \xi \text{ _____} \quad (3)$$

340

### 341 2.3.2 Surface Source Fields

342 Geophysical surface source fields of remotely sensed and reanalysis data included a combination  
343 of sea ice concentration, chl *a*, absorption due to ocean detrital material, and downward  
344 shortwave radiation at the ocean surface.

345 We used daily sea ice concentration data (<https://nsidc.org/data/nsidc-0081>) at a 25 km x 25 km  
346 spatial resolution between 39.23° S and 90° S, 180° W – 180° E from the NASA National Snow  
347 and Ice Data Center Distributed Active Archive Center (NSIDC; Maslanik et al., 1999). This  
348 data reports the fraction of sea-ice cover, land-ice cover, and open water. Unfortunately, these  
349 data do not provide any information on sea ice thickness, or the presence of brine channels or  
350 melt ponds, which may modulate emissions from sea-ice covered regions. Sea ice concentration  
351 data were calculated using measurements of near-real-time passive microwave brightness  
352 temperature from the Special Sensor Microwave Image/Sounder (SSMIS) on the Defense  
353 Meteorological Satellite Program (DMSP) satellites. NSIDC sea ice concentration data were  
354 arithmetically averaged to yield 0.25° x 0.25° binned sea ice fraction for use with gridded surface  
355 influences.

356 Due to persistent cloud cover over the Southern Ocean, which often precludes the retrieval of  
357 remotely sensed ocean color data, we used 8-day mean composite Aqua MODIS L3 distributions  
358 of chl *a* from the Ocean Color Index (OCI) algorithm and absorption due to gelbstoff and detrital  
359 material at 443 nm from the Generalized Inherent Optical Properties (GIOP) model (NASA  
360 Goddard Space Flight Center, 2014). Absorption due to gelbstoff and detrital material at 443 nm  
361 is used as a proxy for colored dissolved organic matter (CDOM;  
362 <https://oceancolor.gsfc.nasa.gov/atbd/giop/>). CDOM is hypothesized to be an important source of  
363 carbon for the photochemical production of CH<sub>3</sub>I (Moore et al., 1994). The GIOP model also  
364 publishes an uncertainty in the absorption due to gelbstoff and detrital material at 443 nm. Raw  
365 4 km x 4 km data were geometrically averaged, based on lognormal probability density  
366 functions, to a spatial resolution of 0.25° x 0.25° for use with gridded surface influences. We  
367 used the ratio of the 0.25° x 0.25° gridded uncertainty in the detrital material absorption to the  
368 absorption as the relative uncertainty for flux calculations (see Sect. 3.4.2).

369 The National Center for Environmental Prediction (NCEP) provides Final Global Data  
370 Assimilation System (GDAS/FNL) global data of downward shortwave radiation at the surface  
371 at 0.25 degree and 6-hour resolution (NCEP, 2015). We chose downward shortwave radiation  
372 for use with gridded surface influences because the photo-production of CH<sub>3</sub>I has been observed  
373 at all visible wavelengths (Moore et al., 1994). This reanalysis data is available at a higher

Elizabeth Asher 7/5/2019 2:55 PM

Formatted: Font:

temporal resolution and better spatial coverage than satellite retrievals of photosynthetically active radiation (PAR) or temperature.

### 3 Results and discussion

#### 3.1 Observed HVOC patterns and relationships

Zonal cross-sections of HVOC data collected on ORCAS and ATom-2 illustrate unprecedented spatial sampling across our study area between the surface and 12 km (Fig. 2). Above average mixing ratios of  $\text{CH}_3\text{I}$ ,  $\text{CHBr}_3$ , and  $\text{CHClBr}_2$  typically remain confined to the lower ~2-4 km of the atmosphere (Fig. 2a, b, d). These compounds have lifetimes of approximately two months or less. Conversely, weak sources and longer lifetimes ( $\geq 3$  months) may have contributed to similar concentrations of  $\text{CH}_2\text{Br}_2$  and  $\text{CHBrCl}_2$  throughout the troposphere and above average mixing ratios as high as 8 km (Fig. 2c, e). Unfortunately, the availability of data above the detection limit and absence of BL enhancements for  $\text{CHBrCl}_2$  preclude the identification of strong regional sources at this time. Meridional distributions also indicate lower latitude sources of  $\text{CH}_3\text{I}$  and  $\text{CH}_3\text{Br}$  ( $< 50^\circ \text{S}$ ), potentially resulting from terrestrial and anthropogenic contributions, and higher latitude sources ( $> 60^\circ \text{S}$ ) of  $\text{CHBr}_3$ ,  $\text{CH}_2\text{Br}_2$ , and  $\text{CHClBr}_2$  (Fig. 2a-d,f).

##### 3.1.1 Observed HVOC interrelationships

Across our study area in both 2016 and 2017, we found that  $\text{CHBr}_3$  and  $\text{CH}_2\text{Br}_2$  exhibit a consistent enhancement ratio with each other in the bottom 2 km of the atmosphere both in Region 1 and Region 2, which suggests that these bromocarbon fluxes are closely coupled. Previous studies have documented co-located source regions of  $\text{CHBr}_3$  and  $\text{CH}_2\text{Br}_2$  in the Southern Ocean (e.g. Hughes et al., 2009; Carpenter et al., 2000; Nightingale et al., 1995; Laturnus et al., 1996), and laboratory studies have demonstrated that phytoplankton and their associated bacteria cultures, including a cold water diatom isolated from coastal waters along the Antarctic Peninsula and common to the Southern Ocean, produce both  $\text{CHBr}_3$  and  $\text{CH}_2\text{Br}_2$  (Hughes et al., 2013; Tokarczyk and Moore 1994, Sturges et al., 1993). The non-linearity observed in ratios of these two gases at low  $\text{CHBr}_3$  may reflect the different rates of their production or loss in seawater, or possibly, the influence of air masses from distant, more productive low-latitude source regions. Several studies have documented bacterially mediated loss of  $\text{CH}_2\text{Br}_2$ , but not  $\text{CHBr}_3$ , and report distinct ratios of  $\text{CH}_2\text{Br}_2$  to  $\text{CHBr}_3$  in seawater during the growth and senescent phases of a phytoplankton bloom (e.g. Carpenter et al., 2009, Hughes et al., 2013). Although this analysis is restricted to the bottom 2 km of the atmosphere, zonal transport of air masses with lower ratios of  $\text{CH}_2\text{Br}_2$  to  $\text{CHBr}_3$  ratios, as have been observed in the MBL over productive, low-latitude regions, may also have influenced our observations (Yokouchi et al. 2005). Mixing ratios of  $\text{CHBr}_3$  and  $\text{CHClBr}_2$  were also correlated (Fig. 3d) in Region 2, and, a similar, weaker relationship was observed in Region 1 (Fig. 3b).  $\text{CHClBr}_2$  is a

Elizabeth Asher 7/7/2019 11:15 AM

Deleted: ,

Elizabeth Asher 7/7/2019 11:16 AM

Deleted: and d

Elizabeth Asher 7/7/2019 11:16 AM

Deleted: ( $\geq$

Elizabeth Asher 7/7/2019 11:16 AM

Deleted: -

Elizabeth Asher 7/7/2019 11:16 AM

Deleted:  $\leq$  -

Elizabeth Asher 7/7/2019 2:46 PM

Formatted: Font:Bold

Elizabeth Asher 7/8/2019 5:34 PM

Deleted: (Fig. 3a, c)



less well-studied compound than CH<sub>2</sub>Br<sub>2</sub>. Yet these consistent relationships suggest that CHBr<sub>3</sub> and CHClBr<sub>2</sub> may either share some of the same sources or have sources that co-vary.

420

### 3.1.2 Observed HVOC relationships to $\delta(\text{O}_2/\text{N}_2)$ and CO<sub>2</sub>

We sought to test if the biologically mediated production of bromocarbons and oxygen result in similar atmospheric distributions. Conversely, we expected HVOC atmospheric distributions and CO<sub>2</sub> distributions to anticorrelate because CO<sub>2</sub> fixation in surface waters is proportional to the production of oxygen.

For these comparisons, both O<sub>2</sub> and CO<sub>2</sub> mixing ratios from the upper troposphere (5-7 km) were subtracted from the data to detrend for seasonal and inter-annual variability (Fig. 4; Fig. S3). To isolate the contribution of ocean O<sub>2</sub> fluxes, the ORCAS  $\delta(\text{O}_2/\text{N}_2)$  values reported here represent the  $\Delta\delta(\text{O}_2/\text{N}_2)$  to observed values between 5-7 km adjusted for CESM O<sub>2</sub> land and fossil fuel contributions and the influence of air-sea N<sub>2</sub> fluxes. In Fig. 4 we present type II major axis regression fits to data (fits were calculated using data scaled to their full range) between the ocean surface and the lowest 7 km for bromocarbons with photochemical lifetimes of  $\geq 1$  month and from the lowest 2 km for CH<sub>3</sub>I with a photochemical lifetime of  $\sim 1$  week. We used a type II major axis regression model to balance the influences of uncorrelated processes and measurement uncertainty in HVOCs (on the y-axis) and uncorrelated processes and measurement uncertainty in O<sub>2</sub> and CO<sub>2</sub> (on the x-axis) on the regression slope (Ayers et al., 2001; Glover et al., 2011). As noted by previous studies, simple least squares linear regressions fail to account for uncertainties in predictor variables (e.g. Cantrell et al., 2008).

The robust correlations of CHBr<sub>3</sub> and CH<sub>2</sub>Br<sub>2</sub> with  $\delta(\text{O}_2/\text{N}_2)$ , in both 2016 and 2017 and in Region 1 and Region 2, provides support for a regional biogenic source of these two HVOCs (Fig. 4a, b and Fig. 4d, e). The air-sea exchange of O<sub>2</sub> during summer in the Southern Ocean is driven by net community production (the excess of photosynthesis over respiration) in the surface mixed layer, surface warming, and to a lesser extent ocean advection and mixing (e.g. Stephens et al., 1998; Tortell and Long 2009; Tortell et al., 2014). Note that we adjust for influences on the  $\delta(\text{O}_2/\text{N}_2)$  from thermal N<sub>2</sub> fluxes (see Equation 1, Sect. 2.1.2 for details). Biological O<sub>2</sub> supersaturation in the surface mixed layer develops quickly in the first several days of a phytoplankton bloom and diminishes as community respiration increases and air-sea gas exchange equilibrates the surface layer with the atmosphere on a timescale of  $\sim 1$  week. CHBr<sub>3</sub> and CH<sub>2</sub>Br<sub>2</sub> are emitted from phytoplankton during the exponential growth phase (Hughes et al., 2013), which often coincides with high net community production and the accumulation of O<sub>2</sub> in surface waters. The bulk air-sea equilibration time for an excess of CHBr<sub>3</sub> and other HVOCs is less than two weeks, although the photochemical loss of HVOCs will alter their ratio over time (see Supplement for details on calculations of bulk sea air equilibration times).

Our observations suggest a biological source for CHBr<sub>3</sub> and CH<sub>2</sub>Br<sub>2</sub> in both Region 1 and Region 2 (Fig. 4). Interestingly, the slope of the regression between CHBr<sub>3</sub> and O<sub>2</sub> appears distinct in Region 1 and Region 2, but between CH<sub>2</sub>Br<sub>2</sub> is the same. Molar enrichment ratios are  $0.20 \pm$

Elizabeth Asher 7/5/2019 2:24 PM

Deleted: 2.5

Elizabeth Asher 7/7/2019 11:17 AM

Deleted:

Elizabeth Asher 7/8/2019 5:43 PM

Deleted: (bivariate)

Elizabeth Asher 7/7/2019 11:28 AM

Deleted: the

Elizabeth Asher 7/7/2019 11:28 AM

Deleted: oxygen

Elizabeth Asher 7/7/2019 11:28 AM

Formatted: Subscript

Elizabeth Asher 7/7/2019 11:29 AM

Deleted: 3

Elizabeth Asher 7/7/2019 11:29 AM

Deleted: (

Elizabeth Asher 7/7/2019 11:29 AM

Deleted: ) is

0.01, and  $0.07 \pm 0.004$  pmol : mol for  $\text{CHBr}_3$  and  $\text{CH}_2\text{Br}_2$  to  $\text{O}_2$  in Region 1, and  $0.32 \pm 0.02$ , and  $0.07 \pm 0.004$  pmol : mol in Region 2. We observe a weaker relationship between  $\text{CH}_3\text{I}$  and  $\text{CHClBr}_2$  and  $\text{O}_2$  in Region 1 (Fig. 4c, d), consistent with the existence of other, non-biological sources of  $\text{CH}_3\text{I}$  in this region. Figure 4f illustrates a strong relationship between  $\text{CH}_3\text{I}$  and  $\text{O}_2$ , as well as  $\text{CHClBr}_2$  and  $\text{O}_2$ , in Region 2, however, which implies that the dominant sources of  $\text{CH}_3\text{I}$  and  $\text{CHClBr}_2$  emissions over the Patagonian Shelf are biological. The corresponding molar enrichment ratios of  $\text{CH}_3\text{I}$  to  $\text{O}_2$  and  $\text{CHClBr}_2$  to  $\text{O}_2$  in Region 2 are  $0.38 \pm 0.03$  pmol : mol and  $0.19 \pm 0.04$  pmol : mol, respectively.

In contrast to  $\text{O}_2$ , air-sea fluxes of  $\text{CO}_2$  over the Southern Ocean during summer reflect the balance of opposing thermal and biological drivers (e.g. Stephens et al., 1998; 2018). Ocean buffering chemistry results in  $\text{CO}_2$  equilibration across the air-sea interface on a timescale of several months. ORCAS observations showed a depletion of  $\text{CO}_2$  in the MBL, indicating that uptake driven by net photosynthesis dominated over thermally driven outgassing during the several months preceding the campaign (Stephens et al., 2018).  $\text{CHBr}_3$  and  $\text{CH}_2\text{Br}_2$  in the lowest 7 km were negatively correlated with  $\text{CO}_2$  in both years in Region 1 and Region 2 (Fig. S3a, b, d, e). Interestingly,  $\text{CH}_3\text{I}$  was not correlated with  $\text{CO}_2$  in Region 1, likely due to the long air-sea equilibration timescale of  $\text{CO}_2$  compared with a 9-day air-sea equilibration time and a  $\sim 7$ -day photochemical lifetime for  $\text{CH}_3\text{I}$ . For longer lived species, correlations for HVOCs to  $\text{CO}_2$  have similar  $r^2$ -values as those for HVOCs to  $\delta(\text{O}_2/\text{N}_2)$ , but model and climatological estimates of Southern Ocean  $\text{CO}_2$  fluxes are much less certain than for  $\text{O}_2$  (Anav et al., 2015; Nevison et al., 2016). As a result, we use modeled  $\text{O}_2$  fluxes as the basis for our HVOC flux estimates (see Sect. 3.4.1 for details).

488

### 3.2 Model-observation comparisons

The ORCAS dataset provides an exceptional opportunity to evaluate the CAM-Chem HVOC emission scheme (Ordoñez et al., 2012) at high latitudes in the Southern Hemisphere. We compared modeled HVOC constituents to corresponding observations along the ORCAS flight track (Fig. 5; Fig. 6). In these figures, we used type II major axis regression models to balance the measurement uncertainty (on the y-axis) and the inherent, yet difficult to quantify representativeness and errors in a global atmospheric chemistry model (on the x-axis). We note that this comparison may favor constituents with longer photochemical lifetimes, when transport and mixing dominate over source heterogeneity.

In Region 1 and Region 2, both the model and observations indicate that elevated mixing ratios of  $\text{CH}_3\text{I}$  remain confined to the MBL (Fig. 5a and Fig. 6a), presumably due to its relatively short photochemical lifetime. Modeled and observed  $\text{CH}_3\text{I}$  are poorly correlated in Region 1 ( $r^2 = 0.20$ ; Fig. 5b) and better correlated in Region 2 ( $r^2 = 0.70$ ; Fig. 6b). In both regions, the model underpredicts  $\text{CH}_3\text{I}$  in the upper troposphere and lower stratosphere (UTLS), likely stemming from the poleward transport of lower latitude air masses, where CAM-Chem also exhibits a negative bias. Mixing ratio comparisons with CAM-Chem over the tropics (see Figure 10 in Ordoñez et al., 2012) depict similar or larger discrepancies, and have been attributed to stronger

Elizabeth Asher 7/7/2019 11:31 AM

Deleted: s

Elizabeth Asher 7/8/2019 5:44 PM

Deleted:



than anticipated convective cells in the tropics. We found strong correlations and agreement to within a factor of ~2 between modeled and observed  $\text{CHBr}_3$  and  $\text{CH}_2\text{Br}_2$  (Fig. 5c-f and Fig. 6c-f). Relatively long lifetimes ( $\geq 1$  month) in Region 1 likely enable vertical and zonal transport of  $\text{CHBr}_3$  and  $\text{CH}_2\text{Br}_2$  to the mid and upper troposphere (Fig. 5c and e). The model was biased low with respect to measurements of  $\text{CH}_3\text{Br}$  by ~25% in Region 1 and Region 2 (Fig. 5g-h and Fig. 6g-h), potentially as a result of an incorrect surface lower boundary condition. The model underpredicted the mean vertical gradient in  $\text{CHClBr}_2$ , although it did a reasonable job of representing the mean vertical gradient in  $\text{CHBrCl}_2$ , in both Region 1 and Region 2. In both cases, however, the model failed to capture the spatial variability in both  $\text{CHClBr}_2$  and  $\text{CHBrCl}_2$  observations (Fig. 5i-l and Fig. 6i-l). Region 2 contains stronger sources of HVOCs than Region 1, which has been documented in numerous ship-based campaigns and archived in the Halocarbons in the Ocean and Atmosphere database (HalOcAt; <https://halocat.geomar.de/>). Region 2 also has much higher chl *a* (Fig. S4), supporting biogenic sources for these gases.

### 3.3 Relationships between STILT surface influence functions and observations

We used the STILT model to explore the relationships between observed mixing ratios and the upstream surface influence functions (Equations 2-3) of sea ice, chl *a*, absorption due to detritus, and downward shortwave radiation at the surface, which relate to various regional hypothesized sources of HVOCs such as marine phytoplankton, phytoplankton in sea ice brines, and decomposing organic matter in surface seawater (e.g. Moore and Zafiriou 1994; Moore et al., 1996; Tokarczyk and Moore 1994; Sturges et al., 1992).

We found no positive relationships between upstream sea-ice influence and any measured HVOC Region 1 (Fig. 7). We interpret this result to mean that increased summertime sea ice acts either to reduce the production of HVOCs by blocking sunlight or as a physical barrier to oceanic emissions of HVOCs from under-ice algae. Both of these mechanisms are also consistent with a link between enhanced  $\text{CHBr}_3$  and  $\text{CH}_2\text{Br}_2$  emissions due to sea-ice retreat and surface sea-ice melt water (Carpenter et al., 2007).

In other studies, it has also been proposed that sea ice could be an important source for  $\text{CHBr}_3$  and other HVOCs, since high mixing ratios of  $\text{CHBr}_3$  have been observed at the sea-ice and ice-snow interface in the austral winter (Abrahamsson et al., 2018) and in under-ice algae in the austral spring (Sturges et al., 1993). At present, CAM-Chem v1.2 with very short-lived halogen chemistry does not include a regional flux of HVOCs over sea-ice covered waters in summer, and our results do not indicate a need to include one. Our data, which were collected in January and February, however, cannot assess the importance of sea ice as a source of HVOCs in other seasons, such as winter or spring (Abrahamsson et al., 2018; Sturges et al., 1993). More field campaigns are needed to further study the seasonality and regional strength of sea ice related HVOC emissions.

Elizabeth Asher 7/7/2019 11:37 AM

Deleted:

Elizabeth Asher 7/7/2019 11:44 AM

Deleted: . High concentrations of  $\text{CHBr}_3$  have been linked to sea ice retreat

549 We observed a statistically significant positive correlation between the surface influence function  
 550 of 8-day satellite composites of chl *a* concentration, which is widely used as a proxy for near-  
 551 surface phytoplankton biomass, and mixing ratios of CHBr<sub>3</sub> and CH<sub>2</sub>Br<sub>2</sub> in Region 1 (Fig. 8a, b).  
 552 This finding corroborates previous findings from ship-borne field campaigns and laboratory  
 553 studies that have suggested a biogenic source for these two bromocarbons (e.g., Moore et al.,  
 554 1996; Hughes et al., 2013), and further substantiates the current CAM-Chem parameterization of  
 555 regional bromocarbon emissions using satellite retrievals of chl *a* in polar regions. CH<sub>3</sub>Br  
 556 mixing ratios were not significantly correlated with chl *a* surface influence functions (Fig. 8c).  
 557 Although potentially suggesting that marine phytoplankton and microalgae were not a strong  
 558 regional source of CH<sub>3</sub>Br during ORCAS, it is also possible that the relatively long lifetime of  
 559 CH<sub>3</sub>Br precludes a definitive analysis of its origin based on chl *a* using 7-day back-trajectories.  
 560 Neither CHClBr<sub>2</sub> nor CHBrCl<sub>2</sub> were significantly correlated with chl *a* composite surface  
 561 influence functions (data not shown); however, more observations of these short-lived species in  
 562 the remote MBL are needed to substantiate this result.

563 Similar to Lai et al. (2011), we observed a significant correlation between mixing ratios of CH<sub>3</sub>I  
 564 and total weekly upstream influence functions of 8-day chl *a* composites (Fig. 8d). Weaker  
 565 correlations were observed with upstream influence functions on shorter timescales than seven  
 566 days. We found that CH<sub>3</sub>I, particularly in Region 1, was better explained by a multi-linear  
 567 regression with two predictors: 1) the influence function of downward shortwave radiation at the  
 568 surface (Fig. 9a) and 2) the absorption of light due to detrital material (Fig. 9b), yielding  
 569 improved agreement between predicted and observed CH<sub>3</sub>I (Fig. 9c). Several previous studies  
 570 have correlated mixing ratios of CH<sub>3</sub>I to satellite retrievals of PAR and surface ocean  
 571 temperature, revealing a link to solar radiation (e.g. Happell et al., 1996; Yokouchi et al., 2001).

572 Although certain species of phytoplankton are capable of producing CH<sub>3</sub>I (e.g. Manley and de la  
 573 Cuesta 1997; Hughes et al., 2011), several studies also indicate a non-biological source for CH<sub>3</sub>I  
 574 in the surface ocean. This non-biological source, though not fully understood, requires light, a  
 575 humic like substance at the surface ocean supplying a carbon source and methyl group, and  
 576 reactive iodine (Moore and Zarifou 1994; Richter and Wallace 2004). Thus far, two chemical  
 577 mechanisms have been proposed for the non-biological production of methyl iodide, one – a  
 578 radical recombination of a methyl group and iodine involving UV photolysis (e.g. Moore and  
 579 Zarifou 1994), and two, a substitution reaction involving the reduction of an oxidant, such as iron  
 580 III (e.g. Williams et al. 2007).

## 581

### 582 3.4 Flux estimation

#### 583 3.4.1 O<sub>2</sub>-based emission estimates

584 We present a novel approach that facilitates a basin-wide HVOC flux estimate using the robust  
 585 relationship between airborne observations of O<sub>2</sub> and HVOCs combined with modeled O<sub>2</sub> fluxes.  
 586 Unlike the existing CAM-Chem HVOC biogenic flux parameterization, this method does not  
 587 rely on weekly retrievals of chl *a* at high latitudes, which are often patchy. In addition, our study

Elizabeth Asher 7/8/2019 3:54 PM

Deleted: footprints

Elizabeth Asher 7/7/2019 11:44 AM

Deleted: the

Elizabeth Asher 7/7/2019 11:44 AM

Deleted: and Fig. 8

Elizabeth Asher 7/8/2019 3:54 PM

Deleted: footprints

Elizabeth Asher 7/7/2019 11:44 AM

Deleted:

Elizabeth Asher 7/8/2019 3:55 PM

Deleted: footprints

Elizabeth Asher 8/4/2019 4:08 PM

Deleted:

Elizabeth Asher 8/4/2019 4:08 PM

Deleted: Several previous studies have correlated mixing ratios of CH<sub>3</sub>I to satellite retrievals of PAR and temperature (e.g. Happell et al., 1996; Yokouchi et al., 2001). We note that chl *a*, which is a proxy for living algal biomass, was correlated with CDOM in Region 1 and Region 2, ( $r^2 = 0.24$ ; data not shown).

603 indicates that  $\text{CHBr}_3$ ,  $\text{CH}_2\text{Br}_2$ , and  $\text{CHClBr}_2$  and  $\text{CH}_3\text{I}$  are better correlated with marine derived  
604  $\text{O}_2$  than the upstream influence of chl  $\alpha$ .

605 For  $\text{CHBr}_3$ ,  $\text{CH}_2\text{Br}_2$ , and  $\text{CHClBr}_2$  we construct ocean emission inventories for January and  
606 February using a scaled version of gridded modeled air-sea  $\text{O}_2$  fluxes and the slopes (i.e. molar  
607 ratios) of linear correlations between  $\delta(\text{O}_2/\text{N}_2)$  and HVOC mixing ratios (Fig. 10).  $\text{O}_2$  fluxes  
608 were obtained from simulations using a configuration of the CESM model nudged to reanalysis  
609 temperatures and winds as described in Stephens et al. (2018). An earlier free running version of  
610 CESM was one of the best evaluated for reproducing the seasonal cycle of  $\delta(\text{O}_2/\text{N}_2)$  over the  
611 Southern Ocean (Nevinson et al., 2015; 2016). To date, the north-south gradient in atmospheric  
612  $\text{O}_2$  has not been well reproduced by any models (Resplandy et al., 2016). Vertical gradients in  $\text{O}_2$   
613 on ORCAS indicate that CESM overestimated gradients by 47% on average; accordingly,  $\text{O}_2$   
614 fluxes were adjusted downward by 47% to better match the observations. This is obviously a  
615 very simple adjustment to the modeled fluxes, and the actual air-sea  $\text{O}_2$  flux biases in CESM  
616 likely have a great deal of spatial and temporal heterogeneity. We calculated an uncertainty for  
617 the CESM flux using a second, independent estimate of  $\text{O}_2$  fluxes based on dissolved  $\text{O}_2$   
618 measurements in surface seawater. The Garcia and Keeling (2001) climatology has much  
619 smoother temporal and spatial patterns than CESM flux estimates but also results in  
620 overestimated atmospheric  $\text{O}_2$  spatial gradients. We calculate the relative uncertainty in  $\text{O}_2$  flux  
621 as the ratio of the mean absolute difference between gridded Garcia and Keeling values (2001;  
622 also adjusted down by 51 % everywhere to better match ORCAS observations) to the CESM  
623 model flux estimates in Regions 1 and 2 (adjusted down by 47% everywhere). These  
624 disagreements were 7.3 % and 3.4 % for Regions 1 and 2, respectively. Based on the ratios of  
625 HVOC to  $\text{O}_2$  mixing ratios in bivariate least squares regressions and these adjusted  $\text{O}_2$  fluxes, we  
626 estimate mean emissions of  $\text{CHBr}_3$  and  $\text{CH}_2\text{Br}_2$  in Region 1 and Region 2. Relative uncertainty  
627 in the slopes (i.e., the standard deviation of the slopes) from these regressions and the mean  
628 relative uncertainties in regional  $\text{O}_2$  fluxes were added in quadrature to yield uncertainties in  
629 calculated HVOC emission rates.

630  
631 Figure 10 shows the mean emissions for Jan. and Feb. of  $\text{CHBr}_3$ ,  $\text{CH}_2\text{Br}_2$ , and  $\text{CHClBr}_2$  in  
632 Region 1 and Region 2. Mean regional emissions of  $\text{CHBr}_3$  and  $\text{CH}_2\text{Br}_2$  and  $\text{CHClBr}_2$  are  $91 \pm 8$ ,  
633  $31 \pm 17$ , and  $11 \pm 4$   $\text{pmol m}^{-2} \text{hr}^{-1}$  in Region 1 and  $329 \pm 23$ ,  $69 \pm 5$ , and  $24 \pm 5$   $\text{pmol m}^{-2} \text{hr}^{-1}$  in  
634 Region 2 (Table 1). The mean flux of  $\text{CH}_3\text{I}$  in Region 2 is  $392 \pm 32$  (Table 1). Table 1 also lists  
635 the mean Jan. and Feb. CAM-Chem emissions from Region 1 and Region 2, as well as emissions  
636 from several other observational and modeling Antarctic polar studies. Our estimates fall within  
637 the range of these other studies, which span every month of the year and whose estimated fluxes  
638 range from negative (i.e. from the atmosphere into the ocean) to  $3500 \text{ pmol m}^{-2} \text{hr}^{-1}$   $\text{CHBr}_3$  in a  
639 coastal bay during its peak in primary production. CAM-Chem emissions for all species are  
640 significantly lower than our observationally derived values in Region 1, with the exception of  
641  $\text{CH}_3\text{I}$ . Conversely, CAM-Chem emissions are significantly higher than our estimated emissions  
642 in Region 2, with the exception of  $\text{CHClBr}_2$  in Region 1, which remains underpredicted by the

Elizabeth Asher 7/8/2019 5:45 PM

Deleted: to facilitate comparisons across regions and atmospheric models

Elizabeth Asher 7/7/2019 11:47 AM

Deleted:  $\text{O}_2/\text{N}_2$

Elizabeth Asher 7/7/2019 11:49 AM

Deleted: Region

Elizabeth Asher 7/7/2019 11:49 AM

Deleted: (7.3% in Region 1 and 3.4 % in Region 2)

Elizabeth Asher 7/7/2019 11:50 AM

Deleted: Antarctic polar

Elizabeth Asher 7/7/2019 11:50 AM

Deleted: biological

Elizabeth Asher 7/8/2019 5:46 PM

Deleted:

652 model (Table 1). We note that in Region 2, CAM-Chem fluxes of  $\text{CHBr}_3$  and  $\text{CH}_2\text{Br}_2$ , although  
653 still significantly different, are more similar to our estimated fluxes.

654

### 655 3.4.2 STILT-based emission estimates

656 Similar to our  $\text{O}_2$ -based emission estimates, we used the relationship between surface influence  
657 functions and  $\text{CH}_3\text{I}$  mixing ratios (Fig. 9) to predict a flux field in Region 1 (Fig. 11). We used a  
658 multiple linear regression ( $\pm 1$  standard deviations; Equation 2), where  $H_{s1}$  and  $H_{s2}$  are the  
659 downward shortwave radiation and detrital absorption surface influence functions, respectively,  
660 with an intercept  $b = 0.19 \pm 0.01$ , and influence coefficients  $a_1 = 3.7\text{E-}5 \pm 1.3\text{E-}5$ ,  $a_2 = 3.5 \pm 0.74$ ,  
661 and an interaction term with the coefficient  $a_3 = -5.2\text{E-}4 \pm 1.5\text{E-}4$  (Fig. 9c). These regression  
662 coefficients and interaction term were used to estimate an average non-biological flux of  $\text{CH}_3\text{I}$   
663 (Fig. 11; Table 1). This method could be used in place of the current Bell et al. (2002)  
664 climatology to update near weekly (~8 day) emissions of  $\text{CH}_3\text{I}$  in future versions of CAM-Chem.  
665 Our estimated mean  $\text{CH}_3\text{I}$  flux in Region 1 ( $35 \pm 29 \text{ pmol m}^{-2} \text{ hr}^{-1}$ ) is significantly lower than the  
666 current CAM-Chem estimated emissions (Table 1). As noted in Sect. 3.2, our observations of  
667  $\text{CH}_3\text{I}$  are also much lower than the modeled mixing ratios. As discussed above, the strong  
668 correlations between  $\text{CH}_3\text{I}$  and  $\text{O}_2$  in Region 2 also suggest a dominant biological source for this  
669 compound in this region. As a result, we have not used this relationship to parameterize a flux  
670 for  $\text{CH}_3\text{I}$  in Region 2 (see Sect. 3.1.2 and 3.4.1 for details). We note that although it would be  
671 possible to provide STILT-based emission estimates for other HVOCs (e.g.  $\text{CHBr}_3$  and  $\text{CH}_2\text{Br}_2$ ),  
672 the correlations these compounds were less strong with surface influence functions than those  
673 with  $\text{O}_2/\text{N}_2$ .

674

### 675 4 Conclusions

676 Our work combined TOGA and AWAS HVOC airborne observations from the ORCAS and  
677 ATom-2 campaigns, with coincident measurements of  $\text{O}_2$  and  $\text{CO}_2$ , geophysical datasets and  
678 numerical models, including the global atmospheric chemistry model CAM-Chem, and the  
679 Lagrangian transport model, STILT. We evaluated model predictions, calculated molar  
680 enrichment ratios, inferred regional sources, and provided novel means of parameterizing ocean  
681 fluxes. We found that the Southern Ocean MBL is enriched in HVOCs, but that these MBL  
682 enhancements are less pronounced at higher latitudes, i.e., poleward of  $60^\circ \text{ S}$  (Region 1) than  
683 over the productive Patagonian shelf (Region 2). Overall, our results indicated that the Southern  
684 Ocean is a moderate regional sources of  $\text{CHBr}_3$ ,  $\text{CH}_2\text{Br}_2$ , and  $\text{CH}_3\text{I}$ , and a weak source of  
685  $\text{CHClBr}_2$  and  $\text{CHBrCl}_2$  in January and February. Good model-measurement correlations were  
686 obtained between our observations and simulations from the Community Earth System Model  
687 (CESM) atmospheric component with chemistry (CAM-Chem) for  $\text{CHBr}_3$ ,  $\text{CH}_2\text{Br}_2$ ,  $\text{CH}_3\text{I}$ , and  
688  $\text{CHClBr}_2$  but all showed significant differences in model:measurement ratios. The  
689 model:measurement comparison for  $\text{CH}_3\text{Br}$  was satisfactory and for  $\text{CHBrCl}_2$  the low levels  
690 present precluded us from making a complete assessment.

691  $\text{CHBr}_3$  and  $\text{CH}_2\text{Br}_2$  exhibited strong and robust correlations with each other and with  $\text{O}_2$  and  
692 weaker but statistically significant correlations with the influence of chl  $a$ , which is a proxy for

Elizabeth Asher 7/7/2019 11:52 AM

Formatted: Subscript

Elizabeth Asher 7/7/2019 11:53 AM

Deleted: The shortwave radiation and detrital material influence function

Elizabeth Asher 7/7/2019 11:53 AM

Deleted: an

Elizabeth Asher 7/7/2019 11:53 AM

Deleted: from a multi-linear regression (Fig. 9)

Elizabeth Asher 7/7/2019 11:53 AM

Deleted: regional

Elizabeth Asher 7/7/2019 11:54 AM

Deleted: .

Elizabeth Asher 7/7/2019 11:55 AM

Formatted: Subscript

Elizabeth Asher 7/7/2019 11:55 AM

Formatted: Subscript

Elizabeth Asher 7/7/2019 11:55 AM

Formatted: Subscript

Elizabeth Asher 7/7/2019 11:55 AM

Deleted: 6

Elizabeth Asher 7/7/2019 11:56 AM

Deleted: climate model

Elizabeth Asher 7/8/2019 5:49 PM

Deleted: and

Elizabeth Asher 7/8/2019 5:49 PM

Deleted:

Elizabeth Asher 7/8/2019 5:49 PM

Deleted: in Region 1 (at higher latitudes) than in Region 2 over the productive Patagonian shelf

Elizabeth Asher 7/8/2019 5:50 PM

Deleted: poleward of  $60^\circ \text{ S}$  (Region 1) and Patagonian Shelf (Region 2) are

Elizabeth Asher 7/8/2019 5:50 PM

Deleted: s

Elizabeth Asher 7/8/2019 5:53 PM

Deleted:

711 phytoplankton biomass.  $\text{CHClBr}_2$  and  $\text{CHBr}_3$  were well correlated with one another, particularly  
 712 in Region 2. Together, these correlations suggested a biological source for these gases over the  
 713 Southern Ocean. We found that  $\text{CH}_3\text{I}$  mixing ratios in Region 1 were best correlated with a non-  
 714 biological surface influence function, although biogenic  $\text{CH}_3\text{I}$  emissions appear important in  
 715 Region 2.

716  
 717 Our flux estimates based on the relationship of HVOC mixing ratios to  $\text{O}_2$  and remotely sensed  
 718 parameters (for  $\text{CH}_3\text{I}$ ) were compared with those derived from global models and ship-based  
 719 studies (Table 1). Our emission estimates of  $\text{CHBr}_3$ ,  $\text{CH}_2\text{Br}_2$ , and  $\text{CHClBr}_2$  are significantly  
 720 higher than CAM-Chem's globally prescribed emissions in Region 1, where HVOC mixing  
 721 ratios are under predicted (Table 1; Fig. 5). Similarly, our estimate of  $\text{CHClBr}_2$  emissions is also  
 722 significantly higher than CAM-Chem's in Region 2, where  $\text{CHClBr}_2$  mixing ratios remained  
 723 underpredicted. Yet, to the best of our knowledge, CAM-Chem's global parameterization of  
 724 HVOC fluxes has not been compared with data at high latitudes. Indeed, our emission estimates  
 725 of  $\text{CHBr}_3$ ,  $\text{CH}_2\text{Br}_2$ ,  $\text{CH}_3\text{I}$  fall within a range of CAM-Chem's estimates (on the low end) and  
 726 most prior estimates based on either other models or localized studies using seawater-side  
 727 measurements from the Antarctic polar region in summer (on the high end). In the case of  $\text{CH}_3\text{I}$ ,  
 728 our estimated emissions suggest that the prescribed emissions in CAM-Chem may be too high in  
 729 Region 1 and Region 2. Our parameterizations of the  $\text{CH}_3\text{I}$  flux could be used to explore inter-  
 730 annual variability in emissions, which is not captured by the Bell et al. (2002)  $\text{CH}_3\text{I}$  climatology  
 731 currently employed in CAM-Chem.

732 To extend these relationships to year-round and global parameterizations for use in global  
 733 climate models, they must be studied using airborne observations in other seasons and regions.  
 734 These approaches may help parameterize emissions of new species that can be correlated with  
 735 surface influence functions or the biological production of oxygen or may improve existing  
 736 emissions, where persistent biases exist. Finally, future airborne observations of HVOCs have  
 737 the potential to further improve our understanding of air-sea flux rates and their drivers for these  
 738 chemically and climatically important gases over the Southern Ocean.

739 *Data Availability.* The ORCAS and ATom-2 datasets are publically available at  
 740 <https://doi.org/10.5065/D6SB445X> ; ([www.eol.ucar.edu/field\\_projects/orcas](http://www.eol.ucar.edu/field_projects/orcas)) and  
 741 <https://doi.org/10.3334/ORNLDAAAC/1581>.

742 *Author Contributions.* EA is responsible for the bulk of the conceptualization, formal analysis,  
 743 writing, review, and editing with contributions from all authors. BBS and ECA were  
 744 instrumental in the investigation and supervision related to this manuscript. RSH contributed to  
 745 the conceptualization, as well as the investigation and HVOC data curation for this project. BBS,  
 746 EJM, and RFK were responsible for the data curation of  $\delta(\text{O}_2/\text{N}_2)$  data and contributed to formal  
 747 analysis involving these data. MSHM along with EAK were responsible for STILT data curation  
 748 and formal analysis, and the conceptualization and formal analysis of SITLT-based geostatistical  
 749 influence functions and flux estimates were also informed by these two. DK, along with ST, JFL  
 750 and ASL were responsible for constructing CAM HVOC emissions and conducting CAM runs.  
 751 MCL was responsible for CESM simulations yielding  $\text{O}_2$  fluxes and comparing this product  
 752 alongside the Garcia and Keeling  $\text{O}_2$  climatology in CAM. KMC and CM were responsible for  
 753 the data curation of  $\text{CO}_2$  observations. AJH contributed to the investigation for HVOC data.

Elizabeth Asher 7/8/2019 5:53 PM

**Deleted:** CAM-Chem provided a good foundation for HVOC, particularly for  $\text{CHBr}_3$  and  $\text{CH}_2\text{Br}_2$  in Region 1 and Region 2. Conversely,  $\text{CHClBr}_2$  and  $\text{CHBrCl}_2$  were underestimated by a factor of two or three in the model, while  $\text{CH}_3\text{I}$  were overestimated by a factor of more than three, and airborne observations indicated that the CAM-Chem  $\text{CH}_3\text{Br}$  surface boundary condition may be too low by ~25%. ... [1]

Elizabeth Asher 7/8/2019 5:53 PM

**Formatted:** Subscript

Elizabeth Asher 7/8/2019 5:53 PM

**Deleted:** other airborne observations

Elizabeth Asher 7/8/2019 5:54 PM

**Deleted:** relatively well

Elizabeth Asher 7/7/2019 12:02 PM

**Deleted:** emission estimates of  $\text{CHBr}_3$ ,  $\text{CH}_2\text{Br}_2$ ,  $\text{CH}_3\text{I}$ , lower than most prior estimates from the Antarctic polar region in summer

Elizabeth Asher 7/7/2019 12:10 PM

**Deleted:** Nevertheless,

Elizabeth Asher 7/7/2019 12:10 PM

**Deleted:** t

Elizabeth Asher 7/7/2019 12:29 PM

**Deleted:**

Elizabeth Asher 7/7/2019 12:30 PM

**Deleted:**

Elizabeth Asher 7/7/2019 12:30 PM

**Deleted:** (

Elizabeth Asher 7/7/2019 12:31 PM

**Deleted:** )

Elizabeth Asher 7/7/2019 12:31 PM

**Deleted:** (

Elizabeth Asher 7/7/2019 12:31 PM

**Deleted:** )

Elizabeth Asher 7/7/2019 12:33 PM

**Deleted:**  $\text{O}_2/\text{N}_2$

779

780 *Acknowledgements.* We would like to thank the ORCAS and ATom-2 science teams and the  
781 NCAR Research Aviation Facility and NASA DC-8 pilots, technicians and mechanics for their  
782 support during the field campaigns. In addition, we appreciate the NCAR EOL staff who have  
783 facilitated computing and data archival. In particular, we thank Tim Newberger for his help in  
784 supporting the NOAA Picarro CO<sub>2</sub> observations and Andrew Watt for his help in supporting the  
785 AO2 O<sub>2</sub> observations. This work was made possible by grants from NSF Polar Programs  
786 (1501993, 1501997, 1501292, 1502301, 1543457), NSF Atmospheric Chemistry Grants  
787 1535364, 1623745, and 1623748 and NASA funding of the EVS2 Atmospheric Tomography  
788 (ATom) project, as well as the support of the NCAR Advanced Study Program (ASP)  
789 Postdoctoral Fellowship Program and computing support from Yellowstone, provided by  
790 NCAR's Computational and Information Systems Laboratory. The National Center for  
791 Atmospheric Research is sponsored by the National Science Foundation.

792



## 793 References

- 794 Abrahamsson, K., Lorén, A., Wulff, A. and Wängberg, S.-Å.: Air–sea exchange of halocarbons: the influence of  
 795 diurnal and regional variations and distribution of pigments, *Deep Sea Research Part II: Topical Studies in*  
 796 *Oceanography*, 51(22–24), 2789–2805, doi:10.1016/j.dsr2.2004.09.005, 2004a.
- 797 Abrahamsson, K., Bertilsson, S., Chierici, M., Fransson, A., Froneman, P. W., Lorén, A. and Pakhomov, E. A.:  
 798 Variations of biochemical parameters along a transect in the Southern Ocean, with special emphasis on volatile  
 799 halogenated organic compounds, *Deep Sea Research Part II: Topical Studies in Oceanography*, 51(22–24), 2745–  
 800 2756, doi:10.1016/j.dsr2.2004.09.004, 2004b.
- 801 Abrahamsson, K., Granfors, A., Ahnoff, M., Cuevas, C. A. and Saiz-Lopez, A.: Organic bromine compounds  
 802 produced in sea ice in Antarctic winter, *Nature Communications*, 9(1), doi:10.1038/s41467-018-07062-8, 2018.
- 803 Anav, A., Friedlingstein, P., Beer, C., Ciais, P., Harper, A., Jones, C., Murray-Tortarolo, G., Papale, D., Parazoo, N.  
 804 C., Peylin, P., Piao, S., Sitch, S., Viovy, N., Wiltshire, A. and Zhao, M.: Spatiotemporal patterns of terrestrial gross  
 805 primary production: A review: GPP Spatiotemporal Patterns, *Reviews of Geophysics*, 53(3), 785–818,  
 806 doi:10.1002/2015RG000483, 2015.
- 807 Apel, E.: ORCAS Trace Organic Gas Analyzer (TOGA) VOC Data. Version 1.0, [online] Available from:  
 808 <https://data.eol.ucar.edu/dataset/490.018> (Accessed 29 January 2019), 2017.
- 809 Apel, E. C., Hornbrook, R. S., Hills, A. J., Blake, N. J., Barth, M. C., Weinheimer, A., Cantrell, C., Rutledge, S. A.,  
 810 Basarab, B., Crawford, J., Diskin, G., Homeyer, C. R., Campos, T., Flocke, F., Fried, A., Blake, D. R., Brune, W.,  
 811 Pollack, I., Peischl, J., Ryerson, T., Wennberg, P. O., Crounse, J. D., Wisthaler, A., Mikoviny, T., Huey, G., Heikes,  
 812 B., O’Sullivan, D. and Riemer, D. D.: Upper tropospheric ozone production from lightning NO<sub>x</sub>-impacted  
 813 convection: Smoke ingestion case study from the DC3 campaign, *Journal of Geophysical Research: Atmospheres*,  
 814 120(6), 2505–2523, doi:10.1002/2014JD022121, 2015.
- 815 Atkinson, H. M., Huang, R.-J., Chance, R., Roscoe, H. K., Hughes, C., Davison, B., Schönhardt, A., Mahajan, A. S.,  
 816 Saiz-Lopez, A., Hoffmann, T. and Liss, P. S.: Iodine emissions from the sea ice of the Weddell Sea, *Atmospheric*  
 817 *Chemistry and Physics*, 12(22), 11229–11244, doi:10.5194/acp-12-11229-2012, 2012.
- 818 Atlas, E.: ORCAS Advanced Whole Air Sampler (AWAS) Data. Version 1.0, [online] Available from:  
 819 <https://data.eol.ucar.edu/dataset/490.027> (Accessed 29 January 2019), 2017.
- 820 Ayers, G. P.: Comment on regression analysis of air quality data, *Atmospheric Environment*, 35(13), 2423–2425,  
 821 doi:10.1016/S1352-2310(00)00527-6, 2001.
- 822 Bates, T. S.: Preface [to special section on First Aerosol Characterization Experiment (AGE 1)], *Journal of*  
 823 *Geophysical Research: Atmospheres*, 104(D17), 21645–21647, doi:10.1029/1999JD900365, 1999.
- 824 Bell, N., Hsu, L., Jacob, D. J., Schultz, M. G., Blake, D. R., Butler, J. H., King, D. B., Lobert, J. M. and Maier-  
 825 Reimer, E.: Methyl iodide: Atmospheric budget and use as a tracer of marine convection in global models:  
 826 GLOBAL ATMOSPHERIC METHYL IODIDE, *Journal of Geophysical Research: Atmospheres*, 107(D17), ACH  
 827 8–1–ACH 8–12, doi:10.1029/2001JD001151, 2002.
- 828 Blake, N. J., Blake, D. R., Wingenter, O. W., Sive, B. C., Kang, C. H., Thornton, D. C., Bandy, A. R., Atlas, E.,  
 829 Flocke, F., Harris, J. M. and Rowland, F. S.: Aircraft measurements of the latitudinal, vertical, and seasonal  
 830 variations of NMHCs, methyl nitrate, methyl halides, and DMS during the First Aerosol Characterization  
 831 Experiment (ACE 1), *Journal of Geophysical Research: Atmospheres*, 104(D17), 21803–21817,  
 832 doi:10.1029/1999JD900238, 1999.
- 833 Blei, E. and Heal, M. R.: Methyl bromide and methyl chloride fluxes from temperate forest litter, *Atmospheric*  
 834 *Environment*, 45(8), 1543–1547, doi:10.1016/j.atmosenv.2010.12.044, 2011.
- 835 [Bloss, W. J., J. D. Lee, G. P. Johnson, R. Sommariva, D. E. Heard, A. Saiz-Lopez, J. M. C. Plane, G. McFiggans,](#)  
 836 [M. Flynn, P. Williams, A. R. Rickard and Z. L. Fleming: Impact of halogen monoxide chemistry upon boundary](#)  
 837 [layer OH and HO<sub>2</sub> concentrations at a coastal site, \*Geophysical Research Letters\*, 32\(6\),](#)  
 838 [doi:10.1029/2004GL022084, 2005.](#)

839 |  
840 Boden, T., Andres, R. and Marland, G.: Global, Regional, and National Fossil-Fuel CO<sub>2</sub> Emissions (1751 - 2014)  
841 (V. 2017), [online] Available from: <https://www.osti.gov/servlets/purl/1389331/> (Accessed 25 November 2018),  
842 2017.

843 Boucher, O., Moulin, C., Belviso, S., Aumont, O., Bopp, L., Cosme, E., von Kuhlmann, R., Lawrence, M. G., Pham,  
844 M., Reddy, M. S., Sciare, J. and Venkataraman, C.: DMS atmospheric concentrations and sulphate aerosol indirect  
845 radiative forcing: a sensitivity study to the DMS source representation and oxidation, *Atmospheric Chemistry and*  
846 *Physics*, 3(1), 49–65, doi:10.5194/acp-3-49-2003, 2003.

847 Butler, J. H., King, D. B., Lobert, J. M., Montzka, S. A., Yvon-Lewis, S. A., Hall, B. D., Warwick, N. J., Mondeel,  
848 D. J., Aydin, M. and Elkins, J. W.: Oceanic distributions and emissions of short-lived halocarbons: OCEANIC  
849 EMISSIONS OF SHORT-LIVED HALOCARBONS, *Global Biogeochemical Cycles*, 21(1),  
850 doi:10.1029/2006GB002732, 2007.

851 Cantrell, C. A.: Technical Note: Review of methods for linear least-squares fitting of data and application to  
852 atmospheric chemistry problems, *Atmospheric Chemistry and Physics*, 8(17), 5477–5487, doi:10.5194/acp-8-5477-  
853 2008, 2008.

854 Carpenter, L. J., Liss, P. S. and Penkett, S. A.: Marine organohalogens in the atmosphere over the Atlantic and  
855 Southern Oceans: MARINE ORGANOHALOGENS IN THE ATMOSPHERE, *Journal of Geophysical Research:*  
856 *Atmospheres*, 108(D9), n/a–n/a, doi:10.1029/2002JD002769, 2003.

857 Carpenter, L. J., Wevill, D. J., Palmer, C. J. and Michels, J.: Depth profiles of volatile iodine and bromine-  
858 containing halocarbons in coastal Antarctic waters, *Marine Chemistry*, 103(3-4), 227–236,  
859 doi:10.1016/j.marchem.2006.08.003, 2007.

860 Carpenter, L. J., Jones, C. E., Dunk, R. M., Hornsby, K. E. and Woeltjen, J.: Air-sea fluxes of biogenic bromine  
861 from the tropical and North Atlantic Ocean, *Atmospheric Chemistry and Physics*, 9(5), 1805–1816,  
862 doi:10.5194/acp-9-1805-2009, 2009.

863 Chuck, A. L.: Oceanic distributions and air-sea fluxes of biogenic halocarbons in the open ocean, *Journal of*  
864 *Geophysical Research*, 110(C10), doi:10.1029/2004JC002741, 2005.

865 Colomb, A., Yassaa, N., Williams, J., Peeken, I. and Lochte, K.: Screening volatile organic compounds (VOCs)  
866 emissions from five marine phytoplankton species by head space gas chromatography/mass spectrometry (HS-  
867 GC/MS), *Journal of Environmental Monitoring*, 10(3), 325, doi:10.1039/b715312k, 2008.

868 Drewer, J., Heal, K. V., Smith, K. A. and Heal, M. R.: Methyl bromide emissions to the atmosphere from temperate  
869 woodland ecosystems, *Global Change Biology*, doi:10.1111/j.1365-2486.2008.01676.x, 2008.

870 Emmons, L. K., Walters, S., Hess, P. G., Lamarque, J.-F., Pfister, G. G., Fillmore, D., Granier, C., Guenther, A.,  
871 Kinnison, D., Laepple, T., Orlando, J., Tie, X., Tyndall, G., Wiedinmyer, C., Baughcum, S. L. and Kloster, S.:  
872 Description and evaluation of the Model for Ozone and Related chemical Tracers, version 4 (MOZART-4),  
873 *Geoscientific Model Development*, 3(1), 43–67, doi:10.5194/gmd-3-43-2010, 2010.

874 Fernandez, R. P., Salawitch, R. J., Kinnison, D. E., Lamarque, J.-F. and Saiz-Lopez, A.: Bromine partitioning in the  
875 tropical tropopause layer: implications for stratospheric injection, *Atmospheric Chemistry and Physics*, 14(24),  
876 13391–13410, doi:10.5194/acp-14-13391-2014, 2014.

877 Finlayson-Pitts, B. J.: The Tropospheric Chemistry of Sea Salt: A Molecular-Level View of the Chemistry of NaCl  
878 and NaBr, *Chemical Reviews*, 103(12), 4801–4822, doi:10.1021/cr020653t, 2003.

879 Garcia, H. E. and Keeling, R. F.: On the global oxygen anomaly and air-sea flux, *Journal of Geophysical Research:*  
880 *Oceans*, 106(C12), 31155–31166, doi:10.1029/1999JC000200, 2001.

881 Gent, P. R., Danabasoglu, G., Donner, L. J., Holland, M. M., Hunke, E. C., Jayne, S. R., Lawrence, D. M., Neale, R.  
882 B., Rasch, P. J., Vertenstein, M., Worley, P. H., Yang, Z.-L. and Zhang, M.: The Community Climate System Model  
883 Version 4, *Journal of Climate*, 24(19), 4973–4991, doi:10.1175/2011JCLI4083.1, 2011.

Elizabeth Asher 8/4/2019 2:02 PM

**Deleted:** Bloss, W. J.: Impact of halogen monoxide chemistry upon boundary layer OH and HO<sub>2</sub> concentrations at a coastal site, *Geophysical Research Letters*, 32(6), doi:10.1029/2004GL022084, 2005.



889 von Glasow, R. and Crutzen, P. J.: Model study of multiphase DMS oxidation with a focus on halogens,  
890 Atmospheric Chemistry and Physics, 4(3), 589–608, doi:10.5194/acp-4-589-2004, 2004.

891 von Glasow, R., von Kuhlmann, R., Lawrence, M. G., Platt, U. and Crutzen, P. J.: Impact of reactive bromine  
892 chemistry in the troposphere, Atmospheric Chemistry and Physics, 4(11/12), 2481–2497, doi:10.5194/acp-4-2481-  
893 2004, 2004.

894 Glover, D. M., Jenkins, W. J. and Doney, S. C.: Modeling Methods for Marine Science, Cambridge University  
895 Press., 2011.

896 Guenther, A. B., Jiang, X., Heald, C. L., Sakulyanontvittaya, T., Duhl, T., Emmons, L. K. and Wang, X.: The Model  
897 of Emissions of Gases and Aerosols from Nature version 2.1 (MEGAN2.1): an extended and updated framework for  
898 modeling biogenic emissions, Geoscientific Model Development, 5(6), 1471–1492, doi:10.5194/gmd-5-1471-2012,  
899 2012.

900 Happell, J. D., Wallace, D. W. R., Wills, K. D., Wilke, R. J. and Neill, C. C.: A purge-and-trap capillary column gas  
901 chromatographic method for the measurement of halocarbons in water and air. [online] Available from:  
902 <http://www.osti.gov/servlets/purl/366493-84sOfy/webviewable/> (Accessed 26 July 2018), 1996.

903 Hossaini, R., Mantle, H., Chipperfield, M. P., Montzka, S. A., Hamer, P., Ziska, F., Quack, B., Krüger, K.,  
904 Tegtmeier, S., Atlas, E., Sala, S., Engel, A., Bönisch, H., Keber, T., Oram, D., Mills, G., Ordóñez, C., Saiz-Lopez,  
905 A., Warwick, N., Liang, Q., Feng, W., Moore, F., Miller, B. R., Maréchal, V., Richards, N. A. D., Dorf, M. and  
906 Pfeilsticker, K.: Evaluating global emission inventories of biogenic bromocarbons, Atmospheric Chemistry and  
907 Physics, 13(23), 11819–11838, doi:10.5194/acp-13-11819-2013, 2013.

908 Hughes, C., Chuck, A. L., Rossetti, H., Mann, P. J., Turner, S. M., Clarke, A., Chance, R. and Liss, P. S.: Seasonal  
909 cycle of seawater bromoform and dibromomethane concentrations in a coastal bay on the western Antarctic  
910 Peninsula: BROMOCARBON SEASONALITY ANTARCTICA, Global Biogeochemical Cycles, 23(2), n/a–n/a,  
911 doi:10.1029/2008GB003268, 2009.

912 Hughes, C., Johnson, M., Utting, R., Turner, S., Malin, G., Clarke, A. and Liss, P. S.: Microbial control of  
913 bromocarbon concentrations in coastal waters of the western Antarctic Peninsula, Marine Chemistry, 151, 35–46,  
914 doi:10.1016/j.marchem.2013.01.007, 2013.

915 Hurrell, J. W., Hack, J. J., Shea, D., Caron, J. M. and Rosinski, J.: A New Sea Surface Temperature and Sea Ice  
916 Boundary Dataset for the Community Atmosphere Model, Journal of Climate, 21(19), 5145–5153,  
917 doi:10.1175/2008JCLI2292.1, 2008.

918 Keeling, R. F., Manning, A. C., McEvoy, E. M. and Shertz, S. R.: Methods for measuring changes in atmospheric O  
919 <sub>2</sub> concentration and their application in southern hemisphere air, Journal of Geophysical Research: Atmospheres,  
920 103(D3), 3381–3397, doi:10.1029/97JD02537, 1998.

921 Lai, S. C., Williams, J., Arnold, S. R., Atlas, E. L., Gebhardt, S. and Hoffmann, T.: Iodine containing species in the  
922 remote marine boundary layer: A link to oceanic phytoplankton: IODINE SPECIES AND PHYTOPLANKTON,  
923 Geophysical Research Letters, 38(20), n/a–n/a, doi:10.1029/2011GL049035, 2011.

924 Lamarque, J.-F.: Response of a coupled chemistry-climate model to changes in aerosol emissions: Global impact on  
925 the hydrological cycle and the tropospheric burdens of OH, ozone, and NO<sub>x</sub>, Geophysical Research Letters, 32(16),  
926 doi:10.1029/2005GL023419, 2005.

927 Lamarque, J.-F., Emmons, L. K., Hess, P. G., Kinnison, D. E., Tilmes, S., Vitt, F., Heald, C. L., Holland, E. A.,  
928 Lauritzen, P. H., Neu, J., Orlando, J. J., Rasch, P. J. and Tyndall, G. K.: CAM-chem: description and evaluation of  
929 interactive atmospheric chemistry in the Community Earth System Model, Geoscientific Model Development, 5(2),  
930 369–411, doi:10.5194/gmd-5-369-2012, 2012.

931 Laturnus, F.: Volatile halocarbons released from Arctic macroalgae, Marine Chemistry, 55(3-4), 359–366,  
932 doi:10.1016/S0304-4203(97)89401-7, 1996.

933 Liang, Q., Atlas, E., Blake, D., Dorf, M., Pfeilsticker, K. and Schauffler, S.: Convective transport of very short lived  
 934 bromocarbons to the stratosphere, *Atmospheric Chemistry and Physics*, 14(11), 5781–5792, doi:10.5194/acp-14-  
 935 5781-2014, 2014.

936 Lin, J. C.: A near-field tool for simulating the upstream influence of atmospheric observations: The Stochastic Time-  
 937 Inverted Lagrangian Transport (STILT) model, *Journal of Geophysical Research*, 108(D16), ACH 2–1–ACH 2–17,  
 938 doi:10.1029/2002JD003161, 2003.

939 Liu, X., Easter, R. C., Ghan, S. J., Zaveri, R., Rasch, P., Shi, X., Lamarque, J.-F., Gettelman, A., Morrison, H., Vitt,  
 940 F., Conley, A., Park, S., Neale, R., Hannay, C., Ekman, A. M. L., Hess, P., Mahowald, N., Collins, W., Iacono, M.  
 941 J., Bretherton, C. S., Flanner, M. G. and Mitchell, D.: Toward a minimal representation of aerosols in climate  
 942 models: description and evaluation in the Community Atmosphere Model CAM5, *Geoscientific Model*  
 943 *Development*, 5(3), 709–739, doi:10.5194/gmd-5-709-2012, 2012.

944 Manley, S. L. and Dastoor, M. N.: Methyl iodide (CH<sub>3</sub>I) production by kelp and associated microbes, *Marine*  
 945 *Biology*, 98(4), 477–482, doi:10.1007/BF00391538, 1988.

946 Maslanik, J.: Near-Real-Time DMSP SSM/I-SSMIS Daily Polar Gridded Sea Ice Concentrations, Version 1, 1999.

947 Mattson, E., Karlsson, A., Smith, W. O. and Abrahamsson, K.: The relationship between biophysical variables and  
 948 halocarbon distributions in the waters of the Amundsen and Ross Seas, Antarctica, *Marine Chemistry*, 140–141, 1–9,  
 949 doi:10.1016/j.marchem.2012.07.002, 2012.

950 Mattsson, E., Karlsson, A. and Abrahamsson, K.: Regional sinks of bromoform in the Southern Ocean: REGIONAL  
 951 SINKS OF CHBR<sub>3</sub> IN THE ANTARCTIC, *Geophysical Research Letters*, 40(15), 3991–3996,  
 952 doi:10.1002/grl.50783, 2013.

953 Moore, R. M. and Groszko, W.: Methyl iodide distribution in the ocean and fluxes to the atmosphere, *Journal of*  
 954 *Geophysical Research: Oceans*, 104(C5), 11163–11171, doi:10.1029/1998JC900073, 1999.

955 Moore, R. M. and Zafiriou, O. C.: Photochemical production of methyl iodide in seawater, *Journal of Geophysical*  
 956 *Research*, 99(D8), 16415, doi:10.1029/94JD00786, 1994.

957 Moore, R. M., Webb, M., Tokarczyk, R. and Wever, R.: Bromoperoxidase and iodoperoxidase enzymes and  
 958 production of halogenated methanes in marine diatom cultures, *Journal of Geophysical Research: Oceans*, 101(C9),  
 959 20899–20908, doi:10.1029/96JC01248, 1996.

960 Murphy, D. M., Froyd, K. D., Bian, H., Brock, C. A., Dibb, J. E., DiGangi, J. P., Diskin, G., Dollner, M., Kupc, A.,  
 961 Scheuer, E. M., Schill, G. P., Weinzierl, B., Williamson, C. J. and Yu, P.: The distribution of sea-salt aerosol in the  
 962 global troposphere, *Atmospheric Chemistry and Physics Discussions*, 1–27, doi:10.5194/acp-2018-1013, 2018.

963 NASA Goddard Space Flight Center, O. E. L.: SeaWiFS Ocean Color Data, 2014.

964 National Centers For Environmental Prediction/National Weather Service/NOAA/U.S. Department Of Commerce:  
 965 NCEP GDAS/FNL 0.25 Degree Global Tropospheric Analyses and Forecast Grids, 2015.

966 Navarro, M. A., Atlas, E. L., Saiz-Lopez, A., Rodriguez-Lloveras, X., Kinnison, D. E., Lamarque, J.-F., Tilmes, S.,  
 967 Filus, M., Harris, N. R. P., Meneguz, E., Ashfold, M. J., Manning, A. J., Cuevas, C. A., Schauffler, S. M. and  
 968 Donets, V.: Airborne measurements of organic bromine compounds in the Pacific tropical tropopause layer,  
 969 *Proceedings of the National Academy of Sciences*, 112(45), 13789–13793, doi:10.1073/pnas.1511463112, 2015.

970 Neale, R. B., Richter, J., Park, S., Lauritzen, P. H., Vavrus, S. J., Rasch, P. J. and Zhang, M.: The Mean Climate of  
 971 the Community Atmosphere Model (CAM4) in Forced SST and Fully Coupled Experiments, *Journal of Climate*,  
 972 26(14), 5150–5168, doi:10.1175/JCLI-D-12-00236.1, 2013.

973 Nevison, C. D., Manizza, M., Keeling, R. F., Kahru, M., Bopp, L., Dunne, J., Tiputra, J., Ilyina, T. and Mitchell, B.  
 974 G.: Evaluating the ocean biogeochemical components of Earth system models using atmospheric potential oxygen  
 975 and ocean color data, *Biogeosciences*, 12(1), 193–208, doi:10.5194/bg-12-193-2015, 2015.

976 Nevison, C. D., Manizza, M., Keeling, R. F., Stephens, B. B., Bent, J. D., Dunne, J., Ilyina, T., Long, M.,  
 977 Resplandy, L., Tjiputra, J. and Yukimoto, S.: Evaluating CMIP5 ocean biogeochemistry and Southern Ocean carbon

978 uptake using atmospheric potential oxygen: Present-day performance and future projection: CMIP5 APO AND  
979 SOUTHERN OCEAN CARBON FLUX, *Geophysical Research Letters*, 43(5), 2077–2085,  
980 doi:10.1002/2015GL067584, 2016.

981 Nightingale, P. D., Malin, G. and Liss, P. S.: Production of chloroform and other low molecular-weight halocarbons  
982 by some species of macroalgae, *Limnology and Oceanography*, 40(4), 680–689, doi:10.4319/lo.1995.40.4.0680,  
983 1995.

984 Nightingale, P. D., Malin, G., Law, C. S., Watson, A. J., Liss, P. S., Liddicoat, M. I., Boutin, J. and Upstill-Goddard,  
985 R. C.: In situ evaluation of air-sea gas exchange parameterizations using novel conservative and volatile tracers,  
986 *Global Biogeochemical Cycles*, 14(1), 373–387, 2000.

987 Obrist, D., Tas, E., Peleg, M., Matveev, V., Faïn, X., Asaf, D. and Luria, M.: Bromine-induced oxidation of mercury  
988 in the mid-latitude atmosphere, *Nature Geoscience*, 4, 22, 2010.

989 Ordóñez, C., Lamarque, J.-F., Tilmes, S., Kinnison, D. E., Atlas, E. L., Blake, D. R., Sousa Santos, G., Brasseur, G.  
990 and Saiz-Lopez, A.: Bromine and iodine chemistry in a global chemistry-climate model: description and evaluation  
991 of very short-lived oceanic sources, *Atmospheric Chemistry and Physics*, 12(3), 1423–1447, doi:10.5194/acp-12-  
992 1423-2012, 2012.

993 Quack, B. and Wallace, D. W. R.: Air-sea flux of bromoform: Controls, rates, and implications: AIR-SEA FLUX  
994 OF BROMOFORM, *Global Biogeochemical Cycles*, 17(1), doi:10.1029/2002GB001890, 2003.

995 Raimund, S., Quack, B., Bozec, Y., Vernet, M., Rossi, V., Garçon, V., Morel, Y. and Morin, P.: Sources of short-  
996 lived bromocarbons in the Iberian upwelling system, *Biogeosciences*, 8(6), 1551–1564, doi:10.5194/bg-8-1551-  
997 2011, 2011.

998 Read, K. A., Mahajan, A. S., Carpenter, L. J., Evans, M. J., Faria, B. V. E., Heard, D. E., Hopkins, J. R., Lee, J. D.,  
999 Moller, S. J., Lewis, A. C., Mendes, L., McQuaid, J. B., Oetjen, H., Saiz-Lopez, A., Pilling, M. J. and Plane, J. M.  
1000 C.: Extensive halogen-mediated ozone destruction over the tropical Atlantic Ocean, *Nature*, 453(7199), 1232–1235,  
1001 doi:10.1038/nature07035, 2008.

1002 Resplandy, L., Keeling, R. F., Stephens, B. B., Bent, J. D., Jacobson, A., Rödenbeck, C. and Khatiwala, S.:  
1003 Constraints on oceanic meridional heat transport from combined measurements of oxygen and carbon, *Climate*  
1004 *Dynamics*, 47(9–10), 3335–3357, doi:10.1007/s00382-016-3029-3, 2016.

1005 Reygondeau, G., Longhurst, A., Martinez, E., Beaugrand, G., Antoine, D. and Maury, O.: Dynamic biogeochemical  
1006 provinces in the global ocean: DYNAMIC BIOGEOCHEMICAL PROVINCES, *Global Biogeochemical Cycles*,  
1007 27(4), 1046–1058, doi:10.1002/gbc.20089, 2013.

1008 Richter, U. and Wallace, D. W. R.: Production of methyl iodide in the tropical Atlantic Ocean: PRODUCTION OF  
1009 METHYL IODIDE, *Geophysical Research Letters*, 31(23), doi:10.1029/2004GL020779, 2004.

1010 Rienecker, M. M., Suarez, M. J., Todling, R., Bacmeister, J., Takacs, L., Liu, H. C., Gu, W., Sienkiewicz, M.,  
1011 Koster, R. D., Gelaro, R., Stajner, I. and Nielsen, J. E.: The GEOS-5 Data Assimilation System – Documentation of  
1012 Versions 5.0.1, 5.1.0, and 5.2.0, NASA/TM-2008-104606., 2008.

1013 Saiz-Lopez, A., Mahajan, A. S., Salmon, R. A., Bauguitte, S. J.-B., Jones, A. E., Roscoe, H. K. and Plane, J. M. C.:  
1014 Boundary Layer Halogens in Coastal Antarctica, *Science*, 317(5836), 348–351, doi:10.1126/science.1141408, 2007.

1015 Saiz-Lopez, A., Lamarque, J.-F., Kinnison, D. E., Tilmes, S., Ordóñez, C., Orlando, J. J., Conley, A. J., Plane, J. M.  
1016 C., Mahajan, A. S., Sousa Santos, G., Atlas, E. L., Blake, D. R., Sander, S. P., Schauffler, S., Thompson, A. M. and  
1017 Brasseur, G.: Estimating the climate significance of halogen-driven ozone loss in the tropical marine troposphere,  
1018 *Atmospheric Chemistry and Physics*, 12(9), 3939–3949, doi:10.5194/acp-12-3939-2012, 2012.

1019 Saiz-Lopez, A., Fernandez, R. P., Ordóñez, C., Kinnison, D. E., Gómez Martín, J. C., Lamarque, J.-F. and Tilmes,  
1020 S.: Iodine chemistry in the troposphere and its effect on ozone, *Atmospheric Chemistry and Physics*, 14(23), 13119–  
1021 13143, doi:10.5194/acp-14-13119-2014, 2014.

1022 Salawitch, R. J., Canty, T., Kurosu, T., Chance, K., Liang, Q., da Silva, A., Pawson, S., Nielsen, J. E., Rodriguez, J.  
1023 M., Bhartia, P. K., Liu, X., Huey, L. G., Liao, J., Stickel, R. E., Tanner, D. J., Dibb, J. E., Simpson, W. R.,  
1024 Donohoue, D., Weinheimer, A., Flocke, F., Knapp, D., Montzka, D., Neuman, J. A., Nowak, J. B., Ryerson, T. B.,  
1025 Oltmans, S., Blake, D. R., Atlas, E. L., Kinnison, D. E., Tilmes, S., Pan, L. L., Hendrick, F., Van Roozendaal, M.,  
1026 Kreher, K., Johnston, P. V., Gao, R. S., Johnson, B., Bui, T. P., Chen, G., Pierce, R. B., Crawford, J. H. and Jacob,  
1027 D. J.: A new interpretation of total column BrO during Arctic spring: FRONTIER, Geophysical Research Letters,  
1028 37(21), n/a–n/a, doi:10.1029/2010GL043798, 2010.

1029 Schauffler, S. M., Atlas, E. L., Blake, D. R., Flocke, F., Lueb, R. A., Lee-Taylor, J. M., Stroud, V. and Travnicsek,  
1030 W.: Distributions of brominated organic compounds in the troposphere and lower stratosphere, Journal of  
1031 Geophysical Research: Atmospheres, 104(D17), 21513–21535, doi:10.1029/1999JD900197, 1999.

1032 Schroeder, W. H., Anlauf, K. G., Barrie, L. A., Lu, J. Y., Steffen, A., Schneeberger, D. R. and Berg, T.: Arctic  
1033 springtime depletion of mercury, Nature, 394, 331, 1998.

1034 Simpson, W. R., Brown, S. S., Saiz-Lopez, A., Thornton, J. A. and von Glasow, R.: Tropospheric Halogen  
1035 Chemistry: Sources, Cycling, and Impacts, Chemical Reviews, 115(10), 4035–4062, doi:10.1021/cr5006638, 2015.

1036 Sive, B. C., Varner, R. K., Mao, H., Blake, D. R., Wingenter, O. W. and Talbot, R.: A large terrestrial source of  
1037 methyl iodide, Geophysical Research Letters, 34(17), doi:10.1029/2007GL030528, 2007.

1038 Stephens, B.: ORCAS Merge Products. Version 1.0, [online] Available from:  
1039 <https://data.eol.ucar.edu/dataset/490.024> (Accessed 31 December 2018), 2017.

1040 Stephens, B. B., Keeling, R. F., Heimann, M., Six, K. D., Murnane, R. and Caldeira, K.: Testing global ocean  
1041 carbon cycle models using measurements of atmospheric O<sub>2</sub> and CO<sub>2</sub> concentration, Global Biogeochemical  
1042 Cycles, 12(2), 213–230, doi:10.1029/97GB03500, 1998.

1043 Stephens, B. B., Keeling, R. F. and Paplawsky, W. J.: Shipboard measurements of atmospheric oxygen using a  
1044 vacuum-ultraviolet absorption technique, Tellus B, 55(4), 857–878, doi:10.1046/j.1435-6935.2003.00075.x, 2003.

1045 Stephens, B. B., Long, M. C., Keeling, R. F., Kort, E. A., Sweeney, C., Apel, E. C., Atlas, E. L., Beaton, S., Bent, J.  
1046 D., Blake, N. J., Bresch, J. F., Casey, J., Daube, B. C., Diao, M., Diaz, E., Dierssen, H., Donets, V., Gao, B.-C.,  
1047 Gierach, M., Green, R., Haag, J., Hayman, M., Hills, A. J., Hoecker-Martínez, M. S., Honomichl, S. B., Hornbrook,  
1048 R. S., Jensen, J. B., Li, R.-R., McCubbin, I., McKain, K., Morgan, E. J., Nolte, S., Powers, J. G., Rainwater, B.,  
1049 Randolph, K., Reeves, M., Schauffler, S. M., Smith, K., Smith, M., Stith, J., Stossmeister, G., Toohey, D. W. and  
1050 Watt, A. S.: The O<sub>2</sub>/N<sub>2</sub> Ratio and CO<sub>2</sub> Airborne Southern Ocean Study, Bulletin of the American Meteorological  
1051 Society, 99(2), 381–402, doi:10.1175/BAMS-D-16-0206.1, 2018.

1052 Sturges, W. T., Cota, G. F. and Buckley, P. T.: Bromoform emission from Arctic ice algae, Nature, 358, 660, 1992.

1053 Sturges, W. T., Cota, G. F. and Buckley, P. T.: Vertical profiles of bromoform in snow, sea ice, and seawater in the  
1054 Canadian Arctic, Journal of Geophysical Research: Oceans, 102(C11), 25073–25083, doi:10.1029/97JC01860,  
1055 1997.

1056 Tilmes, S., Lamarque, J.-F., Emmons, L. K., Kinnison, D. E., Marsh, D., Garcia, R. R., Smith, A. K., Neely, R. R.,  
1057 Conley, A., Vitt, F., Val Martin, M., Tanimoto, H., Simpson, I., Blake, D. R. and Blake, N.: Representation of the  
1058 Community Earth System Model (CESM1) CAM4-chem within the Chemistry-Climate Model Initiative (CCMI),  
1059 Geoscientific Model Development, 9(5), 1853–1890, doi:10.5194/gmd-9-1853-2016, 2016.

1060 Tohjima, Y.: Preparation of gravimetric standards for measurements of atmospheric oxygen and reevaluation of  
1061 atmospheric oxygen concentration, Journal of Geophysical Research, 110(D11), doi:10.1029/2004JD005595, 2005.

1062 Tokarczyk, R. and Moore, R. M.: Production of volatile organohalogens by phytoplankton cultures, Geophysical  
1063 Research Letters, 21(4), 285–288, doi:10.1029/94GL00009, 1994.

1064 Tortell, P. D. and Long, M. C.: Spatial and temporal variability of biogenic gases during the Southern Ocean spring  
1065 bloom, Geophysical Research Letters, 36(1), doi:10.1029/2008GL035819, 2009.

1066 Tortell, P. D., Asher, E. C., Ducklow, H. W., Goldman, J. A. L., Dacey, J. W. H., Grzyski, J. J., Young, J. N.,  
1067 Kranz, S. A., Bernard, K. S. and Morel, F. M. M.: Metabolic balance of coastal Antarctic waters revealed by  
1068 autonomous  $p\text{CO}_2$  and  $\Delta\text{O}_2/\text{Ar}$  measurements: metabolic balance of Antarctic waters, *Geophysical Research*  
1069 *Letters*, 41(19), 6803–6810, doi:10.1002/2014GL061266, 2014.

1070 Williams, J., Gros, V., Atlas, E., Maciejczyk, K., Batsaikhan, A., Schöler, H. F., Forster, C., Quack, B., Yassaa, N.,  
1071 Sander, R. and Van Dingenen, R.: Possible evidence for a connection between methyl iodide emissions and Saharan  
1072 dust, *Journal of Geophysical Research*, 112(D7), doi:10.1029/2005JD006702, 2007.

1073 WMO (World Meteorological Organization): Scientific Assessment of Ozone Depletion: 2018, Global Ozone  
1074 Research and Monitoring Project-Report, Geneva, Switzerland., 2018.

1075 Wofsy, S. C.: HIPER Pole-to-Pole Observations (HIPPO): fine-grained, global-scale measurements of climatically  
1076 important atmospheric gases and aerosols, *Philosophical Transactions of the Royal Society A: Mathematical,*  
1077 *Physical and Engineering Sciences*, 369(1943), 2073–2086, doi:10.1098/rsta.2010.0313, 2011.

1078 Wofsy, S. C., Afshar, S., Allen, H. M., Apel, E., Asher, E. C., Barletta, B., Bent, J., Bian, H., Biggs, B. C., Blake, D.  
1079 R., Blake, N., Bourgois, L., Brock, C. A., Brune, W. H., Budney, J. W., Bui, T. P., Butler, A., Campuzano-Jost, P.,  
1080 Chang, C. S., Chin, M., Commane, R., Correa, G., Crounse, J. D., Cullis, P. D., Daube, B. C., Day, D. A., Dean-  
1081 Day, J. M., Dibb, J. E., Digangi, J. P., Diskin, G. S., Dollner, M., Elkins, J. W., Erdesz, F., Fiore, A. M., Flynn, C.  
1082 M., Froyd, K., Gesler, D. W., Hall, S. R., Hanisco, T. F., Hannun, R. A., Hills, A. J., Hints, E. J., Hoffmann, A.,  
1083 Hornbrook, R. S., Huey, L. G., Hughes, S., Jimenez, J. L., Johnson, B. J., Katich, J. M., Keeling, R., Kim, M. J.,  
1084 Kupc, A., Lait, L. R., Lamarque, J.-F., Liu, H. B., McKain, K., McLaughlin, R. J., Meinardi, S., Miller, D. O.,  
1085 Montzka, S. A., Moore, F. L., Morgan, E. J., Murphy, D. M., Murray, L. T., Nault, B. A., Neuman, J. A., Newman,  
1086 P. A., Nicely, J. M., Pan, X., Paplawsky, W., Peischl, J., Prather, M. J., Price, D. J., Ray, E., Reeves, J. M.,  
1087 Richardson, M., Rollins, A. W., Rosenlof, K. H., Ryerson, T. B., Scheuer, E., Schill, G. P., Schroder, J. C., Schwarz,  
1088 J. P., St.Clair, J. M., Steenrod, S. D., Stephens, B. B., Strode, S. A., Sweeney, C., Tanner, D., Teng, A. P., Thames,  
1089 A. B., Thompson, C. R., Ullmann, K., Veres, P. R., Vizenor, N., Wagner, N. L., Watt, A., Weber, R., Weinzierl, B.,  
1090 et al.: ATom: Merged Atmospheric Chemistry, Trace Gases, and Aerosols, [online] Available from:  
1091 [https://daac.ornl.gov/cgi-bin/dsviewer.pl?ds\\_id=1581](https://daac.ornl.gov/cgi-bin/dsviewer.pl?ds_id=1581) (Accessed 31 December 2018), 2018.

1092 Xiang, B., Miller, S. M., Kort, E. A., Santoni, G. W., Daube, B. C., Commane, R., Angevine, W. M., Ryerson, T. B.,  
1093 Trainer, M. K., Andrews, A. E., Nehrkorn, T., Tian, H. and Wofsy, S. C.: Nitrous oxide ( $\text{N}_2\text{O}$ ) emissions from  
1094 California based on 2010 CalNex airborne measurements: California  $\text{N}_2\text{O}$  emissions, *Journal of Geophysical*  
1095 *Research: Atmospheres*, 118(7), 2809–2820, doi:10.1002/jgrd.50189, 2013.

1096 Yang, B., Yang, G.-P., Lu, X.-L., Li, L. and He, Z.: Distributions and sources of volatile chlorocarbons and  
1097 bromocarbons in the Yellow Sea and East China Sea, *Marine Pollution Bulletin*, 95(1), 491–502,  
1098 doi:10.1016/j.marpolbul.2015.03.009, 2015.

1099 Yokouchi, Y., Nojiri, Y., Barrie, L. A., Toom-Sauntry, D. and Fujinuma, Y.: Atmospheric methyl iodide: High  
1100 correlation with surface seawater temperature and its implications on the sea-to-air flux, *Journal of Geophysical*  
1101 *Research: Atmospheres*, 106(D12), 12661–12668, doi:10.1029/2001JD900083, 2001.

1102 Yokouchi, Y., Hasebe, F., Fujiwara, M., Takashima, H., Shiotani, M., Nishi, N., Kanaya, Y., Hashimoto, S., Fraser,  
1103 P., Toom-Sauntry, D., Mukai, H. and Nojiri, Y.: Correlations and emission ratios among bromoform,  
1104 dibromochloromethane, and dibromomethane in the atmosphere, *Journal of Geophysical Research*, 110(D23),  
1105 doi:10.1029/2005JD006303, 2005.

1106 Ziska, F., Quack, B., Abrahamsson, K., Archer, S. D., Atlas, E., Bell, T., Butler, J. H., Carpenter, L. J., Jones, C. E.,  
1107 Harris, N. R. P., Hepach, H., Heumann, K. G., Hughes, C., Kuss, J., Krüger, K., Liss, P., Moore, R. M., Orlikowska,  
1108 A., Raimund, S., Reeves, C. E., Reifenhäuser, W., Robinson, A. D., Schall, C., Tanhua, T., Tegtmeier, S., Turner,  
1109 S., Wang, L., Wallace, D., Williams, J., Yamamoto, H., Yvon-Lewis, S. and Yokouchi, Y.: Global sea-to-air flux  
1110 climatology for bromoform, dibromomethane and methyl iodide, *Atmospheric Chemistry and Physics*, 13(17),  
1111 8915–8934, doi:10.5194/acp-13-8915-2013, 2013.

1112

1113

1114 **Tables**

1115 Table 1. Mean ± uncertainty (see Sect. 3.4.1 and 3.4.2 for details) HVOC emission estimates  
1116 (pmol m<sup>-2</sup> hr<sup>-1</sup>) in Region 1 and Region 2 calculated in this study (with method indicated below  
1117 each value), from CAM-Chem (Ordoñez et al., 2012) and from several other modeling and ship-  
1118 based observational studies.

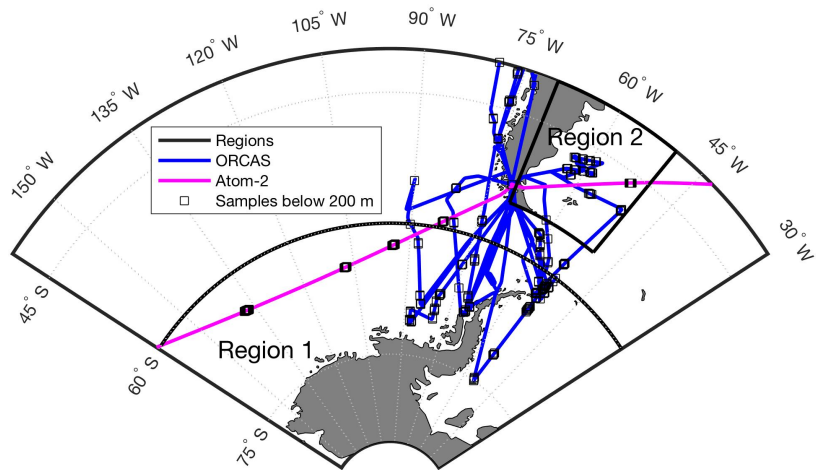
1119

Region/Months	CHBr <sub>3</sub>	CH <sub>2</sub> Br <sub>2</sub>	CH <sub>3</sub> I	CHClBr <sub>2</sub>	Reference
Region 1 (JF) <u>&lt; 60° S</u>	91 ± 8 <u>O<sub>2</sub> Regr.</u>	31 ± 18 <u>O<sub>2</sub> Regr.</u>	35 ± 29 <u>MLR</u>	11 ± 4 <u>O<sub>2</sub> Regr.</u>	This Study
Region 2 (JF) <u>&gt;55° S and</u> <u>&lt;40° S</u>	329 ± 23 <u>O<sub>2</sub> Regr.</u>	69 ± 5 <u>O<sub>2</sub> Regr.</u>	392 ± 32 <u>O<sub>2</sub> Regr.</u>	25 ± 5 <u>O<sub>2</sub> Regr.</u>	This Study
Region 1 (JF)	10	1.9	120	0.38	CAM-Chem
Region 2 (JF)	360	44	800	8.7	CAM-Chem
Southern Ocean (≥50°S), (DJ)	200	200	200	-----	Ziska et al. 2013 (model)
Marguerite Bay (DJF)	3500	875	-----	-----	Hughes et al. 2009 (obs)
70°S-72°S Antarctica	1300	-----	-----	-----	Carpenter et al. 2007 (obs)
Southern Ocean (≥50°S) (Feb. - April)	225	312	708	-----	Butler et al. 2007 (obs)
40°S-52°S S. Atlantic (Sept.- Feb.)	-1670	-----	250	-----	Chuck et al. 2005
Southern Ocean (≥50°S), (DJ)	-330	-----	-----	-----	Mattson et al. 2013 (model)

1120

1121

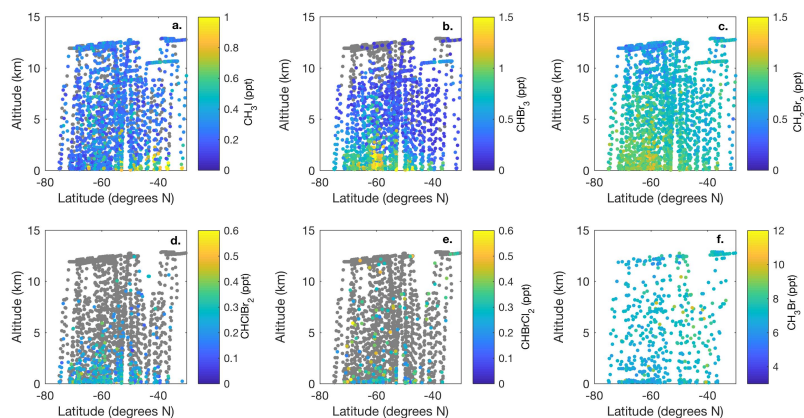
1122



1124  
1125 **Figure 1.** Overview map ORCAS and ATom-2 flight tracks in the study regions: 1) high  
1126 latitudes in the Southern Hemisphere poleward 60° S and 2) the Patagonian Shelf. The ORCAS  
1127 and ATom-2 aircraft flights and dips below 200 m that took place within these regions are also  
1128 shown.

1129  
1130

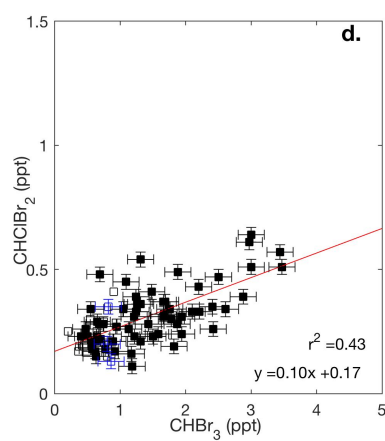
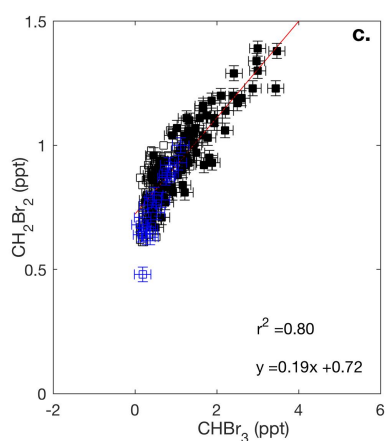
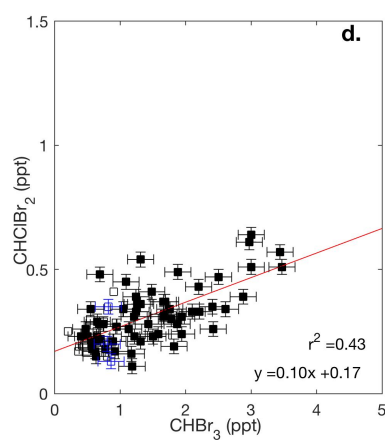
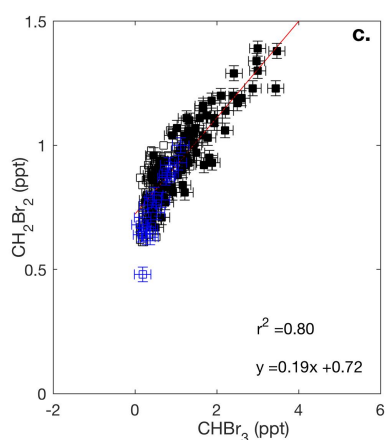
Unknown  
**Formatted:** Font:(Default) Times, 12 pt,  
Bold



Unknown  
Formatted: Font:(Default) Times, 12 pt, Bold

**Figure 2.** Meridional-altitudinal cross-sections of mixing ratios of a)  $\text{CH}_3\text{I}$ , b)  $\text{CHBr}_3$ , c)  $\text{CH}_2\text{Br}_2$ , d)  $\text{CHClBr}_2$ , and e)  $\text{CHBrCl}_2$  from the TOGA and mixing ratios of f)  $\text{CH}_3\text{Br}$  from AWAS and WAS in 2016 and 2017, respectively, during the ORCAS and ATom-2 campaigns over the Southern Ocean in the austral summer. Note the different color bar scales. Gray points denote measurements below the detection limit of each species ( $\text{CH}_3\text{I} - 0.03 \text{ ppt}$ ,  $\text{CHBr}_3 - 0.2 \text{ ppt}$ ,  $\text{CH}_2\text{Br}_2 - 0.03 \text{ ppt}$ ,  $\text{CHClBr}_2 - 0.03 \text{ ppt}$ ,  $\text{CHBrCl}_2 - 0.05 \text{ ppt}$ ,  $\text{CH}_3\text{Br} - 0.2 \text{ ppt}$ ).





Unknown  
Formatted: Font:(Default) Times, 12 pt,  
Bold

**Figure 3.** Mixing ratios of  $\text{CHBr}_3$  vs.  $\text{CH}_2\text{Br}_2$  and  $\text{CHClBr}_2$  across the ORCAS and ATom-2 campaigns in Region 1 (Fig.3a,b) and in (Fig.3c,d), respectively. Type II major axis regression model (bivariate least squares regressions) are based on ORCAS data below 2 km and illustrate regional enhancement ratios. Error bars represent the uncertainty in HVOC measurements.

1150

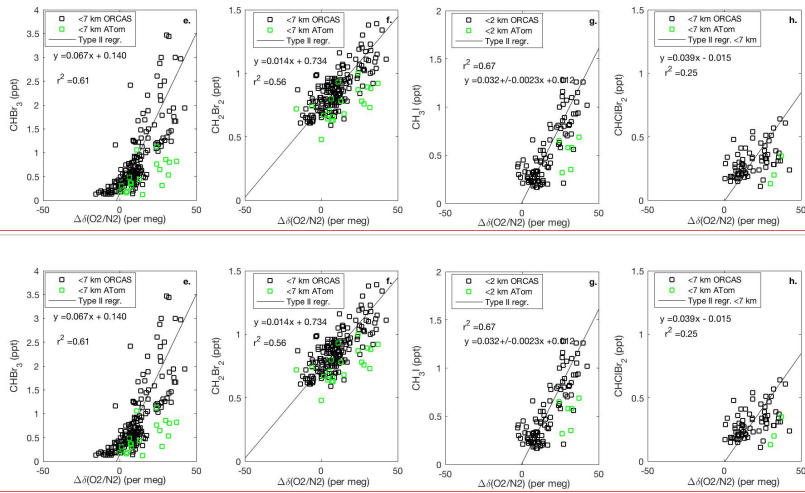
1151

1152

1153

1154 **Figure 4.** Mixing ratios of CHBr<sub>3</sub>, CH<sub>2</sub>Br<sub>2</sub>, and CH<sub>3</sub>I vs. O<sub>2</sub> on ORCAS and ATom-2 in Region  
1155 1, poleward of 60° S (a-d) and Region 2 over the Patagonian Shelf (e-h). Slopes ± standard  
1156 errors from type II major axis regression model (bivariate least squares regression) fits of  
1157 ORCAS data for regressions with  $r^2 > 0.2$  (fits were calculated on variables scaled to their full  
1158 range). The slopes reported in the figure are converted to pmol:mol ratios prior to estimating  
1159 biogenic HVOC fluxes based on modeled CESM O<sub>2</sub> fluxes. Data from above 7 km were  
1160 excluded due to the influence of air masses transported from further north.

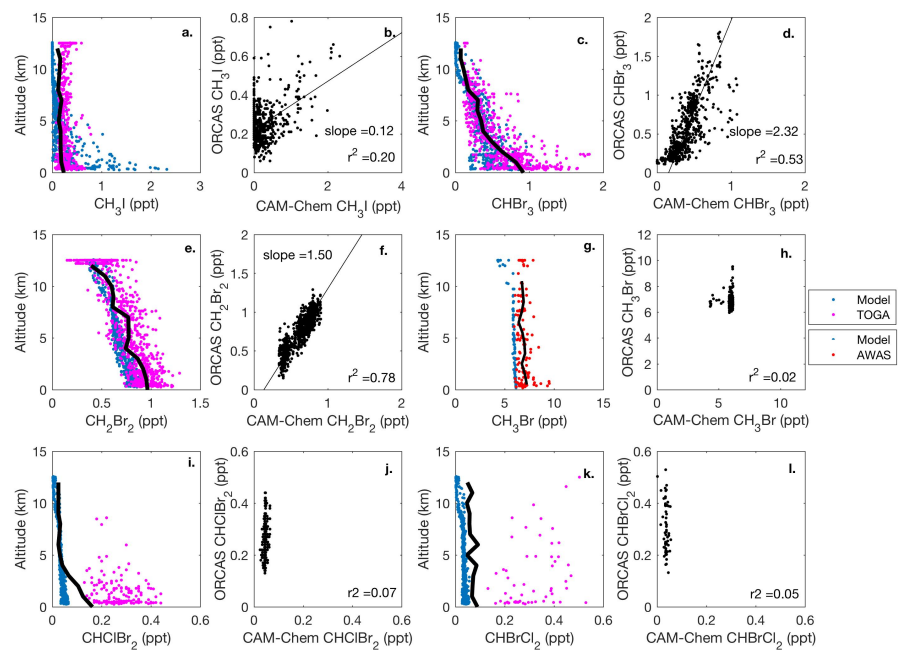
1161



Unknown  
Formatted: Font:(Default) Times, 12 pt

Unknown  
Formatted: Font:(Default) Times, 12 pt

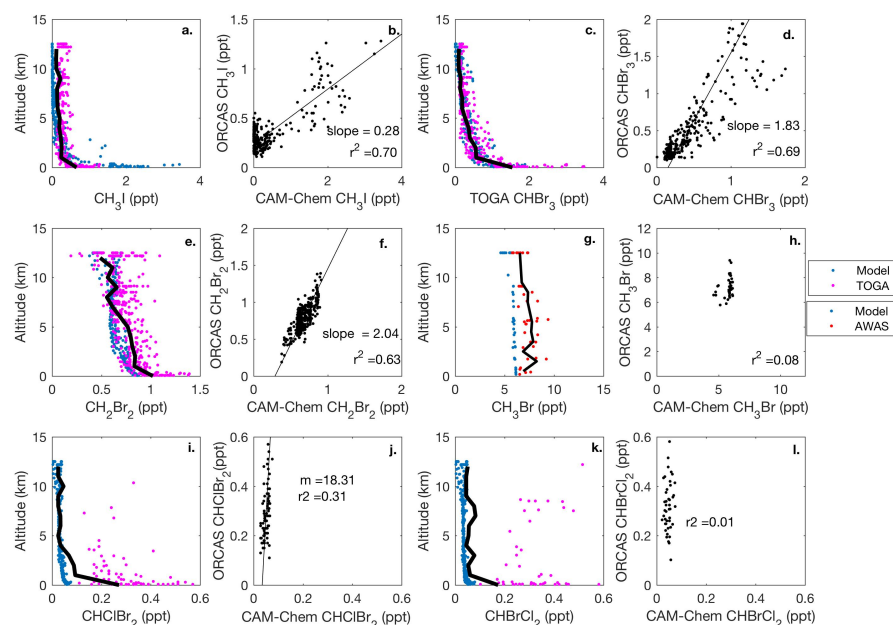
1162  
1163



1164

1165 **Fig 5.** CAM-Chem1.2 model-aircraft measurement comparison during the ORCAS campaign  
1166 between 1-12 km in Region 1, high latitudes in the Southern Hemisphere poleward 60° S. All  
1167 regressions are type II major axis regression models bivariate least squares regressions (slopes  
1168 are shown when the  $r^2 \geq 0.2$ ). The bold, black line in each vertical profile represents the binned  
1169 (mean) mixing ratio of HVOC measurements at that altitude. The binned mean includes  
1170 measurements below the detection limit (DL), which for this calculation are assigned a value  
1171 equal to the DL multiplied by the percentage of data below detection. Modeled values include  
1172 locations where observations were below the DL.

Unknown  
Formatted: Font:(Default) Times, 12 pt



Unknown  
Formatted: Font:(Default) Times, 12 pt

**Figure 6.** CAM-Chem 1.2 model-aircraft measurement (TOGA and AWAS) comparison during ORCAS campaign between 1-12 km in Region 2, the Patagonian Shelf. All regressions are type II major axis regression models bivariate least squares regressions (slopes are shown when the  $r^2 \geq 0.2$ ). The bold, black line in each vertical profile represents the binned (mean) mixing ratio of HVOC measurements at that altitude. Again, the binned mean includes measurements below the detection limit (DL), which for this calculation are assigned a value equal to the DL multiplied by the percentage of data below detection. Modeled values include locations where observations were below the DL.

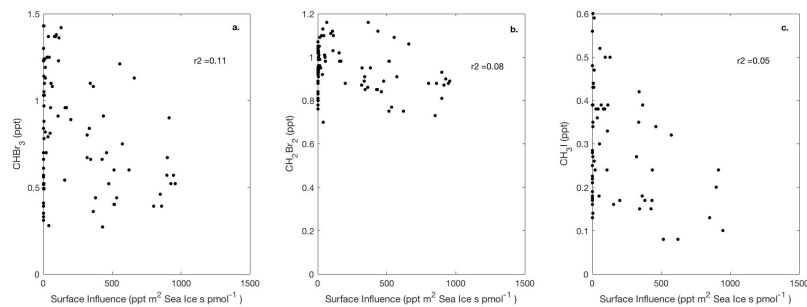
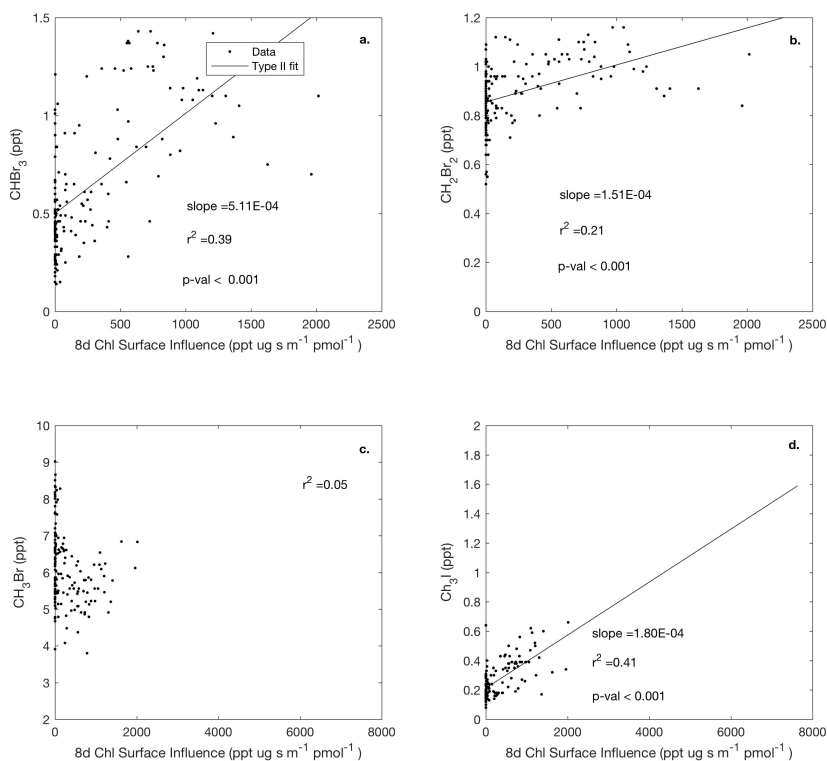


**Figure 7.** Linear type II regressions between influence functions convolved with sea ice distributions, which exclude land ice, and mixing ratios for  $\text{CHBr}_3$ ,  $\text{CH}_2\text{Br}_2$ , and  $\text{CH}_3\text{I}$  in Region 1, poleward of  $60^\circ \text{S}$ . Surface influence ( $\text{ppt m}^2 \text{ s pmol}^{-1}$ ) in each grid cell was multiplied by fractional sea ice concentration surface field, which is unit-less, yielding sea ice surface influence function units of  $\text{ppt m}^2 \text{ s pmol}^{-1}$ , as shown on the x-axis. Linear regression lines are not shown, as  $p \geq 0.001$ .

Unknown  
Formatted: Font:(Default) Times, 12 pt

Elizabeth Asher 7/6/2019 11:31 AM  
Deleted: predictor variable



Unknown

**Formatted:** Font:(Default) Times, 12 pt, Bold

1193

1194

1195 **Figure 8.** Linear type II regressions between influence functions of eight day composites of chl  
 1196 *a* and mixing ratios of HVOCs (a-d) poleward of 60° S (Region 1). Surface influence (ppt m<sup>2</sup> s  
 1197 pmol<sup>-1</sup>) in each grid cell was multiplied by the chl *a* (μg m<sup>-3</sup>) surface field, resulting in surface  
 1198 influence function units of μg ppt s pmol<sup>-1</sup> m<sup>-1</sup>, shown on the x-axis. Linear regression lines are  
 1199 shown where when  $p < 0.001$ .

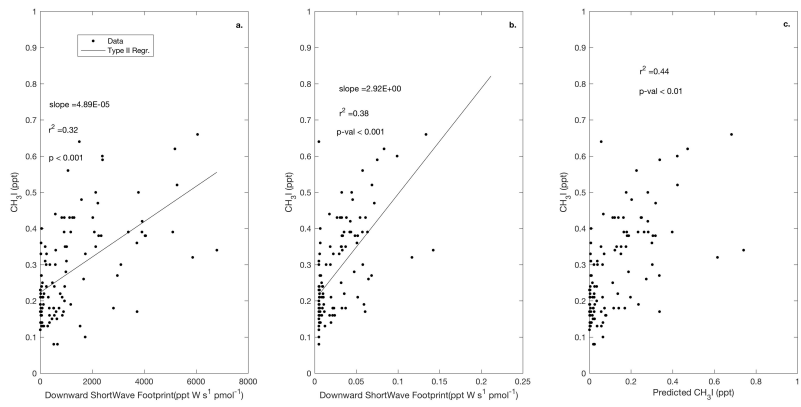
1200

Elizabeth Asher 7/6/2019 11:31 AM

**Deleted:** predictor variables

Elizabeth Asher 7/6/2019 10:26 AM

**Deleted:** .



1204

1205 **Figure 9.** Observed CH<sub>3</sub>I plotted against the surface influence functions of downward shortwave  
1206 radiation (a) and absorption due to detritus (b). Predicted mixing ratios of CH<sub>3</sub>I based on a  
1207 multiple linear regressions (MLR) using these two predictors in Region 1 are shown in Fig. 9c  
1208 according to Equation 3. Surface influence (ppt m<sup>2</sup> s pmol<sup>-1</sup>) in each grid cell was multiplied by  
1209 the surface source field, such as shortwave radiation at the surface (W m<sup>-2</sup>), yielding units of ppt  
1210 Ws pmol<sup>-1</sup>, and the surface ocean's detrital absorption (m<sup>-1</sup>), yielding units of ppt m s pmol<sup>-1</sup>,  
1211 shown on the x-axes.

1212

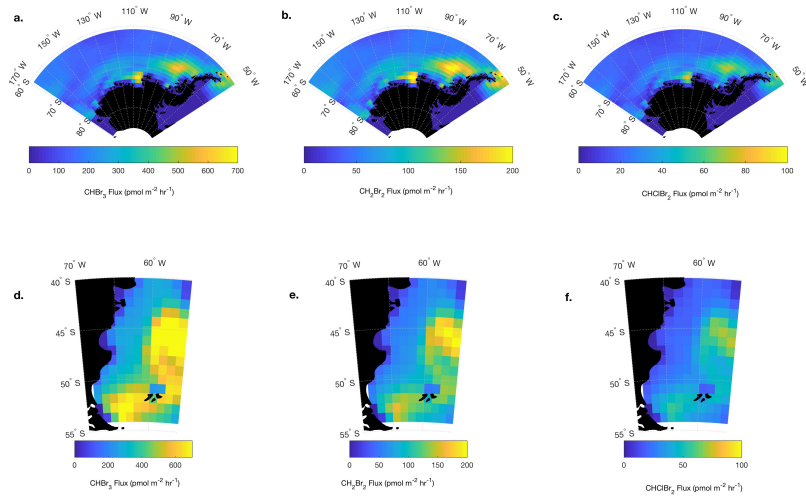
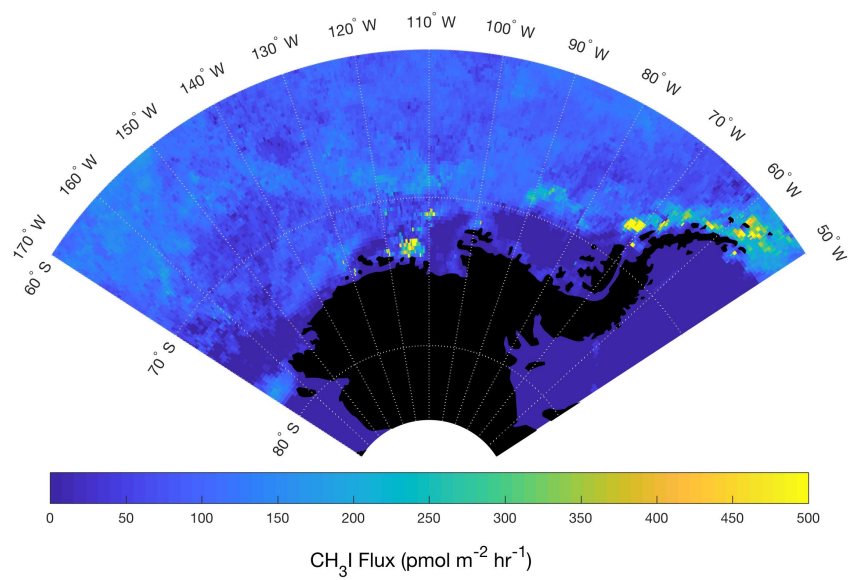


**Figure 10.** Resulting mean Jan. – Feb. 2016 O<sub>2</sub>-based (parameterized) CHBr<sub>3</sub> and CH<sub>2</sub>Br<sub>2</sub> and CHClBr<sub>2</sub> fluxes (pmol m<sup>-2</sup> s<sup>-1</sup>) in Region 1 (a-c) poleward of 60° S and Region 2 (d-f) over the Patagonian Shelf. CESM modeled O<sub>2</sub> fluxes are scaled by the slope between the oceanic contribution to δ(O<sub>2</sub>/N<sub>2</sub>) and CHBr<sub>3</sub> and CH<sub>2</sub>Br<sub>2</sub>, and CHClBr<sub>2</sub> reported in Fig. 4. Note that these fluxes represent mean estimated biogenic fluxes in Jan. -Feb. 2016 (see Sect. 3.4.1 for details).





1220

1221 | **Figure 11.** Mean estimated CH<sub>3</sub>I **fluxes** for Jan. – Feb. The multilinear regression in Fig. 9  
 1222 between CH<sub>3</sub>I mixing ratios and geophysical influence functions related to shortwave radiation  
 1223 and detrital material at the sea surface was used to derive a mean flux field in Jan.-Feb., 2016 for  
 1224 Region 1.

1225

1226 **Supplementary Text**

1227 **Sea air exchange calculations**

1228 To support the interpretation of our results, we calculate nominal equilibration times. For  
1229 estimates of bulk sea air equilibration times for HVOCs, O<sub>2</sub>, and CO<sub>2</sub>, we assume a mixed layer  
1230 depth of 30 m, a temperature of 0° C, a salinity of 35 PSU, and carbonate buffering according to  
1231 eq. 8.3.10 in Sarmiento and Gruber (2006), and transfer velocities according to Nightingale et al.,  
1232 (2000). The Schmidt number (i.e. the ratio of the kinematic viscosity of a gas, divided by the  
1233 molecular diffusivity) for O<sub>2</sub>, CO<sub>2</sub> and CH<sub>3</sub>Br were calculated according to Wanninkhof (2014),  
1234 and the Schmidt numbers for CHBr<sub>3</sub> and CH<sub>3</sub>I were calculated according to Quack and Wallace  
1235 (2003) and Moore and Groszko (1999), respectively. The results are provided in Sect. 3.1.2.

1236 **Comparisons of TOGA, WAS and PFP**

1237 Despite overall good agreement between co-located inflight AWAS, WAS, and PFP samples and  
1238 TOGA measurements, we observed notable discrepancies in several cases (e.g. Fig. S1b; Fig.  
1239 S2a-b). On ORCAS, we observed a non-linear relationship between inflight TOGA  
1240 measurements and co-located AWAS samples of CH<sub>3</sub>I (Fig. S1b), driven by a few samples with  
1241 high mixing ratios. Close inspection of upwind and downwind flights over Region 2 with the  
1242 campaign's high mixing ratios of CH<sub>3</sub>I indicated that TOGA measurements were consistent with  
1243 a modest flux of CH<sub>3</sub>I from the ocean to the atmosphere. On ATom-2, TOGA measurements  
1244 agreed better with co-located PFP samples than with co-located WAS samples; and differences  
1245 on the sixth and seventh research flights (i.e. the data used here) were relatively small.  
1246 Nevertheless these differences motivated an instrument inter-comparison following the ATom  
1247 campaign between these instruments. Thus far, results of this inter-comparison show that TOGA  
1248 and PFP measurements differ by < 25%.

1249

1250

1251 **Supplementary Tables**

1252 Table S1. The TOGA-PFP instrument comparison was done by sampling a 50L SS pontoon,  
1253 created at NCAR from a humidified dilution of the TOGA ATom standard. Data were analyzed  
1254 and reported by Rebecca Hornbrook (NCAR, TOGA) and Steve Montzka (NOAA, PFP).

Pontoon Inter-comparison	Concentration (dilution-based calc.)	TOGA (10/12/2018)	PFP (10/24/2018)
CHBr <sub>3</sub>	34	21.0 ± 0.1	26.6 ± 0.8
CHClBr <sub>2</sub>	26	19.9 ± 1.0	22.9 ± 0.1
CH <sub>2</sub> Br <sub>2</sub>	52	47.7 ± 0.2	51.7 ± 2.0

1255

1256

Elizabeth Asher 7/8/2019 3:47 PM  
Deleted: -

Elizabeth Asher 7/8/2019 3:48 PM  
Deleted: -

Elizabeth Asher 7/7/2019 12:41 PM  
Deleted: ,

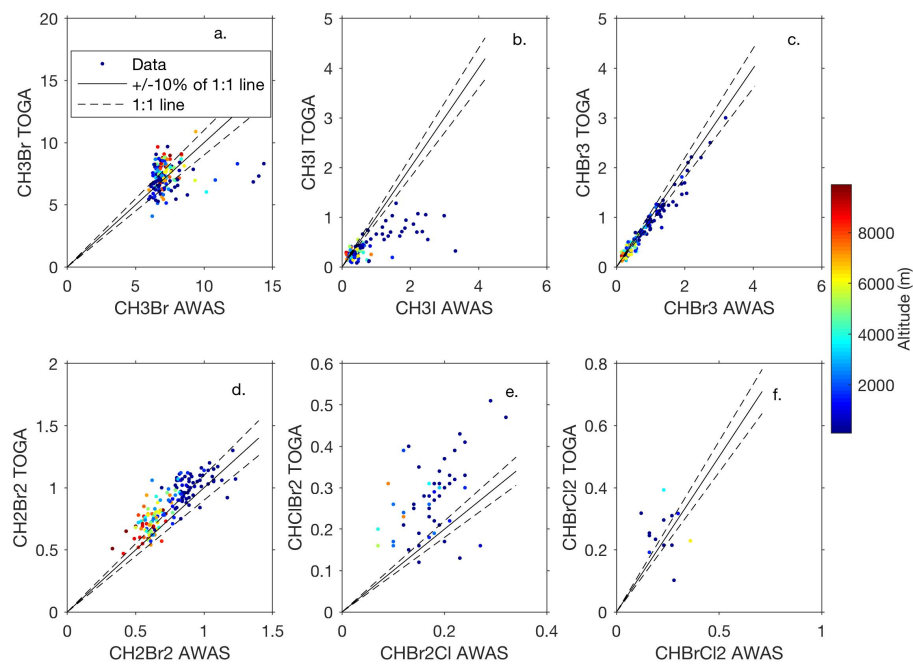
Elizabeth Asher 7/7/2019 12:41 PM  
Formatted: Subscript

Elizabeth Asher 7/7/2019 12:41 PM  
Formatted: Subscript

Elizabeth Asher 7/7/2019 12:41 PM  
Formatted: Subscript

Elizabeth Asher 7/7/2019 12:41 PM  
Formatted: Subscript

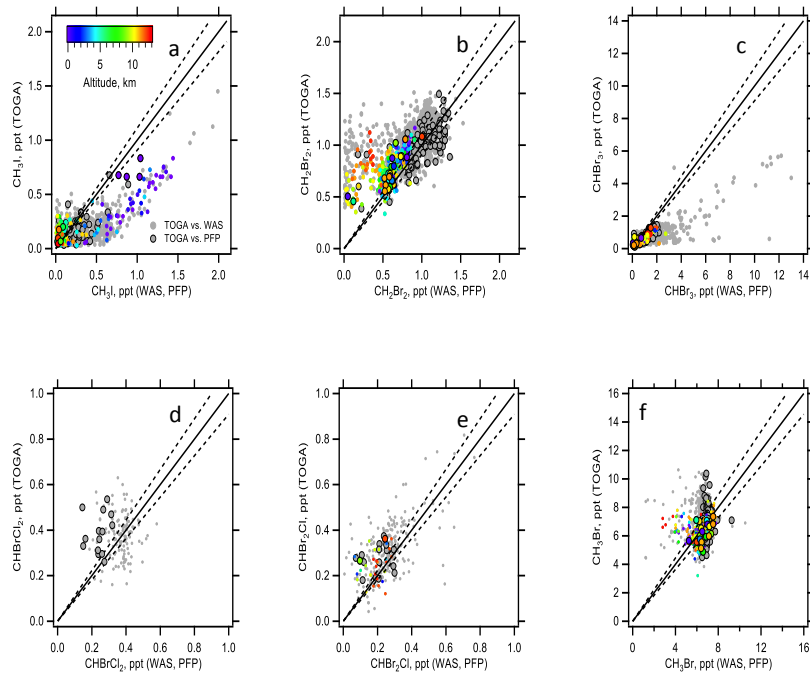
1260  
1261 **Supplementary Figures**  
1262



1263  
1264  
1265 **Figure S1.** Comparison between AWAS samples and TOGA measurements during ORCAS  
1266 below 10 km, when these two shared over half their sampling period. Points are colored by  
1267 altitude. Dashed lines represent  $\pm 10\%$  of the 1:1 line. Sample points below the DL are not  
1268 included in this quantitative comparison.

1269  
1270

1271  
1272  
1273



1274  
1275  
1276  
1277  
1278  
1279  
1280  
1281  
1282  
1283

**Figure S2.** Comparison between WAS, PFP and TOGA measurements during ATom-2 below 10 km, when these instruments shared over half their sampling period. WAS measurements are shown in larger circles, PFP measurements in smaller circles, and measurements from the research flights six and seven used in this analysis are shown in color, while measurements on other research flights in ATom-2 are shown in gray. Dashed lines represent  $\pm 10\%$  of the 1:1 line. Sample points below the DL are not shown.

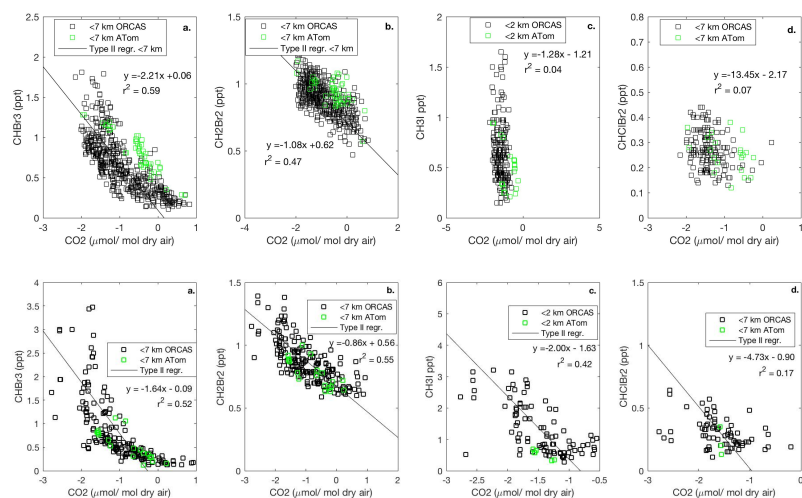


**Figure S3.** Mixing ratios of CHBr<sub>3</sub>, CH<sub>2</sub>Br<sub>2</sub> and CH<sub>3</sub>I vs. CO<sub>2</sub> in Region 1 (a-c) and Region 2 (d-f). Type II major axis regression model (bivariate least squares regression) fits are shown for combined ORCAS and ATom-2 data, using data below 7 km for CHBr<sub>3</sub>, CH<sub>2</sub>Br<sub>2</sub>, and below 2 km for CH<sub>3</sub>I.

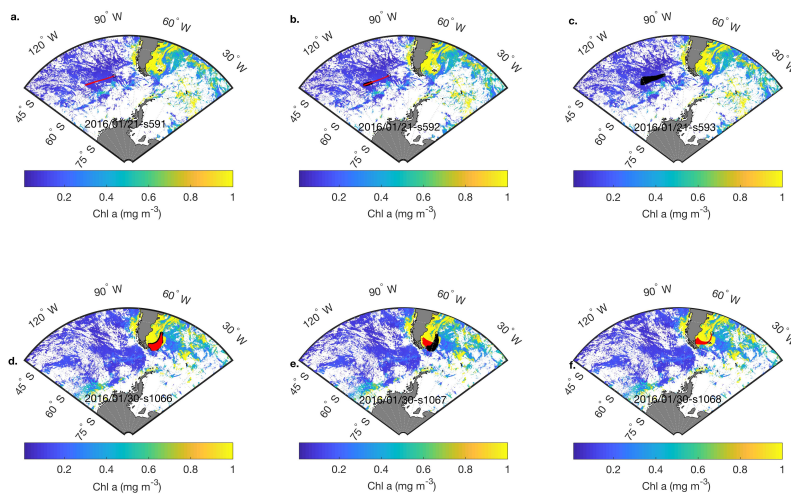


**Figure S4.** Two sets of three consecutive TOGA VOC sample locations, their back-trajectories and surface influences in the lower troposphere on two different flights (a-c; Jan. 21, 2016, and d-f; Jan. 30, 2016). For illustrative purposes, sampling locations are denoted by a black circle, 24-hour back trajectories are shown in red, and surface influences are shown with black squares in each subpanel, overlying weekly composites of remotely sensed chl *a*. Surface influence is multiplied by the underlying chl *a* (or other) surface field and averaged for each sample to yield a surface influence function.